AD NUMBER

AD472558

NEW LIMITATION CHANGE

TO

Approved for public release, distribution unlimited

FROM

Distribution authorized to U.S. Gov't. agencies and their contractors; Administrative/Operational Use; AUG 1965. Other requests shall be referred to Air Force Flight Dynamics Lab., Wright-Patterson AFB, OH 45433.

AUTHORITY

AFFDL ltr, 29 Dec 1971

SECURITY MARKING

The classified or limited status of this report applies to each page, unless otherwise marked.
Separate page printouts MUST be marked accordingly.

1

AFFDL-TR-65-139

PREDICTION OF SPACE VEHICLE THERMAL CHARACTERISTICS

AF33(615)-1755

J. T. Bevans, et al.
TRW Systems Group

TECHNICAL REPORT AFFDL-TR-65-139

AUGUST 1965

AIR FORCE FLIGHT DYNAMICS LABORATORY
RESEARCH AND TECHNOLOGY DIVISION
AIR FORCE SYSTEMS COMMAND
WRIGHT-PATTERSON AIR FORCE BASE, OHIO

27282

NOTICES

When Government drawings, specifications, or other data are used for any purpose other than in connection with a definitely related Government procurement operation, the United States Government thereby incurs no responsibility nor any obligation whatsoever; and the fact that the Government may have formulated, furnished, or in any way supplied the said drawings, specifications, or other data, is not to be regarded by implication or otherwise as in any manner licensing the holder or any other person or corporation, or conveying any rights or permission to manufacture, use, or sell any patented invention that may in any way be related thereto.

Qualified users may obtain copies of this report from the Defense Documentation Center. The distribution of this report is limited because the report contains technology identifiable with items on the strategic embargo lists excluded from export or re-export under U. S. Export Control Act of 1949 (63 STAT. 7) as amended (50 U.S.C. App. 2020.2031) as implemented by AFR 400-10.

Copies of this report should not be returned to the Research and Technology Division unless return is required by security considerations, contractual obligations, or notice on a specific document.

(18) (19)
~~AFFDL~~-TR-65-1~~59~~ 16

(6) PREDICTION OF SPACE VEHICLE THERMAL CHARACTERISTICS.

(10) J. T. Bevans, ~~et al~~ T. Ishimoto, B. R. Loya E. E. Luedke.
TRW Systems Group

(9) TECHNICAL REPORT, ~~AFFDL-TR-65-169~~

(11) AUG ~~1965~~,

(12) 176p.

(16) AF6146 (17) 614617

(15) AF33(615)1725

AIR FORCE FLIGHT DYNAMICS LABORATORY
RESEARCH AND TECHNOLOGY DIVISION
AIR FORCE SYSTEMS COMMAND
WRIGHT-PATTERSON AIR FORCE BASE, OHIO

1473
eef

FOREWORD

The following report was prepared by TRW Systems Group, under USAF Contract No. AF 33(615)-1725 as part of Project 6146, Task 614617. The program was administered by the Air Force Flight Dynamics Laboratory, Research and Technology Division, Wright-Patterson Air Force Base. The Technical Monitor was Mr. C. J. Feldmanis.

The program was performed by J. T. Bevans, T. Ishimoto, B. R. Loya, and E. E. Luedke. Dr. D. K. Edwards of the University of California, at Los Angeles, was consultant throughout the study.

The manuscript was released by the authors 31 August 1965, for publication as an RTD Technical Report.

This technical report has been reviewed and is approved.

William C. Savage
Environmental Control Branch
Vehicle Equipment Division
AF Flight Dynamics Laboratory

ABSTRACT

The work reported herein is the first phase of a program to improve the prediction of spacecraft thermal performance. The study has consisted of measuring actual joint thermal conductances, correlation of the measured joint conductances, programing an improved method of thermal radiation analysis, and performing an experimental comparison of predicted radiation exchange for a simple geometrical system.

Three types of structural and three sizes of component mounting joints were tested and the conductances measured. A successful method of correlation was developed for the unfilled component mounting joints. All joints were selected for their applicability to the next phase of the program, a thermal test of a spacecraft model.

A method of radiation analysis has been programed which uses directional thermal radiation properties and accounts for the specularity and/or diffuseness of these properties. The results of this program can be readily incorporated into most existing thermal analysis programs. The user has the choice of the specular, the diffuse, or the specular-diffuse assumption. The prediction of radiation exchange using these assumptions for simple geometrical arrangements has been compared to experiment. Although the results were within the overall experimental tolerances, further improvement in the predicted values is believed possible.

The study has developed several important technical areas which are worthy of further evaluation. The first is the extension of the correlation techniques to include filled component joints and filled or unfilled structural joints. Continuation of the general measurement of joints to develop a large knowledge of practical joint conductances is also indicated. The comparison of experimental and predicted radiation exchange has shown that a more extensive study is needed of thermal radiation properties to determine the division of these properties into specular and diffuse components. The non-gray error of radiation analysis has also been shown to be an important area for further study.

TABLE OF CONTENTS

ILLUSTRATIONS

ILLUSTRATIONS

TABLES

SYMBOLS

Section 3

A	Area - ft^2
h	Thermal conductance - Btu/hr ft^2 ^oF; h_{eff} = effective h
q	Heat flow - Btu/hr
t	Temperature - ^oF

Section 4

A	Area of a surface -ft^2
B	Quantity introduced by Gebnart - Btu/hr ft^2 $^oR^4$ (Section 4.1)
C	Heat capacity - Btu/hr
D	Diffuse irradiation - Btu/hr ft^2 ster. (Section 4.2)
F	Geometrical shape factor
$\mathcal{F}$	"Script F"
J	Radiosity - Btu/hr ft^2
M	Number of surfaces within the enclosure
N	Number of time intervals
R	Thermal conduction resistance - hr ^oF/Btu (Equation 4-3)
R	Hottel's radiant power leaving a surface - Btu/hr ft^2 $^oR^4$ (Section 4.1)
T	Absolute temperature - ^oR
a	Coefficient (Section 4.2)
b	Coefficient (Section 4.2)
c	Coefficient (Section 4.2)
d	Coefficient (Section 4.2)
i,j,k	Indices representing surfaces within the enclosure
q	Heat flow Btu/hr
x,y,z	Indices
α	Absorptance
ϵ	Emittance
η	Convergence factor (Equation 4-8)
π	3.1415927
ρ	Reflectance
σ	Stefan-Boltzmann constant - Btu/hr ft^2 $^oR^4$
θ	Time

[ ]	Square matrix
$[\ ]^{-1}$	Inverse square matrix
{ }	Column matrix

Section 5

Symbols defined in the text.

Section 6

Q_s	Source heat flow - Btu/hr
$\rho(\theta)$	Directional reflectance at angle θ
θ	Angle between the normal to the surface and the incident or reflected radiation - degrees

Section 7

A	Area, ft^2
Q	Heat flux, Btu/hr ft^2
R	Radius - in.
T	Temperature, ^oF
a	Bolt diameter, in.
b	Twice the plate thickness, in.
c	Effective contact radius, in.
d	Bolt major thread dia.
h	Thermal conductance - Btu/hr ft^2 ^oF
k	Thermal conductivity - Btu/hr ft ^oF
r	Radial position, in.
t	Plate thickness - ft.
η	Nondimensional radius ratio - r/R
η_o	Nondimensional radius constant R_o/R

Appendix IV

T_R = "Receiver" temperature ^oR

T_M = "Mirror" temperature ^oR

T_c = "Sink" (cold wall) temperature ^oR

T_s = "Source" temperature ^oR

1. INTRODUCTION AND SUMMARY

The program, "Prediction of Space Vehicle Thermal Performance," was initiated on 1 July 1964, under Contract AF 33(615)-1725. The purpose of the study can be stated as: Given the necessary analytical methods and experimental data, how well can the thermal performance of a space vehicle be predicted? The subject program was the first step towards securing an answer to this question.

The problem provides two natural divisions. The first is the examination of the analytical procedures needed and the experimental information required for analysis. The second is the verification of the predictions of analysis by a thermal test of a model space vehicle. The present program was intended to satisfy the first need and to provide a transition to the second. Since a model is required to verify analysis, its design will dictate the nature and scope of the experimental studies performed to support analysis. In particular, the subsequent construction of a test model will require the selection of structural and component joints in anticipation of the design. Depending upon the type of joint selected and the degree of experimental measurements made, the thermal resistance of the joints can be critical to the experimental verification of any predictions made. Consequently, it was necessary at the start of the present program to select, in reasonable detail, the model configuration. The experimental measurements of joint thermal resistance were restricted to those joints to be used in the model. Only in this manner could the end purpose of the study, the test of prediction, be achieved within the allocated resources and time.

The specific tasks undertaken in the study were:

(a) Selection of a model for determination of the experimental joint thermal conductance measurements
(b) Experimental measurement of component and structural joint thermal conductance
(c) Examination of the results of the joint thermal conductance results to ascertain if a correlation were possible
(d) Comparison of the analytical techniques of Hottel (1), Gebhart (2), and Oppenheim (3).
(e) Development of a computer program for a specular-diffuse analysis (4)
(f) Experimental measurement of radiation exchange with real surfaces

The following report will consider the above tasks in the order shown. It should be re-emphasized that the purpose of the program and hence, the goal of each task, is to provide the necessary data for a comparison of thermal analysis and thermal test of a spacecraft model.

2. SPACECRAFT MODEL SELECTION

An important initial task was the conceptual design of the model of the space vehicle to be tested in the subsequent phase of the program. The size, method of construction and shape of the model greatly affects the type of fasteners, the physical dimensions and the shape of the joints.

The model which has been selected is shown in Figure 1. Alternative shapes, cylindrical and spherical, were considered but the rectangular parallelepiped was chosen for economy and ease of fabrication. Furthermore, the geometrical shape can not be a critical factor in a test of the prediction of thermal performance. The indicated dimensions, 24" x 24" x 36", are sufficiently large to demonstrate the effects of construction variations, thermal gradients, and internal dissipation. The model will conveniently fit into most environmental test chambers and available solar simulation facilities. Also, the size is representative of many present day space vehicles.

A welded framework is indicated. This method of construction was selected to reduce the number of structural joints that had to be tested. There are three structural joints with the frame: the side panels, the end panels, and the component mounting platform. The side and end panels are 1/16-inch aluminum; i.e., thin enough to sustain a thermal gradient. The mounting platform is 1/8-inch aluminum. In actual space vehicle construction, this mounting plate would probably be a honeycomb structure to reduce weight. Such materials are anisotropic and the thermal conductance in the x, y, and z directions are variable from sample to sample of the same material. The conductance also varies widely for different types of honeycomb. Thus, use of a honeycomb structure would introduce a major undetermined factor in the thermal analysis. This could easily obscure the validity of the comparison of prediction and experiment. The aluminum mounting plate avoids this without affecting the value of the test to be conducted. Thus, if the analysis can properly predict for the aluminum plate, it will be satisfactory for application to a honeycomb material (assuming the properties of the honeycomb are known).

The external panels can be changed to provide different external thermal radiation properties. This may not be important in the initial testing to be performed with the model but will be useful should further testing be desired or required. These panels can be coated to simulate solar cell thermal radiation properties, low α/ε properties or even be insulated without affecting the basic model physically. A louver system could be used in place of any panel to determine the effects of variable emission. Hence, the model will be of much more value than just for the program contemplated in Phase II.

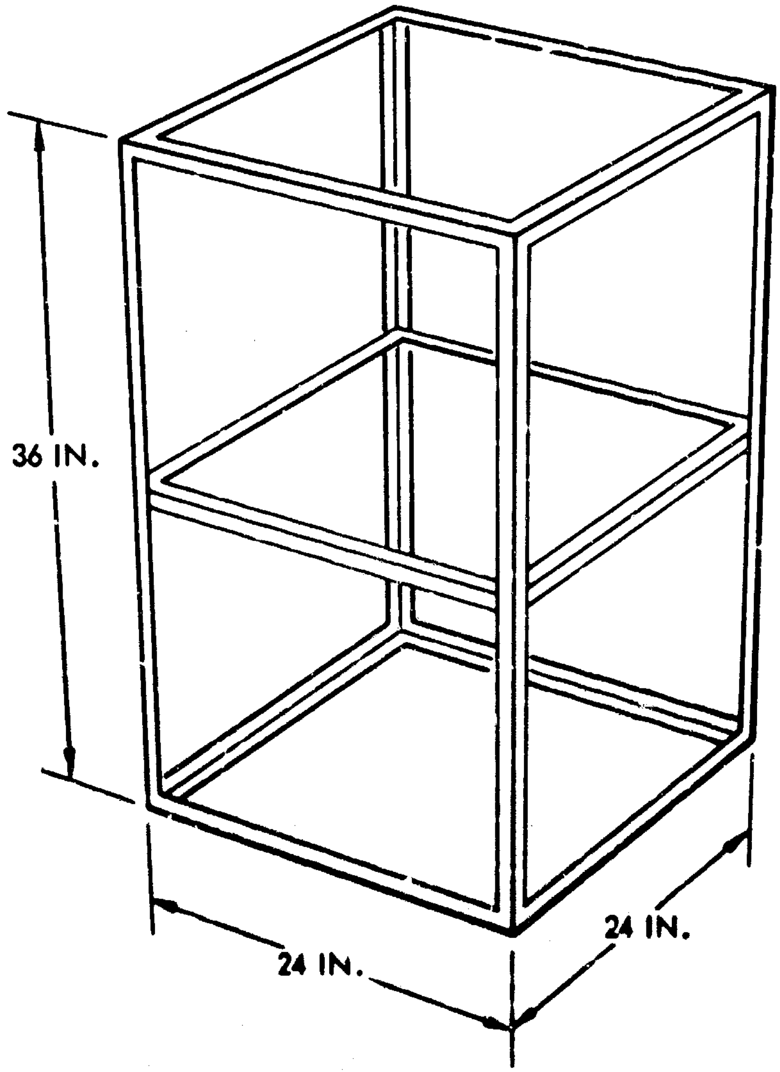

ALUMINUM FRAME-HELI ARC CONSTRUCTION

Figure 1. Spacecraft Model - Size and Shape

3. THERMAL CONDUCTANCE OF JOINTS

Completely riveted joints were excluded from the study. In spacecraft practice, riveted systems are used in order to save weight. However, the thermal conductance of such joints is not considered reproducible and variations of 100 percent have been found in supposedly identical joints (5). Since the goal of the program is to test the ability to predict thermal performance with reliable input information, the introduction of such an uncontrolled thermal resistance is not desired. This would not test the prediction of thermal performance but only the uncertainty of knowledge. The effect of the variable thermal resistance can be demonstrated analytically, once the analysis has been verified.

Two general types of joints were studied: component and structural joints. The component joints are shown in Figure 2. The dimensions were chosen as representative of typical component base sizes. Simulation of the actual component box was not deemed necessary since this would only involve changes in the radiation shape factors used. The assumption was made that the base plates would have a uniform areal power dissipation. The experimental variables examined were bolt-torque, power dissipation level, filler material and reproducibility of the joints. A detailed description of the test method and the results will be given in Section 3.1.

The structural joints tested are presented in Figure 3 and all are bolted joints. The structural joints were selected to satisfy the requirements of the proposed space vehicle model (see Section 2). The first configuration corresponds to the joint between the side panels and the frame. The end panels are bolted to the frame by means of nut plates which are riveted in place (second joint). This joint can be considered to be a combination of a rivet and bolt fastener. The third joint shown represents the joint between the component mounting platform and the frame. As with the component joints, the variables of power dissipation level, filler material and reproducibility were examined. The experimental test method and results are given in Section 3.2.

These joints are "practical" ones; i.e., representing actual fabricated joints. As a result, variations in the thermal conductance must be expected from "identical" joints. An attempt was made to apply idealized theories to these joints to obtain a correlation of the test data. The results of this effort are given in Section 7.

3.1 COMPONENT JOINT EXPERIMENTAL TESTS

The component joints were simulated by bolting a plate 1/16 inch thick of the necessary dimensions to a base plate 1/8 inch thick. The component base plate dimensions used were 6 inches square, 6 inches by 12 inches, and 12 inches square. The plates upon which the base plates were mounted were 2 inches greater in each dimension than the component plate; e.g., 8 inches square for the 6-inch square component plate. The bolt size and placement for each joint are shown in Figure 2. A heater made of 40 gage constantan wire sandwiched between 1 mil Mylar was bonded to the upper surface of each component base plate. The mounting plate had 1/4 inch

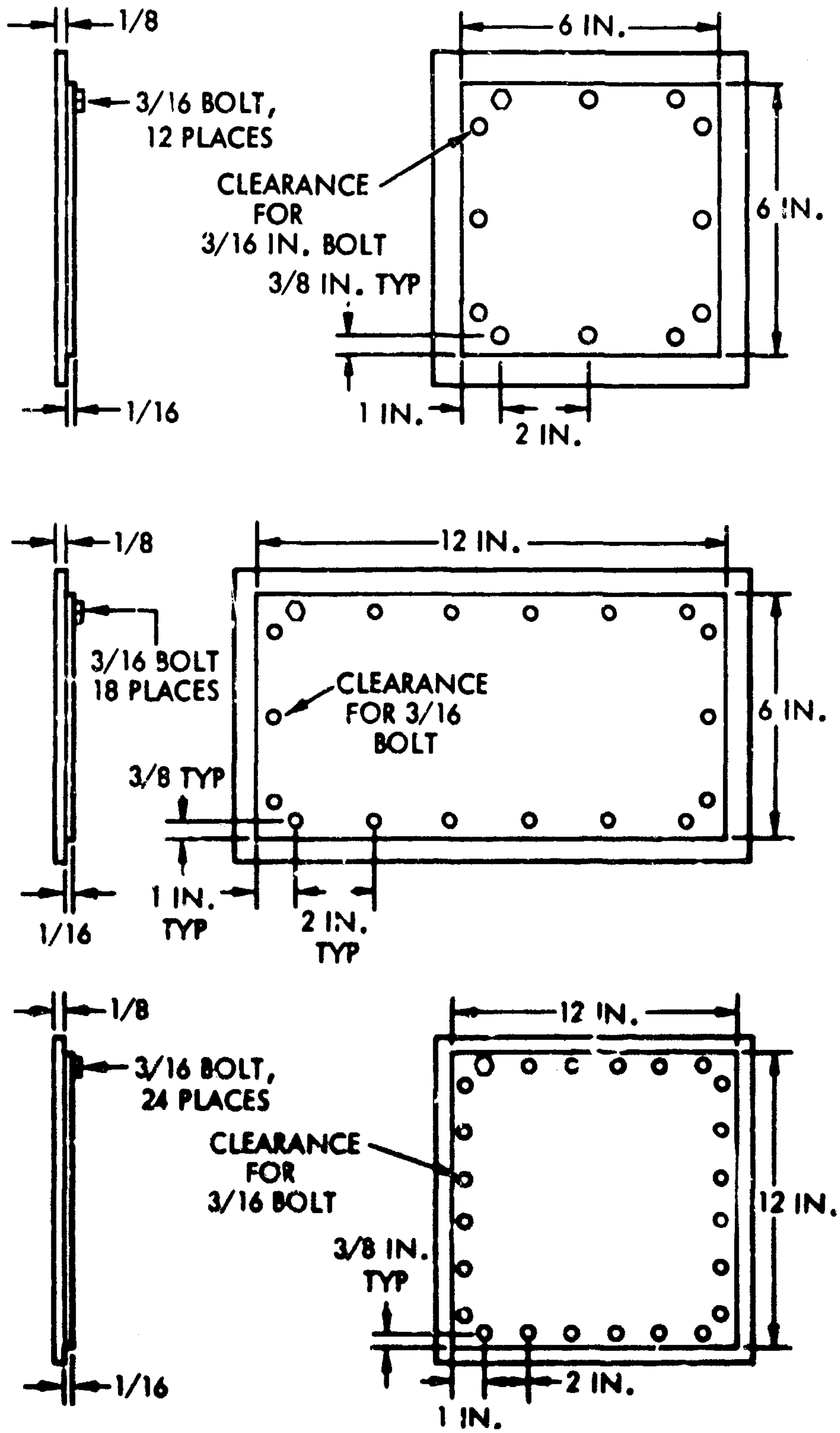

Figure 2. Component Joints

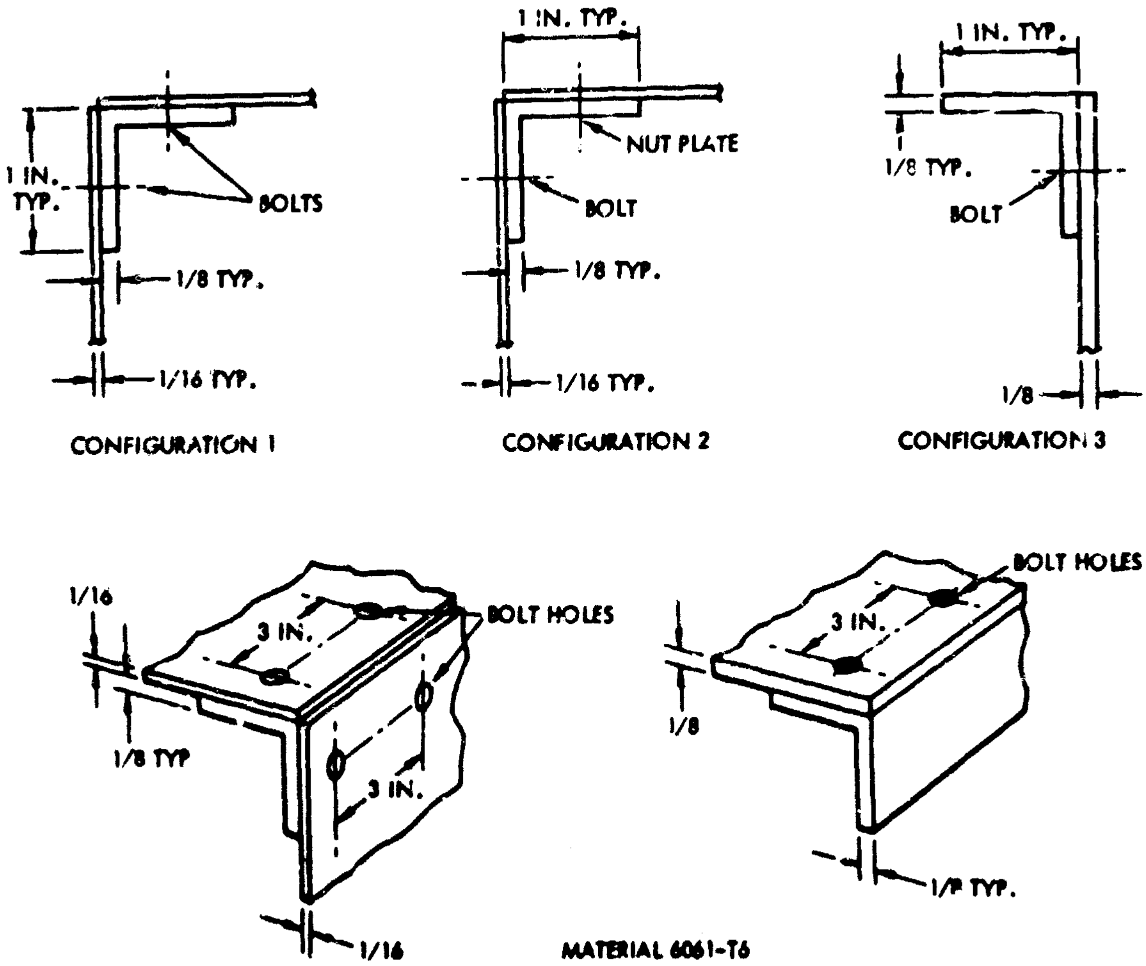

Figure 3. Structural Joints

copper cooling coils attached to its underside. The whole assembly was wrapped in 20 layers of super insulation and suspended within a bell jar. This bell jar was evacuated to a pressure less than 10^{-5} torr. Figure 4 shows a component joint after testing; the final assembly and the vacuum system are illustrated in Figure 5. The thermocouples have been removed from this sample so that surface roughness measurements can be made.

The test procedure consisted of placing the insulated and instrumented joint within the bell jar, securing a vacuum on the system, and setting the initial heating rate. Equilibrium was determined by plotting the various temperatures as a function of time. Once these temperatures had stabilized to less than plus or minus 1°F. per hour, a set of data was taken. The observed temperature drift was caused by drift in the cooling water temperature.

The electrical circuit used to measure the power dissipated by the heater is shown in Figure 6. The power was determined by measuring the voltage across the heater terminals at the component joint and measuring the current flowing in the heater with a standard resistor. This procedure is commonly referred to as the four terminal resistor technique. The potentiometer used for these two measurements was a Leeds and Northrup Type K-3 Potentiometer. This instrument has three ranges: 1.6 volts, 0.16 volts, and 16 millivolts. The least count on these three ranges is 50, 5, and 0.5 microvolts, respectively.

Initially, temperatures were to be measured with nickel resistance temperature sensors. These sensors were obtained from the RdF Corp., Hudson, New Hampshire, and were calibrated by the vendor to within plus or minus 0.5°F. The first tests did not yield consistent results. This was traced to the resistance sensors. Deviations as large as 2°F were found between initial and final calibrations for a run. Since the temperature differences across a joint were generally smaller than 2°F, this initial data had to be discarded and the sensors replaced with differential copper-constantan thermocouples. The subsequent data was reproducible and consistent for a given test configuration.

Resistance thermometry has the inherent advantage of measuring an area rather than a point; i.e., a local average. When properly calibrated, it is also a more accurate sensor since the impurities in the metals used are less important in resistance than in thermoelectric effects. However, this accuracy can only be achieved at a significant increase in cost relative to thermocouples. The instrumentation method required for differential resistance thermometry is quite different than that used for resistance thermometry. The ratio of the resistances of two elements must be measured, the absolute value of one of these elements is needed, and two sets of lead resistance corrections are necessary. This involves two different bridge circuits (and/or instruments) and a means for electrical switching. The alternative use of thermocouples can provide a differential accuracy of approximately plus or minus 0.1°F if the thermocouples are cut from the same roll of wire and careful experimental procedures used. The cost is much less, both in construction and use. This is offset by the "point" measurement characteristics of a thermocouple. For this series of tests, the thermal conductivity of the aluminum joint material was sufficient to minimize this problem.

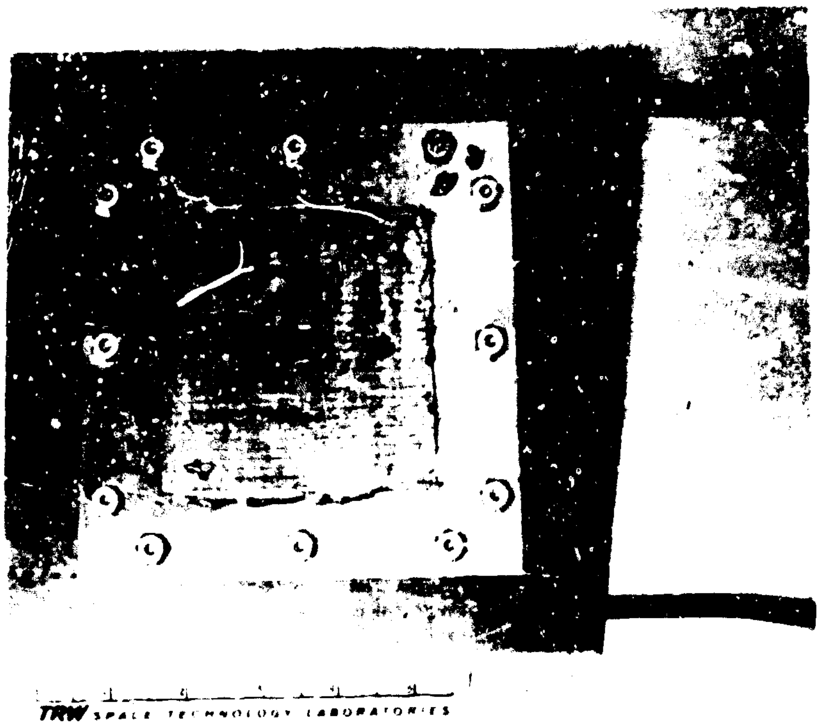

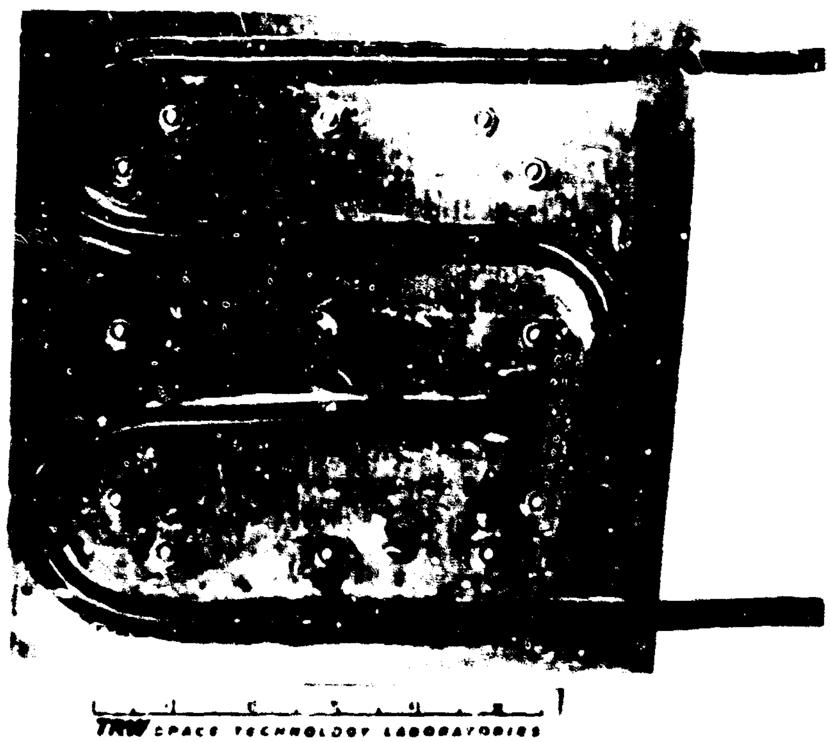

Figure 4. Typical Component Joint

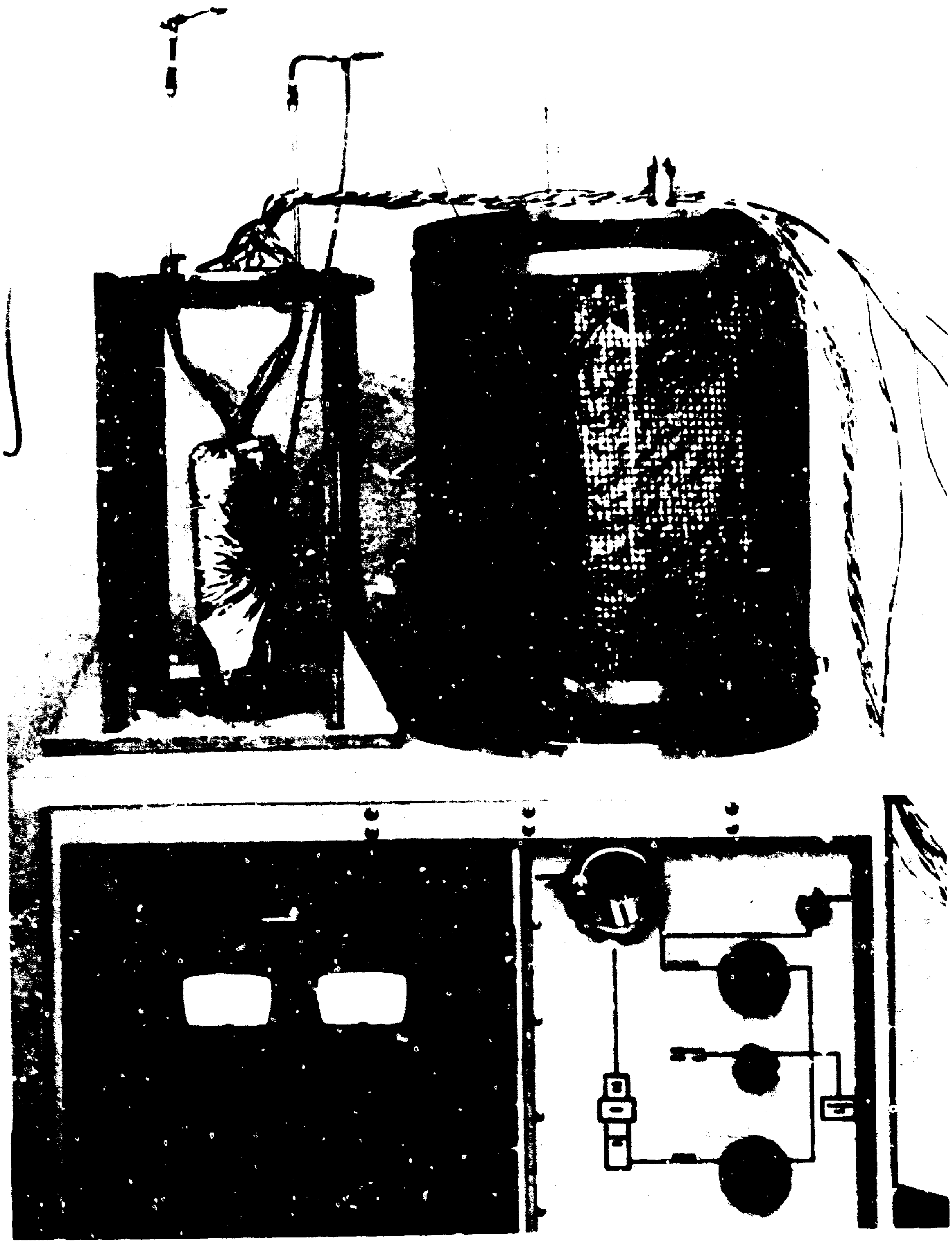

Figure 5. Component Joint Ready for Testing

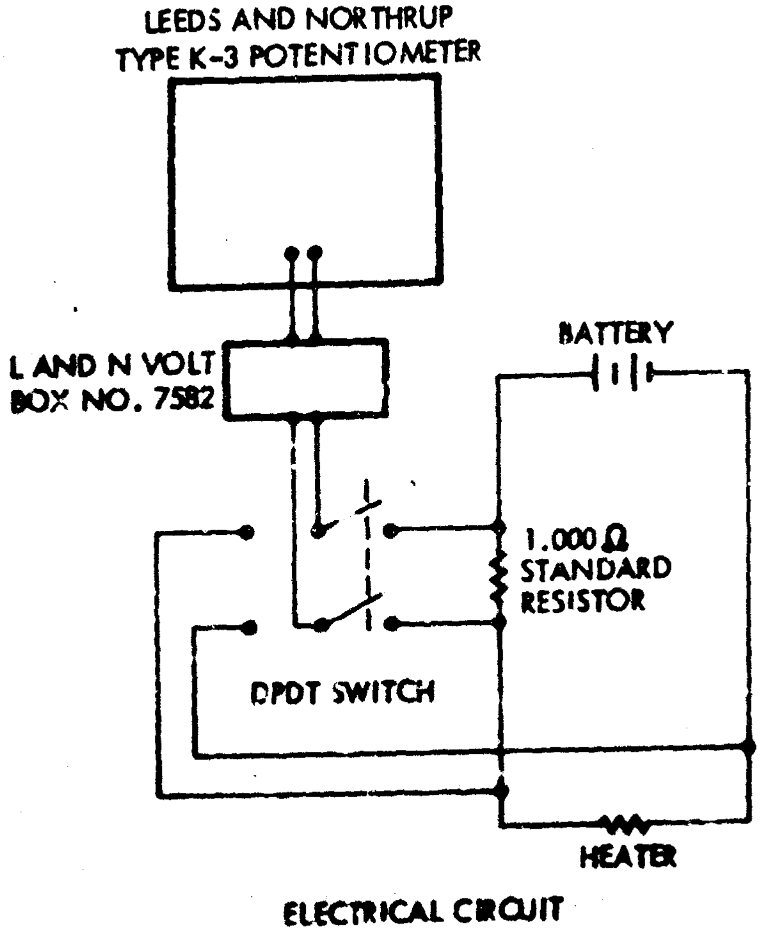

Figure 6. Power Circuit for Joint Testing

The emf of the test thermocouples was measured with a Leeds and Northrup Type K-3 Potentiometer. On the millivolt range, this instrument has a least count of 0.5 microvolts. Deutch No. 14657-37T vacuum feed throughs were used for the thermocouples to avoid a discontinuity in the thermocouple circuitry. When a filler material was used, it was applied by placing two 0.050 inch wires on the surface of the mounting plate, putting an ample quantity of the filler material between the wires and scraping the excess off with a straight edge resting on the wires. Before the material set, in the case of RTV-11* filler material, the component plate was placed on the mounting plate and bolted down. The bolt torques for all joints were set with a calibrated torque wrench. No special instructions were given to the person assembling the joint relative to the order of tightening the bolts. This was intentional since the randomness of a fabricated joint was desired.

The results are summarized in Tables 1, 2, and 3; the actual data and the techniques used in its reduction are given in Appendix I. Included in the Appendix are schematic diagrams showing the placement of the temperature sensors. Three specimens of each joint were run with the exception of the G 683 silicone grease filler.* This material was found to be less suitable for use as filler than the silicone rubber. The primary difficulty with the grease was the contamination of the other areas around the joint; i.e., it was messy. Furthermore, it did not yield joint conductances as large as the RTV-11 material.

The results for the 6-inch square joint (Table 1) shows that the effect of heat flux level was small. This was a temperature gradient effect and for the small range involved in this test (from 2.5°F to 10°F for a typical case), it was not important. Similarly, the change in bolt torque from 12 to 30 inch-pounds was not significant. The effect of the RTV-11 was, however, quite significant. It increased the thermal conductance of the 6-inch square joints by a factor of 4 and the larger joints by a factor between 5 and 6.

The most obvious result of the tests was the inconsistency of the results for "identical" joints. Joint No. 2 of the 6-inch square joints is a good example. An examination of the second joint showed the component base plate to be bowed by 0.007 inches (concave upwards); Joint No. 1 was bowed 0.003 inches (concave downwards); and Joint No. 3 was bowed 0.003 inches (concave upwards). Thus a trend of increased conductance with upward concavity is indicated by these limited tests. In actual fabrication, a flatness tolerance can be imposed, e.g., plus or minus .003 inches, which would minimize this effect. Such a constraint is not unreasonable. The surface roughness of the test plates was measured using a diamond stylus profilometer. The results were consistent for all the plates and yielded 11 μ in. rms across the roll marks and 4 μ in. rms with the roll marks. The surfaces were randomly mated, that is the roll marks placed either parallel or perpendicular, but recorded. The results show no correlation between striation alignment and conductance values.

---

*Manufactured by General Electric Company, Silicone Products Department

TABLE 1

COMPONENT JOINT THERMAL CONDUCTANCE EXPERIMENTAL RESULTS

THERMAL CONDUCTANCE - BTU/HR FT^2 ^{o}F

6 inch by 6 inch plate, 1/16 inch thick, bolted to
8 inch by 8 inch plate, 1/8 inch thick, using 12 bolts

Sample No.	Bolt Torque						Filler
	12 in-lb	24 in-lb				30 in-lb	
		Power Dissipation					
	10 Watts	4.9 Watts	8.6 Watts	13.4 Watts	18.4 Watts	10 Watts	
1		22.8	23.2	22.9	23.1		None
2	28.5	29.1	30.1	30.1	30.0	30.0	None
3	24.8	22.1	25.9	26.2	26.6		None
1*		76.9	81.5	82.5	83.2		RTV-11
2	123.0	128.1	127.0	129.0	130.0	142.0	RTV-11
3	84.1	91.0	93.5	94.8	95.4		RTV-11
1*							G-683
2	55.5	63.0	65.0	66.1	67.1	57.0	G-683
3	47.0	47.3	48.2	48.8	49.5		G-683

*Same samples as above, with filler added.

TABLE 2

COMPONENT JOINT THERMAL CONDUCTANCE EXPERIMENTAL RESULTS

THERMAL CONDUCTANCE - BTU/HR FT^2 ^oF

6 inch by 12 inch plate, 1/16 inch thick, mounted to 8 inch by 14 inch plate, 1/8 inch thick using 18 bolts; bolt torque 24 in-lb

Sample No.	Power Dissipation 10 Watts	20 Watts	40 Watts	Filler Material
1	18.5	18.9	18.5	None
1	103	101.5	98	RTV-11
2	103	101	97	RTV-11
3	90	92	92	RTV-11

TABLE 3

COMPONENT JOINT THERMAL CONDUCTANCE EXPERIMENTAL RESULTS

THERMAL CONDUCTANCE - BTU/HR FT^2 ^oF

12 inch by 12 inch plate, 1/16 inch thick, mounted to 14 inch by 14 inch plate, 1/8 inch thick using 24 bolts; bolt torque 24 in-lb

Sample No.	Power Dissipation 20 Watts	40 Watts	80 Watts	Filler Material
1	8.4	8.3	8.3	None
1	56.6	55.8	56.1	RTV-11
2	51.7	52.8	51	RTV-11
3	51.4	51.9	52.4	RTV-11

The value of the filler for component mounting boxes is apparent. For the proposed test of a spacecraft model, the component boxes will be simulated by resistances dissipating pre-determined values of power. This is very similar to an actual spacecraft system. The higher values of conductance will permit the same heat flow with 1/3 to 1/4 of the temperature difference or conversely, 3 to 4 times the heat flow for the same temperature difference. This should make this type of thermal resistance less critical in the thermal analysis and prediction.

The effect of using filled joints must be investigated for each specific application under consideration. While much higher conductance values were obtained, the scatter in the data was larger for filled than unfilled joints. Therefore, the selection of filled or unfilled joints depends upon whether joints of high conductance, not precisely defined or joints of low conductance, more accurately described, are desired.

The differences in conductance for different sized component mounting plates was also of interest. The filled conductance decreased by a factor of 2 when the dimensions of the square component base was increased from 6 to 12 inches. This decrease is expected since the number of bolts doubled while the total area increased four times. This effectively causes an increase in the conduction pathlength of the mounting plate. These factors will be considered in more detail in Section 7, "Correlation of Experimental Results."

The overall accuracy of the tests is difficult to assess properly. However, the experimental accuracy of the various tests quantities can be given:

Inaccuracy in temperature difference measurement: $\pm 0.1^{\circ}F$

Inaccuracy in temperature measurement: $\pm 0.5^{\circ}F$

Inaccuracy in power dissipation (including insulation loss): $\pm .5\%$

Inaccuracy in area measurement: $\pm .050 \text{ in}^2$

Inaccuracy in bolt torque: ± 0.5 inch-pounds

These values may be combined in a linear error analysis to approximate the total measurement inaccuracy. That is, the error in measured conductance (h) of a typical unfilled joint is:

$$\frac{\Delta h}{h} = \frac{\Delta(\Delta t)}{\Delta t} + \frac{\Delta q}{q} + \frac{\Delta A}{A} = \frac{.1}{1} + \frac{.025}{5} + \frac{.05}{36}$$

or

$$\frac{\Delta h}{h} = 10.5\%$$

The significance of this inaccuracy must be appraised in terms of the application of the data. The error in the measurement of a single joint is less than the lack of reproducibility between joints. Hence, the more important factor is the variation of the conductance of "identical" joints. As shown in Tables 1, 2, and 3, this is approximately plus or minus 25 percent. However the influence of such a variation upon a thermal analysis can be either large or small, depending upon the system examined. For example, if a spacecraft thermal control system is conduction controlled, this variation might be critical; conversely, if it were radiation dominated, the differences might be negligible. To determine the importance of these variations requires an error analysis of the specific configuration.

3.2 STRUCTURAL JOINT EXPERIMENTAL TESTS

The test procedures used for the structural joint measurements were identical to those used with the component joints. The structural joints tested are shown schematically in Figure 3; an actual test joint is shown in Figure 7. A 40 gage constantan and Mylar heater was bonded to one edge of the joint. On the opposite edge, a 1/4 inch copper cooling tube was bonded to provide the necessary heat sink. This whole assembly was wrapped in 20 layers of super insulation and suspended in a bell jar (similar to Figure 5). The remainder of the test procedure was identical to that used for the component joints, e.g., the electrical measurement circuit was that given in Figure 6. Based upon the experience with the component joints, only thermocouples were used as the temperature sensors. The Leeds and Northrup Type K-3 Potentiometer was again used for measuring the thermocouple voltages.

The test results are given in Tables 4, 5, and 6; the actual data from which these results were reduced are given in Appendix II. The first joint tested, Configuration 1 of Figure 3, is representative of the trends indicated for all three joints. Within the range of power dissipations used, no dependency upon power level is indicated for the unfilled joint; i.e., for small temperature differences, the conductance is a constant. A much higher value of joint conductance was obtained with the use of a filler material along with an apparent heat flow dependency. Configuration 2 used nut plates on one side instead of bolts. This had little effect upon conductance for the unfilled case. However, opposite results were obtained for two different RTV-11 filled joints with this configuration; i.e., in one case the nut plate side had a higher conductance and in the other, it had a lower one. No difference between a bolted joint and a nut plate joint could be concluded from the results for Configuration 1 and 2 because of this conflicting data. A strong dependency with heat flow is also noted for the filled joint.

The results of the filled structural joint tests show wide variations in calculated conductance. The most probable reason for these variations is the temperature measurement error. The temperature difference across the interface was of the same order of magnitude as the expected temperature error. In ideal joint conductance tests appearing in the literature (see Section 3.3), the temperature profile of the mating parts is accurately plotted and the data projected to the interface to obtain the temperature difference. The heat flows are normally much higher than in the present study and much higher temperature differences result. In the

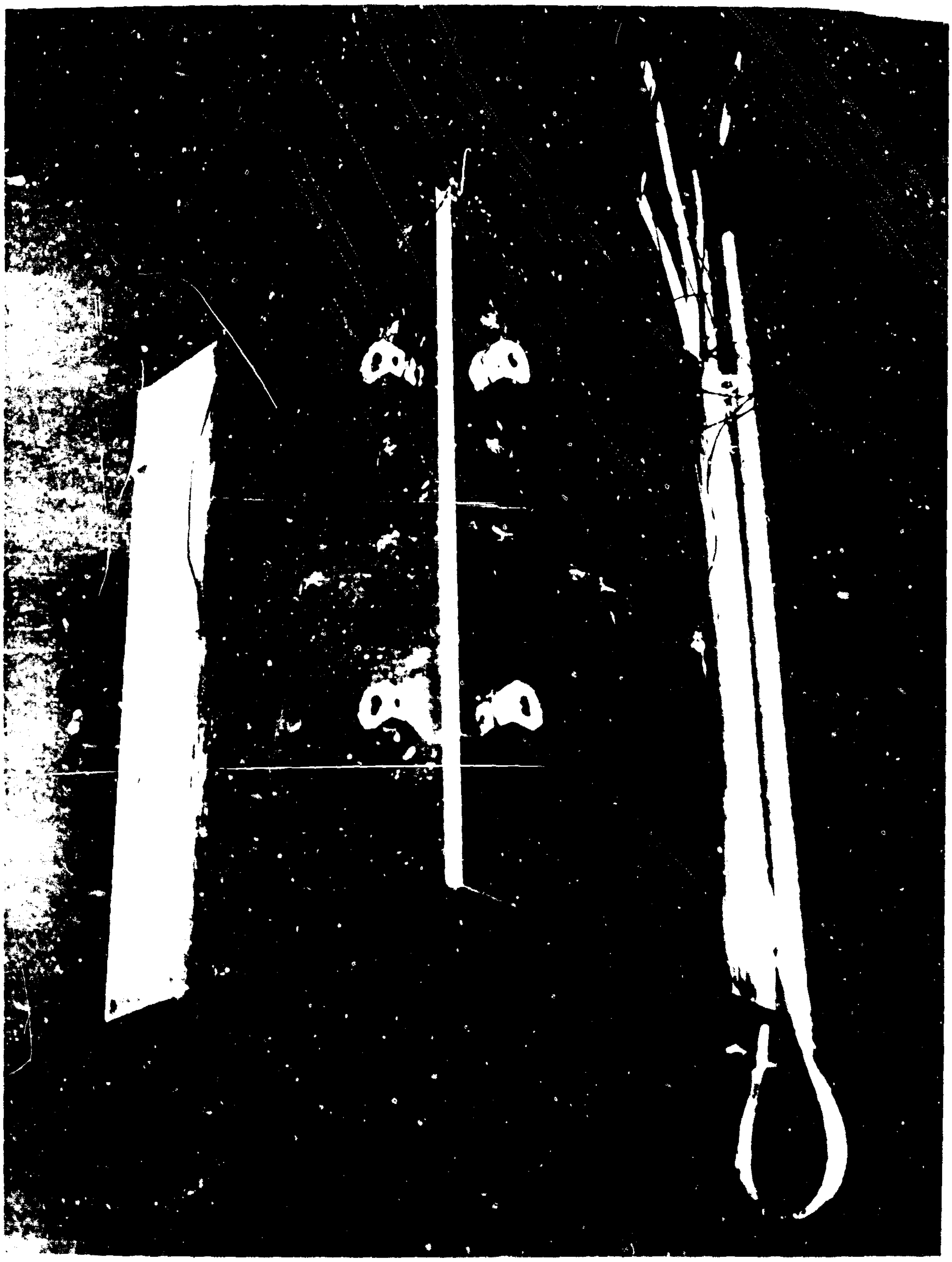

Figure 7. Typical Structural Joint

TABLE 4

STRUCTURAL JOINT CONDUCTANCE - BTU/HR FT^2 $^\circ$F

6 inch joint, 2 bolts, 24 inch-pounds torque, Configuration 1

Joint No.*	Q - Heat Supplied 5 Watts	15 Watts	25 Watts	Filler
1a	70.3	74.2	75.7	None
1b	80.5	80.6	85.3	None
2a	103.5	100.1	100.9	None
2b	88.5	90	96.5	None
3a	78.5	79.4	77.0	None
3b	77.5	79.8	81.8	None
1a	1042	906	715	RTV-11
1b	1042	995	895	RTV-11
1a	502	595	542	G-683
1b	681	652	645	G-683

9 inch joint, 3 bolts, 24 inch-pounds torque, Configuration 1

Joint No.*	7.5 Watts	22.5 Watts	37.5 Watts	Filler
1a	116.0	98.5	100.8	None
1b	74.0	75.3	77.9	None

*The notation a and b are used to distinguish the side of the joint next to the heater and the cooling coil, respectively.

TABLE 5
STRUCTURAL JOINT CONDUCTANCE, BTU HR FT^{2} $^{\circ}$F

6 inch joint, 2 bolts, 24 inch-pounds torque, Configuration 2

Joint No.	5 Watts	15 Watts	25 Watts	Filler
1a (Bolt)	84.2	81.5	85.0	None
1b (Nut Plate)	99.0	100.8	110.3	None
2a (Bolt)	105.5	102	100.8	None
2b (Nut Plate)	82.4	81.4	83.2	None
3a (Bolt)	89.5	88.5	92.6	None
3b (Nut Plate)	93.5	99.3	105.2	None
1a (Bolt)	1427	1227	1050	RTV-11
1b (Nut Plate)	520	514	490	RTV-11
1a (Bolt)	438	425	420	G-683
1b (Nut Plate)	341	345	375	G-683
2a (Bolt)	889	795	669	RTV-11
2b (Nut Plate)	1892	1466	800	RTV-11

9 inch joint, 3 bolts, 24 inch-pounds torque, Configuration 2

Joint No.	7.5 Watts	22.5 Watts	37.5 Watts	Filler
1a (Bolt)	93.5	95.2	94.1	None
1b (Nut Plate)	84.1	87.8	97.6	None

TABLE 6
STRUCTURAL JOINT CONDUCTANCE, BTU HR FT^2 ^oF

6 inch joint, 2 bolts, 24 inch-pounds torque, Configuration 3

Joint No.	5 Watts	15 Watts	25 Watts	Filler
1	147.0	144.2	142.0	None
2	194.0	180.0	174.0	None
3	112.2	108.5	106.5	None
1	1110	1273	1242	RTV-11
1	1328	1262	1231	G-683

9 inch joint, 3 bolts, 24 inch-pounds torque, Configuration 3

Joint No.	7.5 Watts	22.5 Watts	27.5 Watts	Filler
1	142.2	139.0	135.5	None

present investigation, the real joints had two dimensional heat flows. It was not possible to project gradient measurements to the interface. Furthermore, the heat fluxes used were selected as representative of those to be encountered in an actual spacecraft, and the temperature gradients were correspondingly small.

Two values of joint conductance are given in Table 4 and 5 (Configurations 1 and 2) for each test joint. The experimental system was instrumented to obtain the conductance from either plate to the angle. The effective conductance from plate to plate is determined (by analogy to an electrical circuit) as:

$$h_{eff} = \frac{1}{\frac{1}{h_1} + \frac{1}{h_2}}$$

If this effective conductance is computed for "identical" joints and conditions, the variations between the measurements are reduced significantly for the unfilled joints. In the case of Configuration 1, the variations in total conductance are less than plus or minus 15 percent; for Configuration 2, it is less than plus or minus 7.5 percent. The filled joints have a much wider variation as is indicated by the measurements.

Two lengths of joint were tested for all three configurations. No significant differences in the measured conductances were observed. Hence, the end losses from the test joint are considered to have been negligible.

The third configuration tested was the one to be used for connecting the internal mounting plate to the frame. The measured results were similar to those obtained for the other two configurations.

The test results obtained indicate a filled structural joint to be more variable than an unfilled one. The conductance is significantly higher, of course. This variability may be nullified by the higher value obtained. As discussed in Section 3.1, this can only be assessed by performing an analysis of an actual spacecraft system using these opposing conditions. The choice will depend upon the relative importance of the two modes of heat transfer, radiation and conduction, for the joint analyzed and the particular system used. However, if filled joints are used, a formerly conduction dominated system may become radiation controlled. For example, the total effective conductance of an unfilled joint is of the order of 40 to 50 Btu/hr ft^2 ^oF where as an RTV-11 filled joint has a conductance of over 500 Btu/hr ft^2 ^oF.

4. DEVELOPMENT OF ANALYTICAL METHODS FOR THERMAL PERFORMANCE ANALYSIS

The transient energy equation which must be solved for each surface in space vehicle thermal analysis is:

$$C_i \frac{dT_i}{d\theta} = (q_x)_i + (q_r)_i + (q_c)_i \qquad 4\text{-}1$$

where q_x = net heat transfer from an external source or by internal dissipation

q_r = net heat transfer by radiation

q_c = net heat transfer by conduction

The quantity q_x is generally a function of time. This is a result of orbital conditions and/or of mission imposed duty cycles. Solutions of Equation 4-1 are required for each surface of the spacecraft (internal and external) as a function of time in orbit.

For computer solution, the technique of finite differences is used. Equation 4-1 is written

$$T_i(\theta + \Delta\theta) = T_i(\theta) + \left[\frac{\Delta\theta}{C_i}\right] \left\langle \left[q_x(\theta)\right]_i + \left[q_c(\theta)\right]_i + \left[q_r(\theta)\right]_i \right\rangle \qquad 4\text{-}2$$

Thus, the temperature of surface i at time $\theta + \Delta\theta$ is expressed in terms of the temperature and net energy transfers at time θ. The variation of q_x with time is assumed to be known or imposed by external constraints upon the spacecraft. However, both conduction and radiation contain the temperature variable. The expression for q_c is

$$(q_c)_i = \sum_{k=1}^{M} \frac{T_k - T_i}{R_{ki}} \qquad 4\text{-}3$$

The expression for q_r can be given by either the network method or by Hottel's "script F."* The equations which must be solved to obtain $(q_r)_i$ by the two methods is given in Section 4.1. They are

$$\text{Hottel:} \quad (q_r)_i = \sum_{k=1}^{M} A_i \mathcal{F}_{ik} \sigma (T_k^4 - T_i^4) \qquad 4\text{-}4$$

---

*The simple equivalence of Hottel (1) and Gebhart (2) methods (see Section 4.1) is such that for all practical purposes, they may be assumed to be identical.

Network: $(q_r)_i = A_i \left(\frac{\varepsilon_i}{\rho_i}\right) (\sigma T_i^4 - J_i)$ 4-5

$$J_i = \varepsilon_i \sigma T_i^4 + \rho_i \sum_{k=1}^{M} F_{ik} J_k \qquad 4\text{-}6$$

or

$$(q_r)_i = A_i \varepsilon_i \sigma T_i^4 - A_i \varepsilon_i \sum_{k=1}^{M} F_{ik} J_k \qquad 4\text{-}7$$

The difference between the two methods for radiation calculations becomes apparent by examining the above equations. At each time interval, the network method requires a new solution of the radiation problem; the "script F" technique requires the radiation problem to be solved once to determine the values of $\mathfrak{F}_{ik}$. The determination of $\mathfrak{F}_{ik}$ does not need to be repeated unless the properties are changed. It should be noted that if the problem is not transient and no conduction is involved, neither method has any computational advantage over the other.

The procedure for obtaining the "script F" values for a given enclosure can be that described by Hottel (1) or from the network method (6). In both methods of securing $\mathfrak{F}_{ij}$, one matrix inversion is required; if the two matrices are compared (see References 1 and 6), they differ only by the use of the areas of the surfaces in the diagonal of Hottel's matrix; i.e., no computational or accuracy advantage.

The inversion process and the time interval increments used in Equation 4-2 provides a quantitative means for determining the "cost" of solving Equation 4-2 by the radiosity method. A matrix of the coefficients of the various J's must be inverted once at the start of the entire problem and can be used again with the values of temperature obtained at subsequent times. Hottel's method for calculating "script F" requires a similar matrix inversion. In each case, after the matrix inversion, secondary calculations are required to determine the various $\mathfrak{F}_{ij}$ or the new radiosities. However, with "script F," this does not have to be repeated at each time interval. Hence, for N time intervals and M surface enclosure, the number of calculations using radiosities is:

NM^2 + the matrix inversion

The reciprocity relationship $A_i \mathfrak{F}_{ij} = A_j \mathfrak{F}_{ji}$ can be used in conjunction with the method given by Reference 6 to obtain $\mathfrak{F}_{ij}$ in a time corresponding to that given for the network method of:

1/2 (M)(M+1) + the matrix inversion

Consequently, the "script F" method is significantly more economical than the network method.

The steady state case is also more readily solved by the "script F" method when radiation and conduction are both present. Equation 4-1 for the steady state case can be written with the aid of Equation 4-3 as:

$$T_i = T_i\,(1-\eta) + \eta \left\{ \frac{(q_x)_i + (q_r)_i + \sum_{k=1}^{M} \frac{T_k}{R_{ki}}}{\sum_{k=1}^{M} \frac{1}{R_{ki}}} \right\} \qquad 4\text{-}8$$

where η represents the convergence factor; i.e., $\eta \Rightarrow o$ with convergence. Equation 4-8 must be solved for all surfaces i, e.g., by iteration. If, for each iteration, a new solution for the values of $(q_r)_i$ is required, the number of calculations required is identical to the time interval problem. If however, $(q_r)_i$ is represented by Equation 4-4, the iteration process is independent of recalculation of the radiation problem.

This discussion of the relative merits of the network method and the "script F" method is not based upon the assumptions inherent in either procedure. Another technique based on less restrictive assumptions will be described in Section 4.2. It can be used in either a network or a "script F" form, and the same arguments will hold relative to the method of solution to be used.

The accuracy of any method can be separated into two parts. The first is that inherent in the assumptions; e.g., specular versus diffuse properties. The second part is the accuracy of computation. The assumptions of the analysis is the dominant factor in determining the degree to which a method approximates a real system.

4.1 COMPARISON OF THE ANALYTICAL METHODS OF HOTTEL (1), GEBHART (2), AND OPPENHEIM (3) FOR CALCULATION OF RADIATION HEAT TRANSFER

The calculation of radiation heat transfer is generally based upon several simplifying assumptions:

(1) The thermal radiation properties of all surfaces involved in the heat transfer are diffuse (independent of angle), grey (independent of wavelength), not dependent upon temperature, and surfaces are opaque.
(2) An "enclosure" can be constructed which contains and/or bounds all of the surfaces involved in the radiation exchange such that all radiation emitted and/or reflected from any one surface is reflected and/or absorbed by the other surfaces.
(3) Any single surface used in the calculations is isothermal and uniformly irradiated; this may necessitate the subdivision of a large natural surface into several parts in order to approach this condition.
(4) No effects occur as a result of polarization, diffraction or fluorescence.

Three different methods of viewing the solution of this radiation exchange problem are available. These are generally known as the "script F" method (Hottel), Gebhart's method, and the network (Oppenheim). Intuitively, these methods must be identical since they are based upon the same physical assumptions and the conservation of energy. However, it is important that this equivalence be demonstrated. Sparrow (7) has recently shown this by developing the methods of Hottel and Gebhart from the network method. Since the "script F" method has been advocated as a more useful approach in complex transient radiation exchange, the "script F" method will be used here as the method of comparison.

Hottel's method is based upon the superposition of the radiant exchange within an enclosure. To do this, he assumed all of the surfaces except one within the enclosure to be at zero temperature; the remaining surface has an emission rate of unity, i.e., $\sigma T_i^4 = 1$. He then considers the quantity ${}_iR_j$, the power per unit area leaving surface j as a result of the power emitted by surface i; for surface i, the radiation leaving is $\varepsilon_i + {}_iR_i$. The exchange between surfaces i and j are expressed as

$$Q_{ij} = A_i \mathfrak{F}_{ij} \sigma (T_i^4 - T_j^4) \qquad 4\text{-}9$$

where the reciprocity relation has been used, i.e., $A_i \mathfrak{F}_{ij} = A_j \mathfrak{F}_{ji}$. The quantity ${}_iR_j$ is related to $\mathfrak{F}_{ij}$ by:

$$A_i \mathfrak{F}_{ij} = {}_iR_j A_j \left(\frac{\varepsilon_i}{\rho_j} \right) \qquad 4\text{-}10$$

Thus, the incident power per unit area $({}_iR_j/\rho_j)$ is absorbed in the fraction ε_i. This absorbed power is a result of an emission from surface i of unity and must be increased by the factor σT_i^4. Correspondingly, the absorbed power of surface i from emission by surface j must be increased by σT_j^4. The "script F" is, therefore, a quantity which collects the interreflections within the enclosure and provides a measure of the radiant interchange between two surfaces by direct and reflected (from all surfaces) exchange.

The irradiation of surface j by surface i $({}_iR_j/\rho_j)$ can be expressed for an M surface enclosure $(\sigma T_i^4 = 1)$ as:

$$\frac{{}_iR_j}{\rho_j} = F_{ji}\varepsilon_i + \sum_{k=1}^{M} F_{jk}\, {}_iR_k \qquad 4\text{-}11$$

Multiplying through by $\varepsilon_j A_j / A_i$ gives

$$\frac{A_j \varepsilon_j \; {}_iR_j}{A_i \rho_j} = \frac{A_j F_{ji} \varepsilon_i \varepsilon_j}{A_i} + \sum_{k=1}^{M} \frac{\varepsilon_j A_j F_{jk} \; {}_iR_k}{A_i} \left(\frac{\rho_k}{\rho_k}\right)\left(\frac{\varepsilon_k}{\varepsilon_k}\right) \qquad 4\text{-}12$$

With Equation 4-10 and noting $A_i F_{ij} = A_j F_{ji}$, this gives

$$\mathfrak{J}_{ij} = \varepsilon_i \varepsilon_j F_{ij} + \sum_{k=1}^{M} (\varepsilon_j F_{kj}) \; \frac{\rho_k}{\varepsilon_k} \; \frac{A_k}{A_i} \; \frac{\varepsilon_k}{\rho_k} \; {}_iR_k$$

or

$$\mathfrak{J}_{ij} = \varepsilon_i \varepsilon_j F_{ij} + \sum_{k=1}^{M} \varepsilon_j F_{kj} \frac{\rho_k}{\varepsilon_k} \quad \mathfrak{J}_{ik} \qquad 4\text{-}13$$

Equation 4-13 will be developed by the network method in order to indicate the equivalence of the two techniques.

The Gebhart method is a variation of the "script F" phrased in different language. Gebhart utilized a quantity B_{ij} to represent the effects of interreflections within the enclosure. ${}^{i}{}_{j}B_{ij}$ is the fraction of radiation emitted by surface i which is absorbed by surface j. The heat loss of a surface was expressed by Gebhart as:

$$q_j = \varepsilon_j A_j \sigma T_j^{\,4} - \sum_{i=1}^{M} B_{ij} \varepsilon_i A_i \sigma T_i^{\,4} \qquad 4\text{-}14a$$

or

$$q_j = \varepsilon_j A_j \sigma T_j^{\,4} - \sum_{i=1}^{M} q_{ij} \qquad 4\text{-}14b$$

The corresponding expression for Hottel's method is:

$$q_j = \sum_{i \neq j}^{M} A_j \mathfrak{J}_{ji} \sigma T_j^{\,4} - \sum_{i \neq j}^{M} A_i \mathfrak{J}_{ij} \sigma T_i^{\,4} \qquad 4\text{-}15$$

The first term of Equation 4-15 simplifies by noting the total radiation leaving surface j is $\varepsilon_j \sigma T_j^{\,4}$, i.e., $T_i = 0$

$$\sum_{i \neq j}^{M} \sigma T_j^{\,4} \, \mathfrak{J}_{ji} = \varepsilon_j \sigma T_j^{\,4} - \mathfrak{J}_{jj} \sigma T_j^{\,4}$$

or

$$\sum_{i=1}^{M} \mathcal{F}_{ji} = \varepsilon_j \qquad 4\text{-}16$$

Equations 4-14 and 4-15 must represent the same net heat loss by surface j. Equating these two relations gives:

$$\sum_{i=1}^{M} A_i\ \mathcal{F}_{ij}\sigma T_i^{\ 4} = \sum_{i=1}^{M} B_{ij}\varepsilon_i A_i \sigma T_i^{\ 4}$$

This can only be true if:

$$\mathcal{F}_{ij} = \varepsilon_i B_{ij} \qquad 4\text{-}17$$

Consequently, Gebhart's B_{ij} is equal to Hottel's $\mathcal{F}_{ij}$ divided by ε_i.

The equations representing the network method of solution utilize the radiosity* of a surface. The radiosity of a surface can be expressed as:

$$J_i = \varepsilon_i \sigma T_i^{\ 4} + \sum_{k=1}^{M} \rho_i F_{ik} J_k \qquad 4\text{-}18$$

The net heat flux leaving a surface is:

$$q_i = A_i\ \frac{\varepsilon_i}{\rho_i}\ \left(\sigma T_i^{\ 4} - J_i\right) \qquad 4\text{-}19$$

This can also be written as (since $\varepsilon_i + \rho_i = 1$):

$$q_i = A_i J_i - A_i \sum_{k=1}^{M} F_{ik}\ J_k \qquad 4\text{-}20$$

Now consider the case of an enclosure with all surfaces at zero temperature except surface i which has $\sigma T_i^{\ 4} = 1$.

$$J_j = \rho_j\ \sum_{k=1}^{M} F_{jk} J_k \qquad 4\text{-}21$$

$$q_j = q_{ij} = A_j J_j - A_j\ \sum_{k=1}^{M} F_{jk} J_k \qquad 4\text{-}22$$

or

$$q_{ij} = A_j J_j \left(1 - \frac{1}{\rho_j}\right) = -\left(\frac{\varepsilon_j}{\rho_j}\right)\ A_j J_j \qquad 4\text{-}23$$

*Radiosity is the sum of the emitted and reflected radiant power from a surface.

But by Equation 4-9 for the assumed constraints on surface temperatures

$$q_{ij} = - A_i \mathfrak{F}_{ij} = - A_j \mathfrak{F}_{ji}$$

Hence

$$\mathfrak{F}_{ji} = \left(\frac{\varepsilon_j}{\rho_j}\right) J_j \qquad 4\text{-}24$$

Substitution of Equation 4-24 into Equation 4-20 yields

$$\mathfrak{F}_{ij} = \varepsilon_i \varepsilon_j F_{ij} + \sum_{k=1}^{M} \varepsilon_j F_{kj} \left(\frac{\rho_k}{\varepsilon_k}\right) \mathfrak{F}_{ik} \qquad 4\text{-}25$$

This is identical to Equation 4-13.

SUMMARY

The method of Gebhart has been shown to be directly convertible to the "script F" of Hottel by the use of Equation 4-17. Similarly the network method has been shown to yield an expression for $\mathfrak{F}_{ij}$ identical to that obtained from Hottel's method (Equation 4-13 and 4-25). Therefore, there is no difference in the methods and by algebraic manipulation, one method can be expressed in the terms of either of the other two.

4.2 IMPROVED METHOD OF RADIATION ANALYSIS

The available methods for radiation heat transfer analysis have been restricted by the assumptions given in Section 4.1 Recently, a review of the problem has been made and a procedure is now available for eliminating the restriction to nondirectional diffuse properties (4). The use of non-grey thermal radiation properties can be used in the manner described by Bevans and Dunkle (8). Perfectly specular properties can be treated by the method of Eckert and Sparrow (9) but the properties must be considered to be nondirectional. The case of polarization can also be treated (10) but the practicality is limited to a few cases. The most practical new technique is believed to be that given by the second approximation described in Reference 4. The following discussion will describe the adaptation of this method to development of a "script F."

The second approximation of Reference 4 considers surfaces which have directionality and components of reflection which are diffuse and specular. The expression for the heat transfer to a surface within an enclosure under the assumptions of wavelength independent properties is:*

*This later restriction can be easily removed but is not pertinent to the ensuing discussion.

$$q_k = A_k\varepsilon_k\sigma T_k^{\ 4} - \sum_{j=1}^{M} A_k\alpha_{kj}F_{kj}\varepsilon_{jk}\sigma T_j^{\ 4}$$

$$- \sum_{j=1}^{M}\sum_{i=1}^{M} A_k\alpha_{kj}\rho_{ijk}\varepsilon_{ij}F_{kj}F_{ji}\sigma T_i^{\ 4} \qquad 4\text{-}26$$

$$- \pi \sum_{j=1}^{M}\sum_{i=1}^{M} A_k\alpha_{kj}\rho_{ijk}\rho_{ij}F_{kj}F_{ji}D_i$$

This can be written as:

$$q_k = A_k\bar{\varepsilon}_k\sigma T_k^{\ 4} - \sum_{i=1}^{M}\sum_{j=1}^{M} A_k\alpha_{ki}(\varepsilon_{ik}F_{ki} + \rho_{ijk}\varepsilon_{ij}F_{kj}F_{ji})\sigma T_i^{\ 4} \qquad 4\text{-}27$$

$$- \pi \sum_{i=1}^{M}\sum_{j=1}^{M} A_k\alpha_{kj}\rho_{ijk}\rho_{ij}F_{kj}F_{ji}D_i$$

In matrix notation this becomes:

$$\begin{bmatrix} q_1 \\ q_2 \\ \cdot \\ \cdot \\ \cdot \\ q_M \end{bmatrix} = \begin{bmatrix} \varepsilon_1\sigma T_1^{\ 4} \\ \varepsilon_2\sigma T_2^{\ 4} \\ \cdot \\ \cdot \\ \cdot \\ \varepsilon_M\sigma T_M^{\ 4} \end{bmatrix} + \begin{bmatrix} a_{11} & a_{12} & \cdots & a_{1M} \\ a_{21} & a_{22} & \cdots & a_{2M} \\ \cdot & \cdot & & \cdot \\ \cdot & \cdot & & \cdot \\ \cdot & \cdot & & \cdot \\ a_{M1} & a_{M2} & & a_{MM} \end{bmatrix} \begin{bmatrix} \sigma T_1^{\ 4} \\ \sigma T_2^{\ 4} \\ \cdot \\ \cdot \\ \cdot \\ \sigma T_M^{\ 4} \end{bmatrix}$$

$$- \begin{bmatrix} b_{11} & b_{12} & \cdots & b_{1M} \\ b_{21} & b_{22} & \cdots & b_{2M} \\ \cdot & \cdot & & \cdot \\ \cdot & \cdot & & \cdot \\ \cdot & \cdot & & \cdot \\ b_{M1} & b_{M2} & & b_{MM} \end{bmatrix} \begin{bmatrix} D_1 \\ D_2 \\ \cdot \\ \cdot \\ \cdot \\ D_M \end{bmatrix} \qquad 4\text{-}28$$

where

$$a_{xy} = -(A_x\alpha_{xy}\varepsilon_{yx}F_{xy} + \sum_{z=1}^{M} A_x\alpha_{xy}\rho_{yzx}\varepsilon_{yz}F_{xz}F_{zy}) \qquad 4\text{-}29$$

$$b_{xy} = -\sum_{z=1} A_x\pi\alpha_{xz}\rho_{yzx}F_{xz}F_{zy}\rho_{xz} \qquad 4\text{-}30$$

The quantity D_k is given by:

$$D_k = \frac{1}{\pi}\sum_{j=1}^{M} \varepsilon_{jk}\sigma T_j^{\,4}F_{kj} + \frac{1}{\pi}\sum_{j=1}^{M}\sum_{i=1}^{M} \rho_{ijk}\varepsilon_{ij}F_{kj}F_{ji}\sigma T_i^{\,4}$$

$$+ \sum_{j=1}^{M}\sum_{i=1}^{M} \rho_{ijk}\rho_{ij}F_{kj}F_{ji}D_i \qquad 4\text{-}31$$

In matrix notation, these equations can be written:

$$\begin{bmatrix} d_{11} & d_{12} & \cdot & \cdot & d_{1M} \\ d_{21} & d_{22} & \cdot & \cdot & \cdot \\ \cdot & & & & \cdot \\ \cdot & & & & \cdot \\ \cdot & & & & \cdot \\ d_{M1} & d_{M2} & \cdot & \cdot & d_{MM} \end{bmatrix} \begin{bmatrix} D_1 \\ D_2 \\ \cdot \\ \cdot \\ \cdot \\ D_M \end{bmatrix} = \begin{bmatrix} c_{11} & c_{12} & \cdot & \cdot & c_{1M} \\ c_{21} & c_{22} & \cdot & \cdot & c_{2M} \\ \cdot & & & & \cdot \\ \cdot & & & & \cdot \\ \cdot & & & & \cdot \\ c_{M1} & c_{M2} & \cdot & \cdot & c_{MM} \end{bmatrix} \begin{bmatrix} \sigma T_1^{\,4} \\ \sigma T_2^{\,4} \\ \cdot \\ \cdot \\ \cdot \\ \sigma T_M^{\,4} \end{bmatrix} \qquad 4\text{-}32$$

where

$$d_{xy} = \begin{cases} \sum_{z=1}^{M} \rho_{yzx}\rho_{yz}F_{xz}F_{zy} & (x \neq y) \qquad 4\text{-}33 \\ 1 - \sum_{z=1}^{M} \rho_{xzx}\rho_{xz}F_{xz}F_{zx} & (x = y) \end{cases}$$

$$c_{xy} = \frac{1}{\pi}\ \varepsilon_{yx}F_{xy} + \sum_{z=1}^{M} \rho_{yzx}\varepsilon_{yz}F_{xz}F_{zy} \qquad 4\text{-}34$$

If Equation 4-32 is now solved for the quantities D, we have

$$\{D\} = [d]^{-1}\ [c]\ \{\sigma T^4\} \qquad 4\text{-}35^*$$

*The notation [ ] has been introduced to denote a square matrix, e.g., the d or c matrix of Equation 4-32; the { } denotes a column matrix such as the D or σT^4 matrix of Equation 4-32; and $[\ ]^{-1}$ is the inverse of the indicated matrix

Solution of Equation 4-35 yields the various D_k's required in Equation 4-28. Equation 4-28 can then be expressed as:

$$\{q\} = \{\varepsilon\sigma T^4\} + [a]\{\sigma T^4\} + [b]\{D\} \qquad 4\text{-}36$$

A directional diffuse-specular "script F" can be obtained with Equations 4-35 and 4-36. Using Hottel's concept of a "script F," i.e., set all temperatures except one within the enclosure equal to zero and the remaining one equal to unity (say surface k), the heat flows (q) are then q_{kj}. With this condition:

$$\{q_{kj}\} = \{\overset{o}{\varepsilon}_k\} + \{a_{jk}\} + [b]\{D_{jk}\} \qquad 4\text{-}37^*$$

and

$$\{D_{kj}\} = [d]^{-1}\{c_{jk}\} \qquad 4\text{-}38^*$$

The solution then proceeds as follows:

(1) An index k is selected and the pertinent coefficients c_{kj} selected.

(2) D_{jk} is computed for all j by Equation 4-38.

(3) The values of a_{jk} are selected and the values of q_{kj} for all j are computed with Equation 4-37.

(4) $\mathfrak{F}_{kj}$ is then computed with the definition:

$$\mathfrak{F}_{jk} = \frac{q_{kj}}{A_j} \qquad 4\text{-}39$$

(5) The next value of k is selected, and the calculation continues until all M surfaces have been computed. The reciprocity relationship $A_j\mathfrak{F}_{jk} = A_k\mathfrak{F}_{kj}$ is used to reduce the number of computations.

(6) $\mathfrak{F}_{jk}$ is used in the same manner as with Hottel's method and the solution of Equation 4-2 or 4-8.

$$^*\ \{q_{kj}\} = \begin{bmatrix} q_{k1} \\ q_{k2} \\ \cdot \\ \cdot \\ \cdot \\ q_{kM} \end{bmatrix} ; \quad \{\overset{o}{\varepsilon}_k\} = \begin{bmatrix} 0 \\ 0 \\ \cdot \\ \cdot \\ \varepsilon_k \\ \cdot \\ 0 \end{bmatrix} ; \quad \{a_{jk}\} = \begin{bmatrix} a_{1k} \\ a_{2k} \\ \cdot \\ \cdot \\ \cdot \\ a_{Mk} \end{bmatrix} ; \quad \{c_{jk}\} = \begin{bmatrix} c_{1k} \\ c_{2k} \\ \cdot \\ \cdot \\ \cdot \\ c_{Mk} \end{bmatrix}$$

The equations presented in this section may appear to be more complicated and hence, more difficult than with the diffuse property assumption. Mathematically, this is not the case. The computations are more time consuming and require added computer time and storage space. This is only the penalty paid for more exact computations.

5. COMPUTER PROGRAM FOR DIRECTIONAL SPECULAR-DIFFUSE METHOD

The procedural steps required to calculate a "script F" ($\mathfrak{F}$) from the equations for the directional specular-diffuse analysis have been described in Section 4.2 This method has been programmed for an IBM 7094 as a program separate from any general program for thermal analysis. The technical basis for selecting the $\mathfrak{F}$ procedure rather than the network approach have been discussed in the first portion of Section 4. For the reasons given there, most computer programs for thermal analysis have been written in terms of $\mathfrak{F}$. Thus, the existing analysis programs could incorporate a directional specular-diffuse $\mathfrak{F}$ as an input quantity with a minimum of alteration. Furthermore, the direction specular-diffuse $\mathfrak{F}$ requires a much larger working computer storage than a diffuse $\mathfrak{F}$. If an attempt was made to assemble a single $\mathfrak{F}$ and analysis program, the number of surfaces would have been seriously limited. It is for these technical and practical reasons that the $\mathfrak{F}$ calculation was programmed as a separate entity. The flow chart of the program is shown in Figure 8 and a complete printout in Appendix III. The symbols used are those of Section 4.2.

5.1 REQUIRED INPUT DATA

The physical factors which are required for the directional specular-diffuse $\mathfrak{F}$ are:

(a) the areas of the surfaces involved (A_i, $i = 1, 2, 3 \ldots$)

(b) the number of surfaces used to subdivide the enclosure (N; $N \leq 20$)

(c) the directional reflectance of surface i in the direction of surface j (ρ_{ij} of Reference 4; designated RHØ in machine language)

(d) the geometrical bidirectional reflectance of surface j for radiation from surface i which is reflected to surface k by surface j (ρ_{ijk} of Reference 4; designated R_{ijk} in machine language)

(e) the geometrical diffuse shape factors between surfaces (F_{ij})

The only quantities which are not used in conventional diffuse $\mathfrak{F}$ analysis are ρ_{ij} (RHØ) and ρ_{ijk} (R_{ijk}). The use of the usual diffuse shape factors (F_{ij}) is made possible by assigning the deviations from diffuseness to the reflectances. This is described in greater detail in Reference 4 and leads to the concept of geometrical reflectances, i.e., a property which is weighted by the geometry and nondiffuseness of the surface. The directional emittance of a surface is incorporated in the program as: $1 - \rho_{ij}$. This introduces the gray radiation assumption, i.e., properties independent of wavelength. If desired, either a band energy or monochromatic analysis could be performed (see Reference 4).

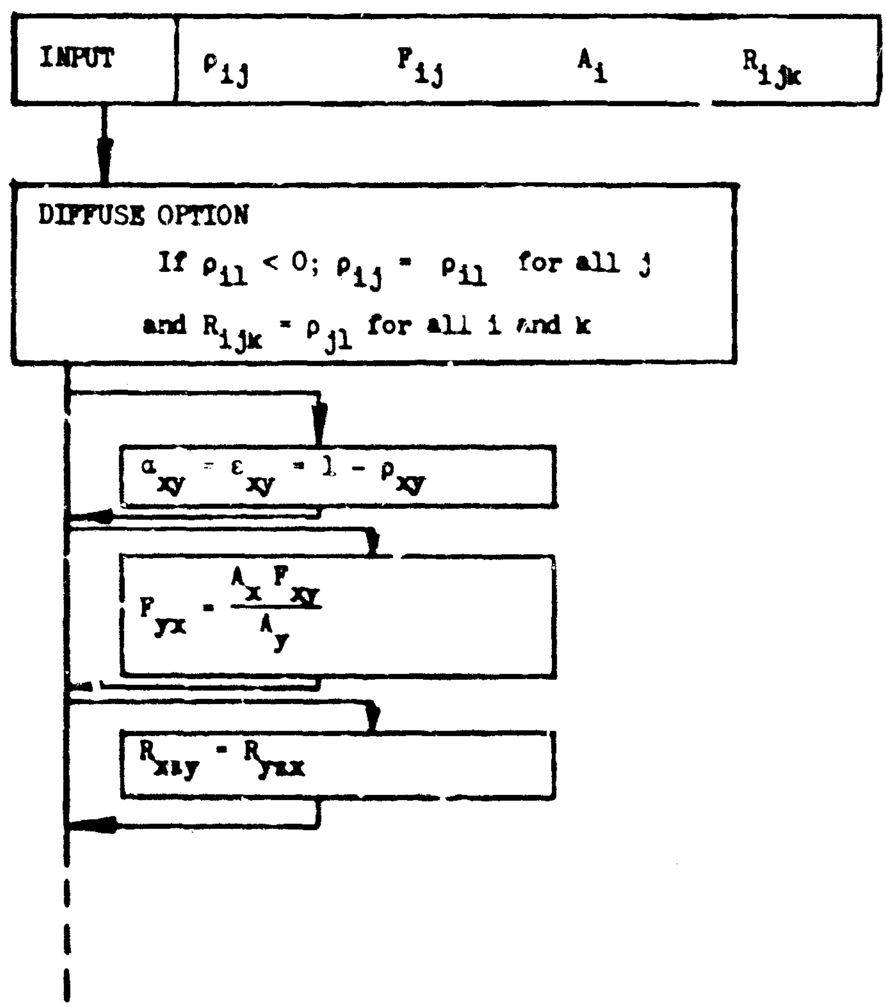

Continued on next page.

Figure 8. Computer Program Flow Chart

$$a_{xy} = -\alpha_{xy}\epsilon_{yx}F_{xy} - \sum_{z=1}^{M} \alpha_{xz}R_{yzx}\epsilon_{yz}F_{xz}F_{zy}$$

A

$$b_{xy} = -\sum_{z=1}^{M} \alpha_{xz}R_{yzx}\rho_{yz}F_{xz}F_{zy}$$

B

$$C_{xy} = \epsilon_{yx}F_{xy} + \sum_{z=1}^{M} R_{yzx}\epsilon_{yz}F_{xz}F_{zy}$$

C

$$d_{xy} = \begin{cases} (y \neq x) = -\sum_{z=1}^{M} R_{yzx}\rho_{yz}F_{xz}F_{zx} \\ (y = x) = 1 - \sum_{z=1}^{M} R_{xzx}\rho_{xz}F_{xz}F_{zx} \end{cases}$$

D

Figure 8. Computer Program Flow Chart (Cont.)

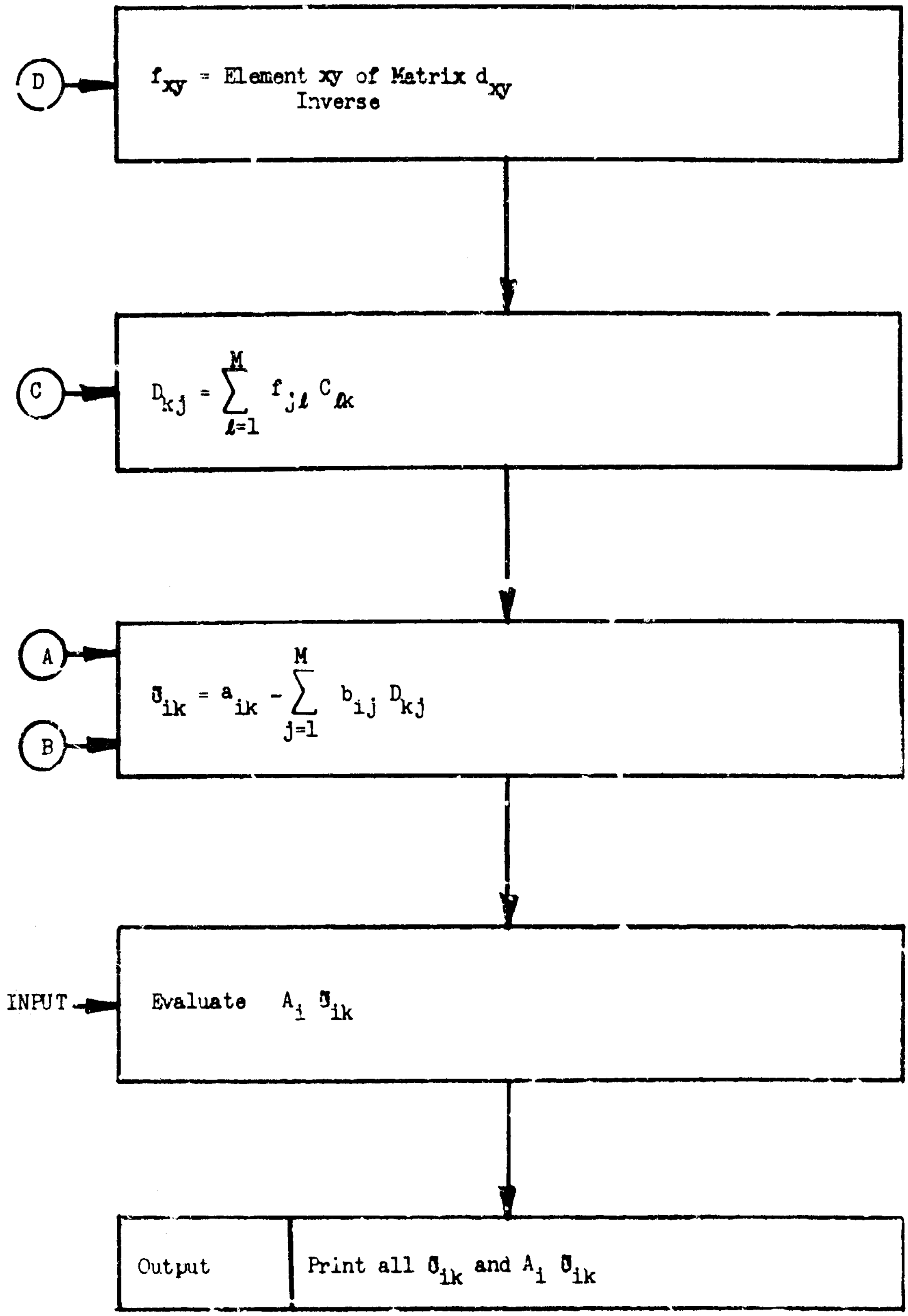

Figure 8. Computer Program Flow Chart (Cont.)

Values of ρ_{ij} and ρ_{ijk} (RHØ and R_{ijk}) can be approximated with data obtained in many Thermophysics Laboratories (4). The methods suggested for this approximation will be illustrated in Section 5.3 and 6.2

5.2 INPUT PROCEDURE

The input format is shown in Figure 9. The quantities indicated are as follows:

N = the number of surfaces within the enclosure to be examined. The present program is storage limited to a maximum of 20 surfaces.

CLR = a flag directing the program to clear itself of input information (CLR = 1), prior to proceeding to the next case, or instructing the program to retain input information (CLR = 0) for the following case. When CLR is set to zero, only those quantities that vary from case to case need be entered, all other information will be retained.

L = a flag used in the column labeled "PRE" of the load sheet. The quantity L is used in conjunction with CLR = 0. An input matrix is not cleared of information if the quantity L is inserted in the column labeled "PRE."

M = a flag used in the column labeled "PRE" of the load sheet. It instructs the program to clear the input matrix of information prior to storing data.

ρ_{ij} = RHØ = the directional reflectivity of surface i in the direction of surface j. For program convenience, ρ_{ii} is set equal to the negative value of the hemispherical reflectance for a diffuse surface.

F_{ij} = F = the shape factor of surface j as viewed by surface i. Only the lower triangular half of the shape factor matrix need be entered; that is: F_{11}, F_{21}, F_{22}, F_{31}, F_{32}, F_{33}, . . . F_{mn}.

R_{ijk} = Geometrical bidirectional reflectance of surface j for incident energy from surface i and reflected to surface k. Bidirectional reflectivities are inputed in block form as indicated by the sample load sheet. The block number corresponds to the third subscript k, and the other two subscripts are contained within the k'th block. Only the upper triangular portion of the three dimensional R_{ijk} matrix need be entered. That is, R_{1j1} for j = 1 to n is entered for the first matrix, K = 1; R_{1j2} R_{2j2}, for j = 1 to n is entered for the second matrix, K = 2; R_{1j3}, R_{2j3}, R_{3j3} for j = 1 to n is entered for the third matrix, K = 3; and so on until the full matrix is entered for K = n.

A_i = A = surface area of node i.

DATE ____________ PAGE ____ OF ____

NAME ____________ PRIORITY ____________

PROBLEM NO. ____________ KEYPUNCHED BY ____________

NO. OF CARDS ____________ VERIFIED BY ____________

1	7	73
H1	HEADERS - LIMITED TO 66 LINES EACH - USED	
H2	AS RUN DESCRIPTION ONLY	

X1

SYMBOL	PRE	LOC.	VALUE	EXP.
		N		
		CLR		
	M	RHØ	20, 20	
		01, 01		
		.		
		.		
		.		
		.		
		.		
	M	F	20, 20	
		01, 01		
		.		
		.		
		.		
		.		
	M	R1	20, 20	
		.		
		.		
		.		
	M	R2	20, 20	
		.		
		.		
		.		
	M	R3	20, 20	
		.		
		.		
	M	RN	20, 20	
		.		
		.		
		.		
		.		

SYMBOL	PRE	LOC.	VALUE	EXP.
		AREA		
		1		
		2		
		3		
		.		
		.		
		.		
		.		
		N		
	E	ND		

X1

Figure 9. Program Input Format

An unlimited number of cases may be "stacked"; all that is required to run several cases together is an END card between cases. Output quantities $\mathfrak{F}$ and $\mathfrak{F}$-area products, are printed out in matrix form.*

The following is a very simple problem which illustrates the input loading. Consider two infinite diffuse strips of unit width and separation, as shown below:

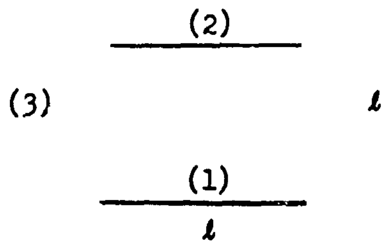

surface (1) and (2)

surface (3) is space

$\rho_1 = \rho_2 = 0.9;\ \rho_3 = 0$

Input information:

(a) $\rho_{12} = \rho_{13} = \rho_{21} = \rho_{23} = 0.9$

$\rho_{31} = \rho_{32} = \rho_{33} = 0$

(b) $F_{12} = F_{21} = F_{33} = 0.414214$

$F_{13} = F_{23} = 0.585786$

(c) $R_{213} = R_{312} = R_{313} = R_{212} = \rho_1 = 0.9$

$R_{123} = R_{321} = R_{323} = R_{121} = \rho_2 = 0.9$

(d) $A_1 = A_2 = 1.0,\ A_3 = 2.0$

The load sheet for the above problem with diffuse surfaces can be found in Figure 10. The result of this computation is 0.0933965, which can be compared to the value given by Reference 9 of 0.09340.

It should be noted that in addition to comparing very favorably with the $\mathfrak{F}$ matrix evaluated by hand, using Hottel's techniques, the following holds

$$\bar{e}_k = \sum_{j=1}^{M} \mathfrak{F}_{kj} = \text{hemispherical emittance}$$

as it should.

*It should be noted that all quantities should be left justified within their respective fields.

DATE
NAME
PROBLEM NO.
NO. OF CARDS

PAGE OF
PRIORITY
KEYPUNCHED BY
VERIFIED BY

H1	SAMPLE PROBLEM TWO PARALLEL INFINITE
H2	DIFFUSE STRIPS OF UNIT WIDTH AND SEPARATION

X1

SYMBOL	PR	LOC.	VALUE	EXP.
		N	3	
		CLR	1	
	M	RHØ	20, 20	
		01, 01	-0.9	
		02, 01	-0.9	
		03, 01	-0.0	
	M	F	20, 20	
		02, 01	0.414214	
		03, 01	0.292893	
		03, 02	0.292893	
		03, 03	0.414214	
		AREA		
		1	1.0	
		2	1.0	
		3	2.0	
	E	ND		

X1

Figure 10. Load Sheet for Two Parallel Infinite Diffuse Strips of Unit Width and Separation

5.3 EXAMPLES OF INPUT FOR DIFFUSE, SPECULAR, AND SPECULAR-DIFFUSE

The following problem has been selected to illustrate the input required for the three cases of diffuse, specular and directional specular-diffuse. The 3 computer program given here can treat these cases by manipulation of the quantity $R_{j\,jk}$ $(\rho_{i\,jk})$. As discussed in Reference 4, this factor is approximated by:

$$\rho_{ijk} = (\rho_D)_j + (\rho_S)_j \left\{\frac{F_{ik(j)}}{F_{kj}\ F_{ji}}\right\} \qquad 5\text{-}1$$

If the perfectly diffuse assumption is to be made, the specular reflectance of surface j (ρ_s) is set equal to zero; if the perfectly specular assumption is made, the diffuse reflectance (ρ_D) is set equal to zero. The configuration to be used to illustrate the input is shown below:

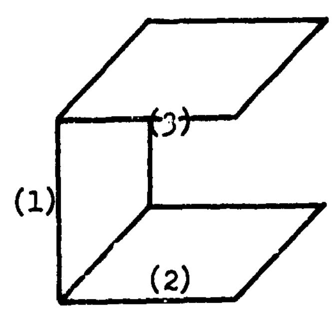

Surface 1: $\rho_1 = 0.973$ (vacuum deposited aluminum)
Surface 2 and 3: $\rho_2 = \rho_3 = 0.116$ (3M black paint)
Surface 4: $\rho_4 = 0$ (surrounding space)

$F_{12} = F_{21} = F_{31} = F_{32} = F_{41} = F_{43} = 0.2$

$F_{44} = 0.4$

$A_1 = A_2 = A_3 = 1$

$A_4 = 3$

The diffuse assumption input sheet is shown in Figure 11.

DATE
NAME
PROBLEM NO.
NO. OF CARDS

PAGE OF
PRIORITY
KEYPUNCHED BY
VERIFIED BY

1	7
H1	SAMPLE PROBLFM
H2	DIFFUSE ASSUMPTION

SYMBOL	PRE	LOC.	VALUE	EXP.
		N	4	
		CLR	1	
	M	RHØ	20, 20	
		01, 01	-0.973	
		02, 01	-0.116	
		03, 01	-0.116	
		04, 01	-0.0	
	M	F	20,20	
		01, 02	0.2	
		02, 01	0.2	
		03, 01	0.2	
		03, 02	0.2	
		04, 01	0.2	
		04, 02	0.2	
		04, 03	0.2	
		04, 04	0.4	
		AREA		
		1	1.0	
		2	1.0	
		3	1.0	
		4	3.0	
	E	ND		

Figure 11. Load Sheet for Sample Problem; Diffuse Assumption

The specular assumption utilizes the same data as above, but the reflection is assumed to be perfectly specular. For this condition,

$$R_{213} = \rho_{12} \left\{ \frac{F_{23(1)}}{F_{21}F_{13}} \right\}$$

$$= 2.0897$$

The quantity R_{412} is obtained by noting for R_{ijk}

$$\rho_{jk} = \sum_{i=1}^{n} R_{ijk} F_{ji} \qquad 5\text{-}2$$

i.e., conservation of energy. Thus,

$$R_{412} = \frac{\rho_{12} - R_{312}F_{13}}{F_{14}} = 0.9323$$

Use is made of reciprocity to find $R_{312} = R_{213}$, $R_{214} = R_{412}$, and $R_{412} = R_{413}$. The load sheet for this problem is shown in Figure 12.

The directional specular-diffuse procedure requires a knowledge of the directional properties of the surfaces. The greatest angle subtended by surface 3 as viewed from surface 2 is less than 55 degrees. For the black surface, the directional reflectance and hence directional emittance is very nearly equal to the near normal value. Therefore, the near normal value was used for ρ_{23} and ρ_{32}. To obtain ρ_{21}, a heat balance was used, i.e., for the general case of surface i

$$(\rho_H)_i = \frac{1}{A_i} \sum_{j=1}^{n} \rho_{ij} A_i F_{ij} \qquad 5\text{-}3$$

where

$(\rho_H)_i$ = hemispherical reflectance of surface i.

The value of ρ_{21} was obtained from:

$$\rho_{21} = \frac{(\rho_H)_2 - F_{23}\rho_{23}}{4\, F_{21}}$$

or

$$\rho_{21} = 0.1275$$

DATE ______ PAGE ___ OF ___

NAME ______ PRIORITY ______

PROBLEM NO. ______ KEYPUNCHED BY ______

NO. OF CARDS ______ VERIFIED BY ______

1	7
H1	SAMPLE PROBLEM
H2	SPECULAR ASSUMPTION

SYMBOL	PR	LOC.	VALUE	EXP.
		N	4	
		CLR	1	
	M	RHØ	20, 20	
		01, 02	0.9733	
		01, 03	0.9733	
		01, 04	0.9733	
		02, 01	-0.116	
		03, 01	-0.116	
		04, 01	-0.[illegible]	
	M	F	20, 20	
		01, 02	0.2	
		02, 01	0.2	
		03, 01	0.2	
		03, 02	0.2	
		04, 01	0.2	
		04, 02	0.2	
		04, 03	0.2	
		04, 04	0.4	
		AREA		
		1	1.0	
		2	1.0	
		3	1.0	
		4	3.0	
	M	R1	20, 20	
		01, 02	0.116	
		01, 03	0.116	
	M	R2	20, 20	
		01, 03	0.116	
		02, 03	0.116	

SYMBOL	PR	LOC.	VALUE	EXP.
	M	R3	20, 20	
		01, 02	0.116	
		02, 01	2.0897	
		03, 02	0.116	
	M	R4	20, 20	
		01, 02	0.116	
		01, 03	0.116	
		02, 01	0.9323	
		02, 03	0.116	
		03, 01	0.9323	
		03, 02	1.0025	
		04, 02	0.116	
		04, 03	0.116	
	END			

STL FORM 1003 REV. 10/63

Figure 12. Load Sheet for Sample Problem; Specular Assumption

Reciprocity was utilized to obtain $\rho_{21} = \rho_{12}$, $\rho_{31} = \rho_{13}$, etc. Using the procedure described for ρ_{21}, the values of the other geometrical reflectances were:

$$\rho_{12} = \rho_{13} = 0.9716$$

$$\rho_{14} = 0.9744$$

$$\rho_{23} = \rho_{32} = 0.07$$

The load sheet for this problem is shown in Figure 13.
The computer results for the above configuration will be found in Section 6.

DATE ______ PAGE

NAME ______ PRIORITY

PROBLEM NO. ______ KEYPUNCHED BY

NO. OF CARDS ______ VERIFIED BY

1	7	73
H1	SAMPLE PROBLEM	
H2	DIRECTIONAL SPECULAR-DIFFUSE ASSUMPTION	

SYMBOL	P/R/E	LOC.	VALUE	EXP.
		N	4	
		CLR	1	
	M	RHØ	20, 20	
		01, 02	0.9716	
		01, 03	0.9716	
		01, 04	0.9744	
		02, 01	0.1275	
		02, 03	0.07	
		02, 04	0.1275	
		03, 01	0.1275	
		03, 02	0.07	
		03, 04	0.1275	
	M	F	20, 20	
		01, 02	0.2	
		02, 01	0.2	
		03, 01	0.2	
		03, 02	0.2	
		04, 01	0.2	
		04, 02	0.2	
		04, 03	0.2	
		04, 04	0.4	
		AREA		
		1	1.0	
		2	1.0	
		3	1.0	
		4	3.0	
	M	R1	20, 20	
		01, 02	0.07	
		01, 03	0.07	

SYMBOL	P/R/E	LOC.	VALUE	EXP.
	M	R2	20, 20	
		01, 03	0.07	
		02, 03	0.07	
	M	R3	20, 20	
		01, 02	0.07	
		02, 01	2.086	
		03, 02	0.07	
	M	R4	20, 20	
		01, 02	0.1658	
		01, 03	0.1658	
		02, 01	0.924	
		02, 03	0.07	
		03, 01	0.924	
		03, 02	0.07	
		04, 01	1.008	
		04, 02	0.1338	
		04, 03	0.1338	
	END			

Figure 13. Load Sheet for Sample Problem, Directional Specular-Diffuse Assumption

6. EXPERIMENTAL COMPARISON OF SPECULAR, DIFFUSE AND DIRECTIONAL SPECULAR-DIFFUSE ANALYSES

The purpose of this task was to obtain an experimental evaluation of the different analytical methods. Such a comparison must utilize an experimental system that is simple conceptually and physically. Otherwise the effects of geometry, conduction, convections, extraneous heat losses, etc., will not be controlled. The experimental configurations chosen are shown in Figure 14. A test consisted of placing the experiment within a cold wall vacuum chamber (to eliminate convection), insulating the non-radiative surfaces, supplying a known quantity of power to one of the surfaces and measuring the equilibrium temperatures of the other surface(s). The experimental results were then compared to the predicted values using the directional specular-diffuse analysis (4), the specular property assumption and the diffuse property assumption.

The following discussion will be divided into three parts: (1) the experimental test method, (2) the analytical results, and (3) a discussion of the comparison of experiment and analysis.

6.1 EXPERIMENTAL METHOD AND PROCEDURE

The configuration selected for test are shown in Figure 14. The test surfaces were six such squares of 1100 aluminum 0.0625 inch thick. In each case the lower surface was selected as the heat source and the remaining surface(s) allowed to reach an equilibrium condition with the environment. The heated surface had a heater of approximately 200 ohms cemented to its underside (the non-radiative side). This heater consisted of 40 gage constantan wire sandwiched between two sheets of 1 mil Mylar. Voltage leads were attached at the heater boundary and the four terminal resistance method used (see Section 3.1) to calculate power dissipation. The electrical measuring circuit was the same as shown in Figure 6 of Section 3 with a Leeds and Northrup 8686 substituted for the Type K 3.

Originally, the back of each surface was insulated with 20 layers of super insulation. However, the edge heat leak was found to be too large relative to the heat absorbed by the unheated surfaces. A guard heat system was found to be necessary. This was obtained by placing a heated plate on the outside of the insulation and adjusting the dissipation until the temperature difference across the insulation was zero, i.e., no heat flow through the insulation. The edges of the insulation, guard heater, and test surface were covered with 1/4 mil thick aluminized Mylar, aluminum side out. These steps reduced the edge and back heat "leak," i.e., uncontrolled loss, to approximately 1 Btu/hr for a test surface temperature of 70°F. This was satisfactory for all test surfaces except the surface coated with vacuum deposited aluminum. The radiative heat loss or gain from such a surface was the same order of magnitude as the edge loss. Hence, this test surface had to be used as a passive surface, i.e., a reflector, and no heat balance could be performed for it.

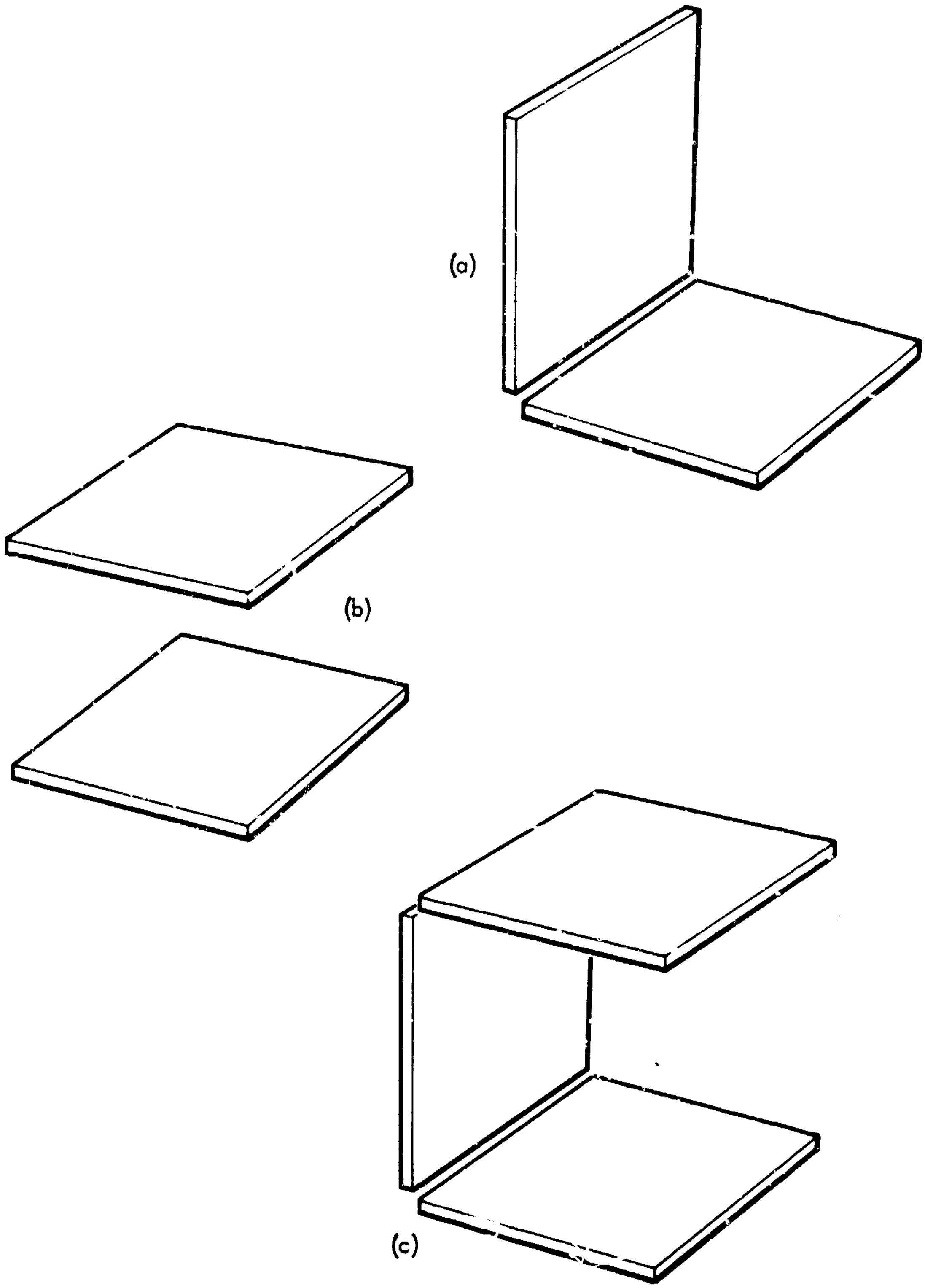

Figure 14. Configuration Used for Test of Radiation Analysis

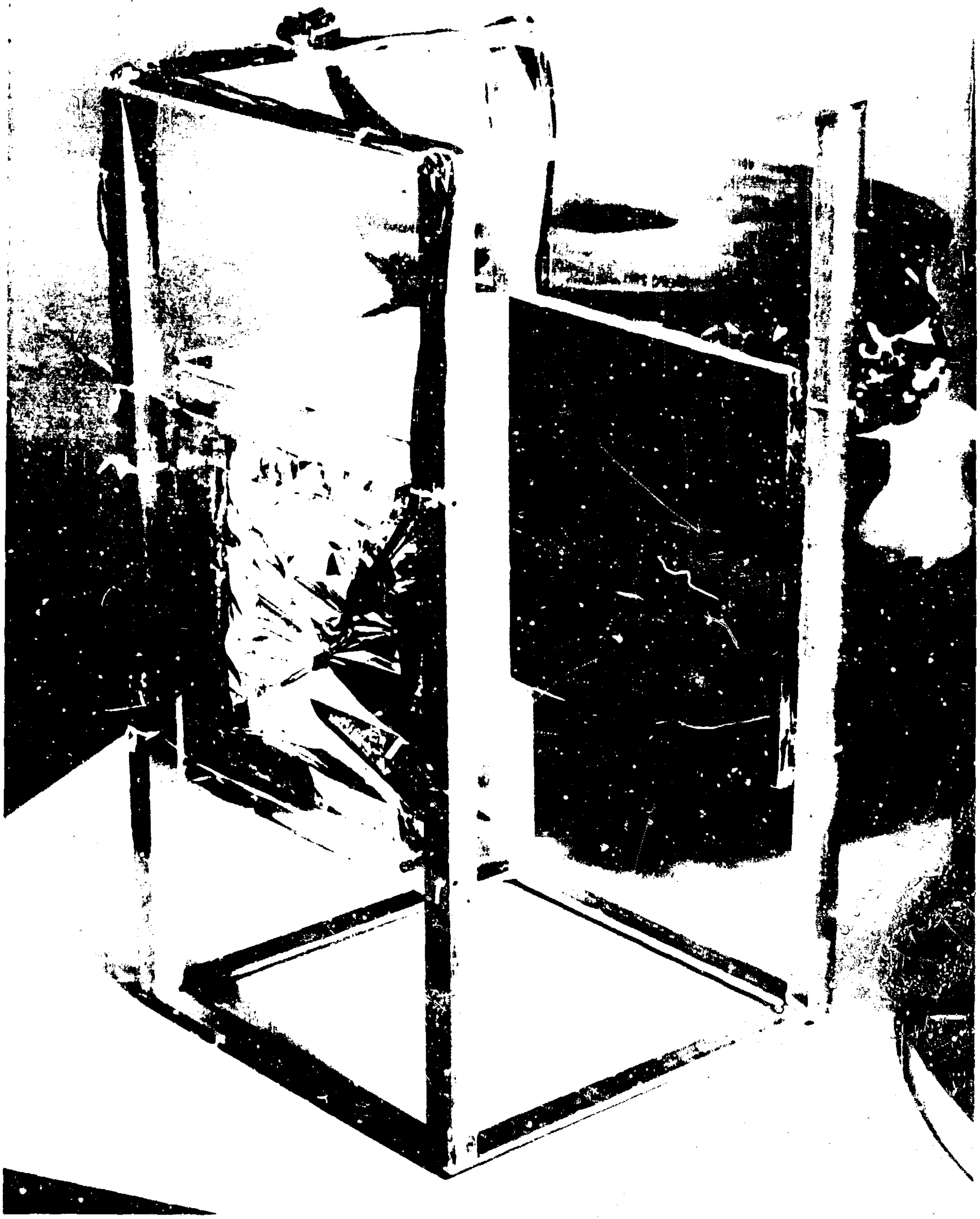

Figure 15. Test Configuration in Test Fixture

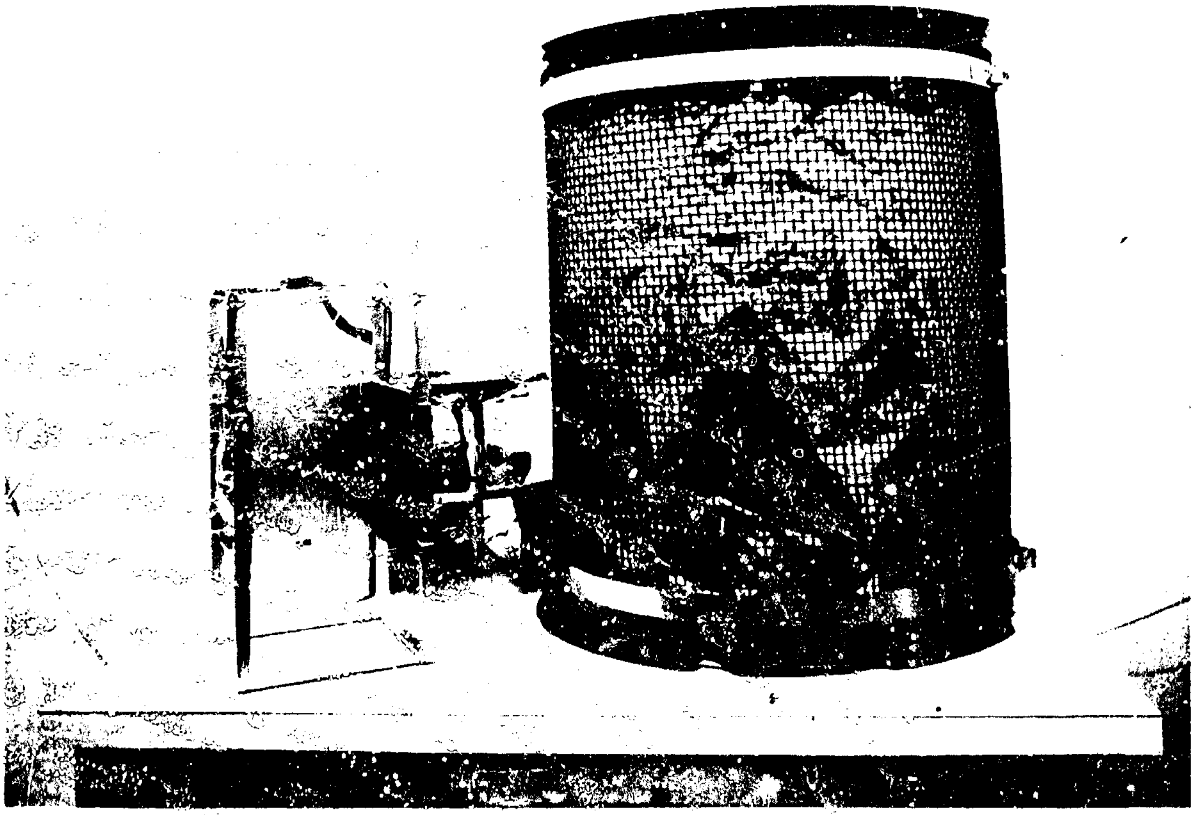

Figure 16. Test Configuration Ready for Testing

Each test surface was supported within a framework by dacron cords attached to phenolic stand-off attachments. In this manner the test surfaces were isolated from the framework but properly positioned and restrained (see Figure 15). This framework was mounted within a LN_2 cooled baffled and the assembly placed within a vacuum system. A pressure of 10^{-5} torr or lower was obtained during the testing. The system is illustrated in Figure 16.

Thermocouples were placed on at least two points of each test surface; one at the center of the surface and one within one-half inch of the edge. No significant gradient across the test surface was observed in any of the tests; i.e., the surfaces were essentially isothermal. The thermocouple material was copper-constantan. All thermocouples were taken from the same roll. The voltages generated by the thermocouples were measured with a Leeds and Northrup Type 8686 potentiometer using a conventional ice junction compensation system.

The test procedure consisted of the following steps:

(1) setting the predicted power dissipation for the source surface
(2) setting estimated guard heat dissipation(s) for the receiving surface(s)
(3) observing the temperature of the receiver surface(s) and adjusting the guard power dissipation(s)
(4) when the receiver surface(s) and guard heater(s) indicated a negligible temperature difference for thirty minutes, at least two sets of data were recorded within the next thirty minutes.

The latter step insured that the surfaces were in equilibrium for approximately one hour. The accuracy of the measurements are estimated to be:

Temperature difference	$\pm$ 0.1°F
Temperature	1°F
Total power dissipated by the heat source	1.5%

A complete summary of the experimental data is given in Appendix III.

6.2 ANALYTICAL PREDICTION

The radiative heat flow from the source surface and the temperature of the receiver surface were predicted by the analytical methods based upon the three different property assumptions: diffuse (1,2,3), specular (7), and the directional specular-diffuse (4). The prediction served to test the utility and practicality of the computer program developed for this study (Section 5) as well as provide a basis of comparison between theory and experiment.

The test configurations have been described in Section 6.1 and illustrated in Figure 14. These three configurations were combined with different surface coatings to give six different test systems. These systems are schematically represented in Figure 17. The directional

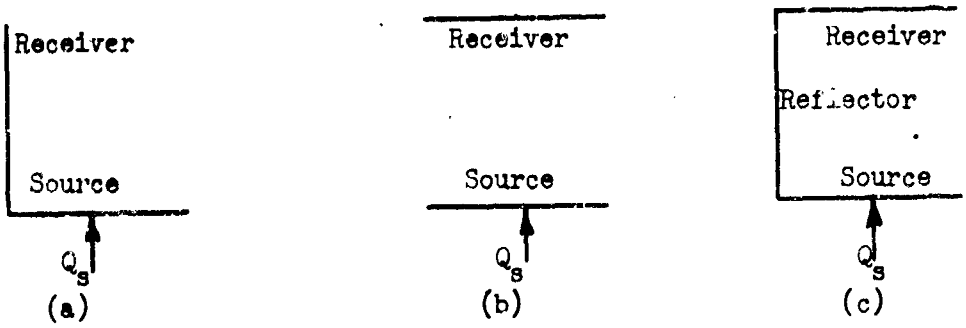

Test	Surface Coatings			
	Source	Receiver	Reflector	Configuration
1.	"3M" Flat Black Paint	"3M" Flat Black Paint		(a)
2.	"3M" Flat Black Paint	"3M" Flat Black Paint		(b)
3.	"3M" Flat Black Paint	"3M" Flat Black Paint	Vacuum Deposited Aluminum	(c)
4.	"3M" Flat Black Paint	"3M" Flat Black Paint	Rinshed-Mason Leafing Aluminum Paint	(c)
5.	"3M" Flat Black Paint	Rinshed-Mason Leafing Aluminum Paint	Vacuum Deposited Aluminum	(c)
6.	"3M" Flat Black Paint	Rinshed-Mason Leafing Aluminum Paint	Anodized Aluminum	(c)

NOTE: The coating material descriptions are described in detail in Figures 18 through 21.

Figure 17. Experimental Matrix for Test of Radiation Analysis

reflectances of these coatings for a black body source at 540°R are shown in Figures 18 through 21. Included in these figures is the specular reflectance for the same radiation source. The specular reflectances were measured with a goniometric reflectometer shown in Figure 22. The directional reflectances were measured with a heated cavity reflectometer similar to that described in Reference 11.

The method of determining the various quantities and establishing the input for the computer program has been described in Section 5.3. The results of the computer calculations are shown in Table 7.

6.3 COMPARISON OF EXPERIMENTAL AND ANALYTICAL RESULTS

An examination of the results presented in Table 7 will quickly show one consistent fact: In every case, the experimentally measured temperature exceeded the value predicted by any of the analytical methods. A hasty conclusion would be that the experiments were in error in some manner. After re-examining the experimental technique for major errors, nothing sufficiently significant could be found. Conversely, many questions can be raised relative to the analytical predictions. The following discussion will be concerned with the errors of prediction. However, the possibility of an unrealized source of error in the experiments is not ruled out.

The difficulties with the predictions are believed to be centered about the thermal radiation properties used. The analyses are based upon the gray radiation assumption, i.e., wavelength independent properties. The source surface was operated at approximately 585°R whereas the receiver surfaces ranged between 340 and 415°R, i.e., a difference of 170 to 245°F. All properties used in the analysis assumed a material and source temperature of 585°R for emittance and reflectance. This "non-gray" error would be particularly noticeable with anodized aluminum and aluminum paint surfaces. To correct for this, the analyses would have to be performed on at least the band energy basis (4).

A second error was in the measurement of the properties. The heated cavity reflectometer is known to have an error due to sample heating (11). This error could be of the order of .02-.04 in directional reflectance (or emittance) and would affect the predicted temperatures slightly. It would have a more direct effect upon the predicted heat loss by the source surface. In only one case (Test 5), was the measured heat loss lower than predicted. In this instance, it was within experimental accuracy for the nearest prediction. The predicted temperatures and heat fluxes are too interrelated to separate them except as a first approximation. Thus, no firm conclusion can be drawn from this one case. However, the problem of sample emission is not considered to have been a major source of the discrepancies as judged from the spectral data.

Polarization of the energy with the monochromator of the heated cavity can also cause an error. For very highly reflective materials, e.g., vacuum deposited aluminum, or smooth dielectrics, polarization may cause an error as large as 10 to 20 percent in the reflectance at high angles.

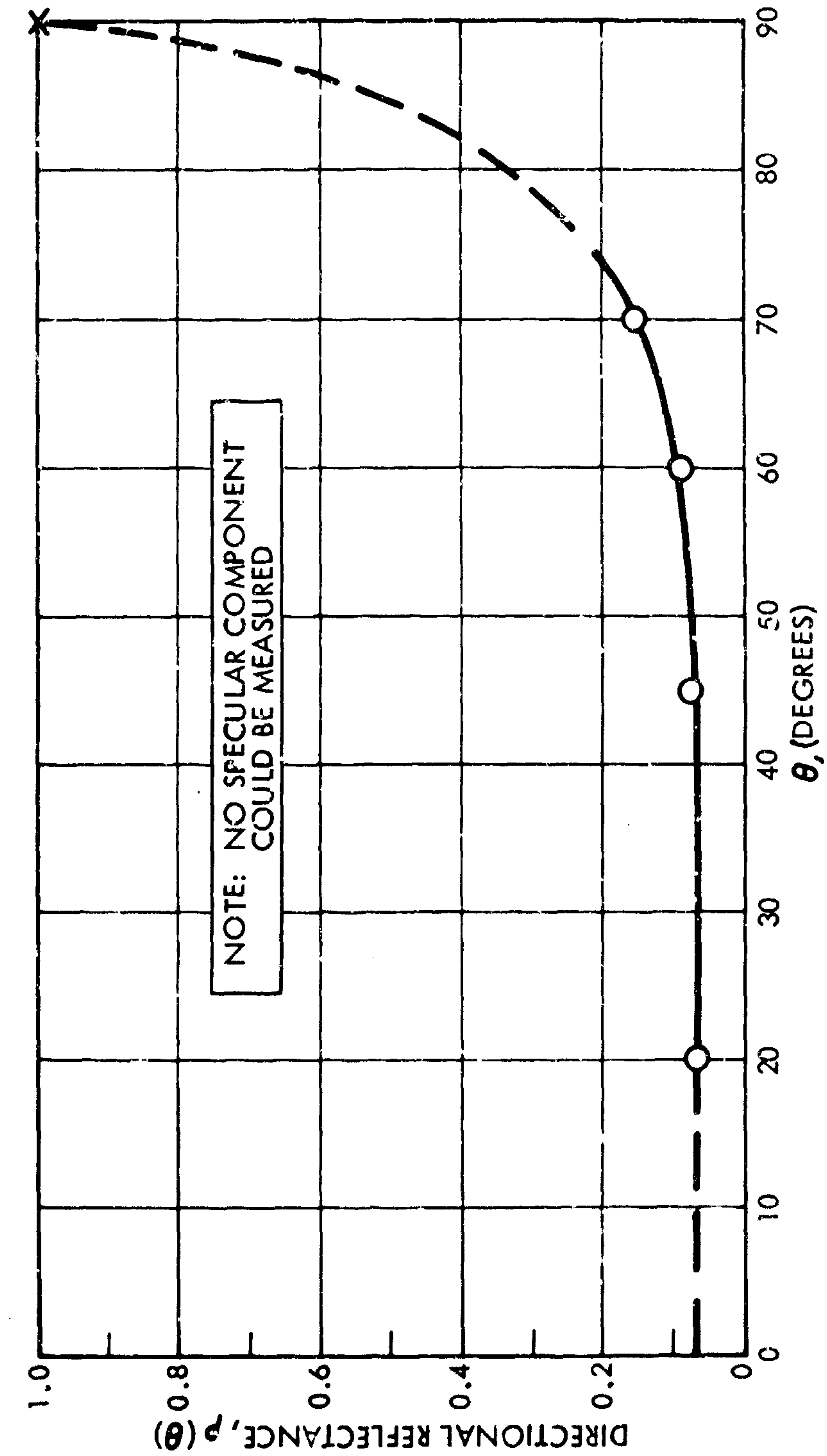

Figure 18. Directional Reflectance of 3M Flat Black Paint to a $540^{\circ}R$ Black Body as a Function of Angle

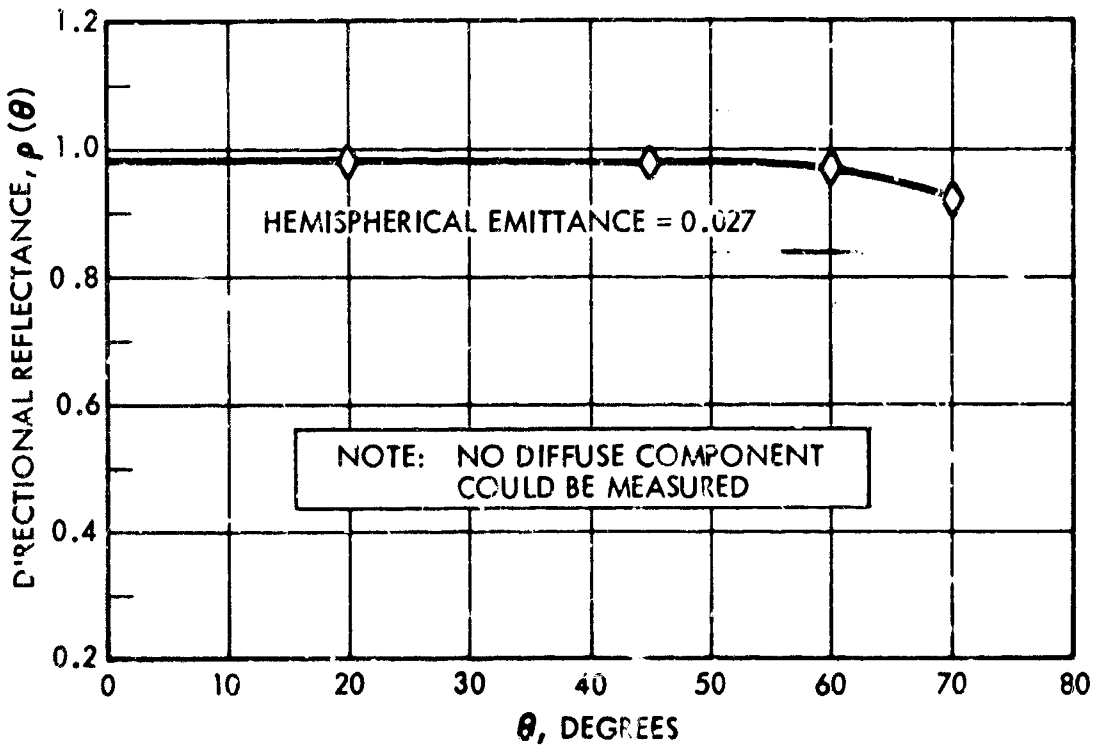

Figure 19. Directional Reflectance of Vacuum Deposited Aluminum to a 540°R Black Body as a Function of Angle

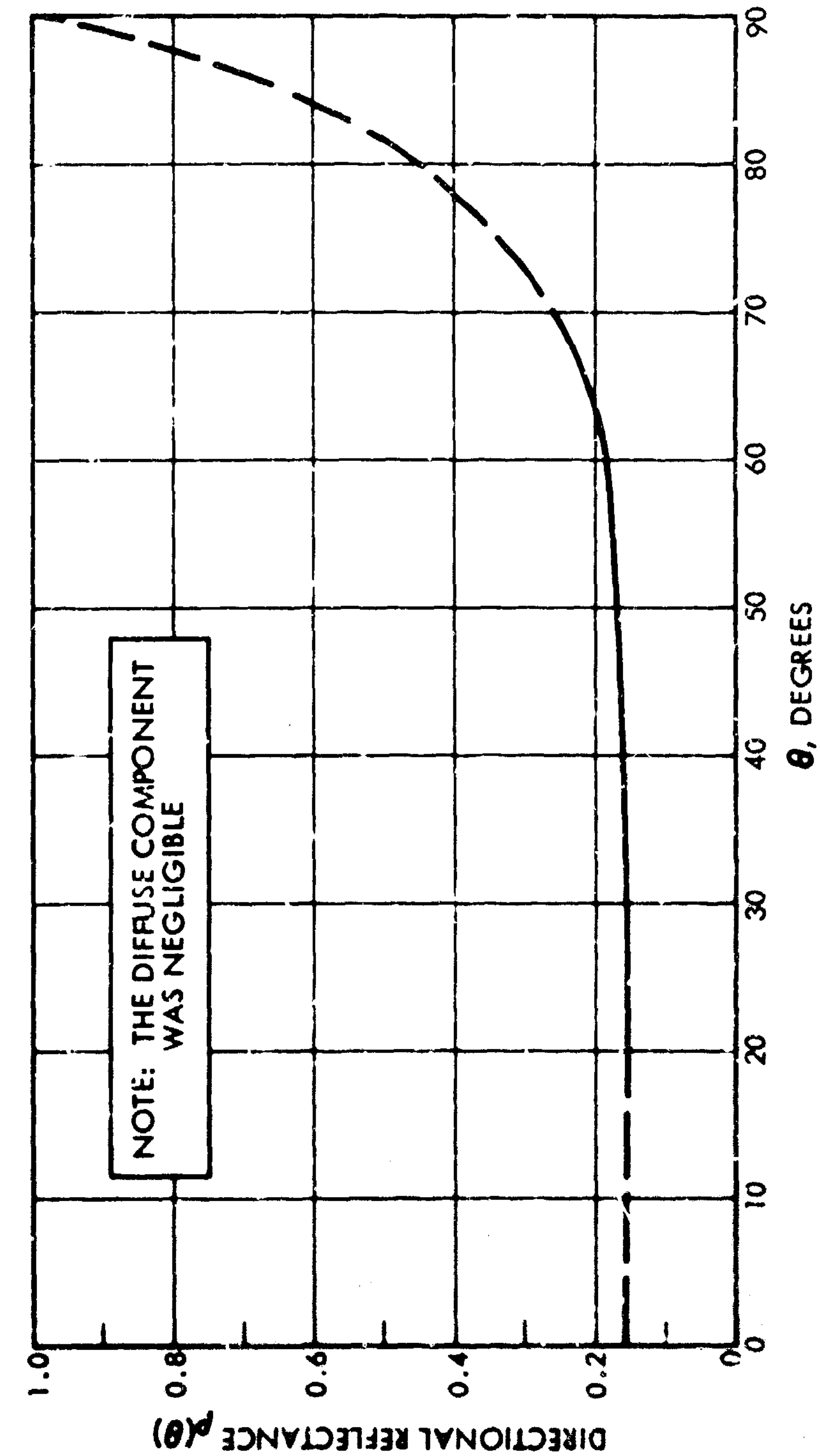

Figure 20. Directional Reflectance of Sulfuric Soft Anodized Aluminum (Type 1100), 0.0005 Inches Thick to a 540°R Black Body as a Function of Angle

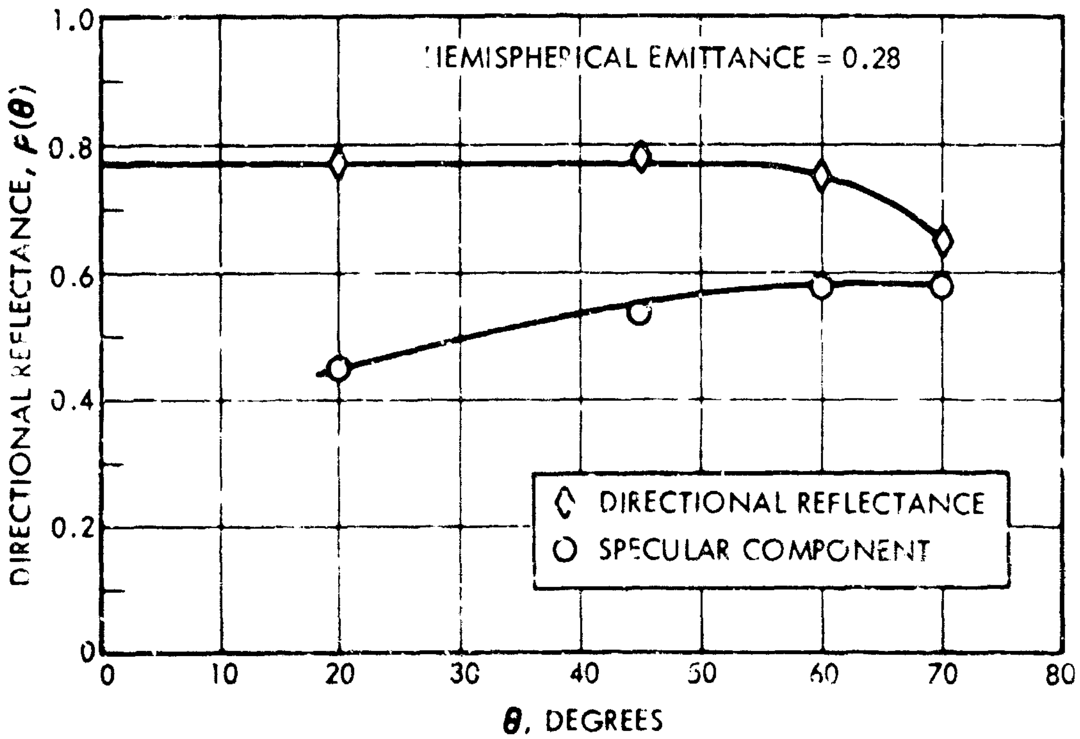

Figure 21. Directional Reflectance of Rinshed-Mason Leafing Aluminum Paint to a 540°R Black Body as a Function of Angle

TABLE 7

SUMMARY OF RADIATION EXCHANGE ANALYSES AND EXPERIMENT

Configuration*		Q_s Source Heat Quantity Btu/hr	T_R Receiver Temperature ^oR
1	Experimental	29.83	345.2
	Directional Specular-Diffuse Analysis	29.41	340.4
	Specular-Assumption	29.17	342.2
	Diffuse Assumption	29.17	342.2
2	Experimental	42.50	393.8
	Directional Specular Diffuse Analysis	42.06	386
	Specular-Assumption	41.2	386.4
	Diffuse Assumption	41.2	386.4
3	Experimental	41.29	428.2
	Directional Specular-Diffuse Analysis	40.68	419.4
	Specular-Assumption	40.93	412.0
	Diffuse Assumption	39.69	393.8
4	Experimental	40.7	423.5
	Directional Specular-Diffuse Analysis	40.33	415.5
	Specular-Assumption	40.25	408.8
	Diffuse Assumption	40.54	397.4
5	Experimental	39.93	409.7
	Directional Specular-Diffuse Analysis	40.0	391.6
	Specular-Assumption	40.3	402.5
	Diffuse Assumption	40.2	383.8
6	Experimental	40.05	398.7
	Directional Specular-Diffuse Analysis	39.21	382.3
	Specular-Assumption	39.56	391.1
	Diffuse Assumption	40.19	387.9

*See Figures 14 and 17.

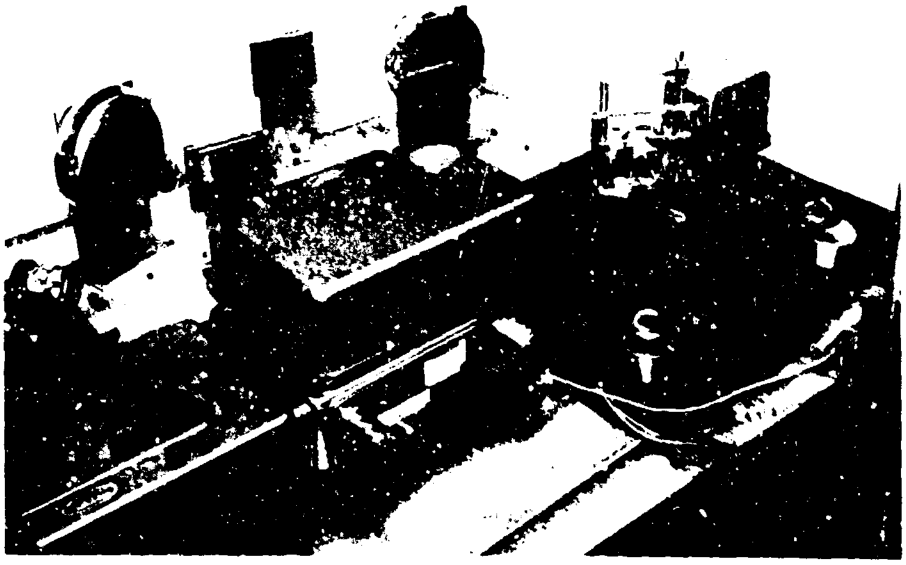

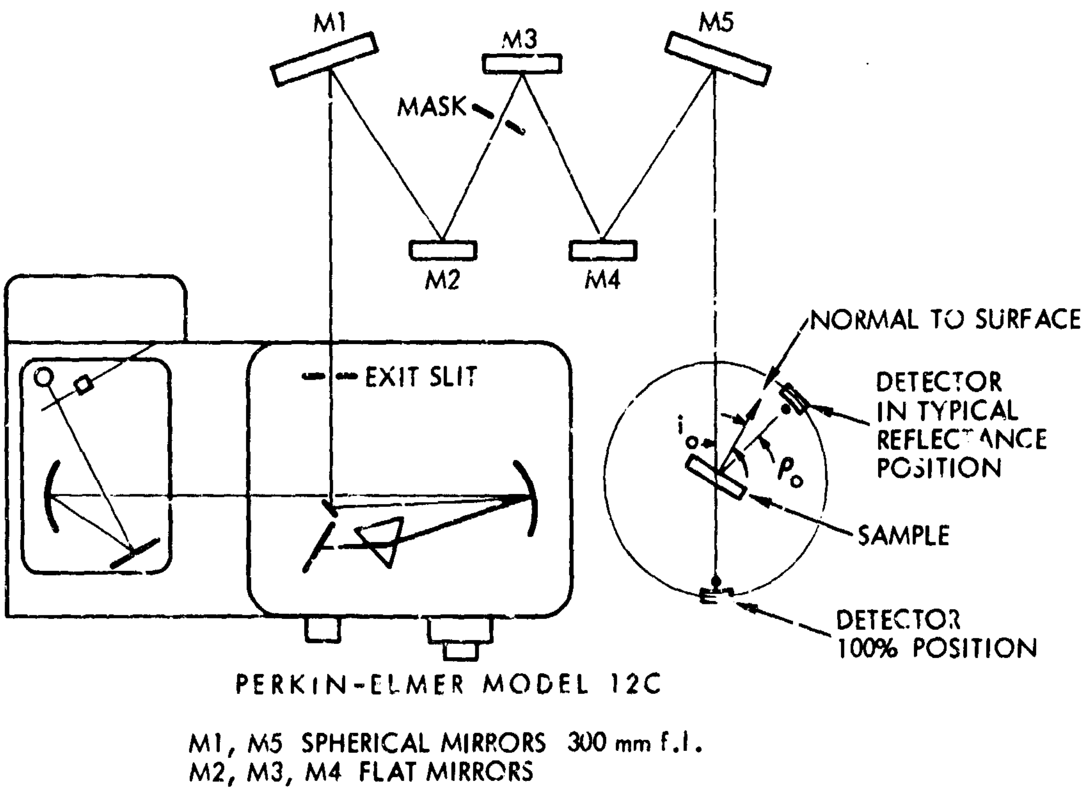

Figure 22. STL Goniometric Reflectometer

This source of error has also been recently recognized and the information required to assess this error is not yet available for the monochromator used. In the case of the tests described, only the 3M flat black paint will be free of this error.

A fourth source of error was the approximations used to obtain the geometrical reflectances; i.e., the interaction between spatial variation of reflectance and the shape factor integral. The methods used to approximate these properties have been described in Section 5.3. Until a spatial distribution of the reflectance property of a number of surfaces have been obtained and incorporated in the integration of a shape factor, the magnitude of this error will not be known. Simple analysis of an extreme case has shown this to be as large as 30 percent (4).

Considering all of these factors together, plus the probable experimental error, leads to the conclusion that the predicted temperatures should be re-examined. This would require the analyses to be performed on a band energy basis and with a more detailed evaluation of the properties.

The analytical results given in Table 7 also offer an opportunity to compare the different methods of analysis. The program described in Section 5 is based upon the method given in Reference 4. The technique is an admitted approximation to the integral equations describing the radiation exchange within an enclosure. The other two methods are also approximations in that an assumption is made relative to the radiation properties, i.e., nondirectional perfectly specular or perfectly diffuse. The approach programed to this study resulted in a set of equations which were very similar to those obtained in the diffuse approximation and could be solved with a slight increase in time. In contrast, an enclosure with perfectly specular surfaces can require extensive preliminary calculation to obtain the "specular interreflections."

The test configurations of Figure 17 are examples of very simple enclosures which are easily solved by any one of the three methods. They do not represent a complex enclosure and cannot adequately demonstrate the differences between the specular, diffuse and directional specular-diffuse methods. A trend can be inferred, however. For example, Test Configurations 1 and 2 should yield identical results for the specular and diffuse assumptions. The directional specular-diffuse analysis yields different results because the emission from source occurs at large angles from the normal. The predicted temperature of the receiver is higher for Test 1 and lower for Test 2 because of the angular effects of absorption. For Test 3, the specular analysis is suitable but does not account for the directional properties. The diffuse analysis does not account for specular reflection and radiation is "diffusely" reflected back to the source. The directional specular-diffuse result is between these two. Similar arguments hold for Test Configurations 4, 5, and 6. These geometries are more complicated by the use of the aluminum paint and anodized aluminum which have directional and/or specular components of reflection. In more complicated enclosures, such a simple explanation of possible differences is not practical. The only comment that can be made is that the directional specular-diffuse analysis is a more realistic approximation to physical fact.

7. CORRELATION OF COMPONENT JOINT EXPERIMENTAL RESULTS

At the request of the Technical Monitor, C. J. Feldmanis, an effort was made to correlate the experimentally measured values of joint conduction. This work was a substitute for the completion of the preliminary design task originally scheduled for the last portion of the program. This correlation effort has resulted in a simplified approach based on the conduction flow pattern to a circular cavity(region of the bolts) in the mating parts. For the thin plates in the component mounting joints, the conduction at the bolts was very high and the apparent contact area small. This led to the conclusion that macroscopic effects were of the greatest significance.

A review of the technical literature revealed little information that would be useful in predicting interface conductance for the bolted joints of this study. A subsequent study of the pressure distribution indicated that the apparent contact area occupies only to a small region near the bolts. This suggested that the predominant thermal resistance lies in the mating plates themselves. This correlation effort has resulted in a simplified expression for the interface conductance based on the heat flow pattern in a large circular region to a circular sink at the center. These comments apply specifically to the mounting plate configuration investigated in this study.

7.1 REVIEW OF LITERATURE

A review of technical literature reveals that the study of vacuum thermal contact resistance is of recent vintage. Past emphasis has been upon joints in a conducting fluid; e.g., air. This is not surprising since the need for information on the behavior of heat flow through connecting elements in a vacuum was not great until the advent of satellites. An excellent review of technical literature is contained in Reference 12 and a bibliography on contact conductance is contained in Reference 13; Appendix V list references that are not reported in Reference 13.

As background to the correlation to be presented, two well known methods that have been proposed will be cited. The applicability (or lack of it) to the type of joints considered in the present study will be indicated.

Fenech and Rohsenow (14) developed an expression for the thermal conductance of a mathematical model with contacting surfaces idealized as cylindrical contacts equally spaced in a triangular array. The thermal conductance was expressed in terms of the thermal conductivity of the metals and of the fluids of filling the voids, the real area in contact, the number of contact points per unit area, and the volume average thickness of the void gaps. A method of obtaining these physical properties of a contact is contained in Reference 15. The need for the profiles of the contacting surfaces precluded the examination of this method.

While most investigators were concerned with microscopic areas of contacts (those due to surface finish), Clausing and Chao (12) concluded that macroscopic resistances (that due to large scale waviness or non-flatness) was predominant over the microscopic resistance for a majority of engineering surfaces. The interface conductance was expressed in terms of the mean thermal conductivity of the two contacting materials, the radius of the macroscopic constriction ratio, the contact pressure, the macroscopic constriction ratio, the harmonic mean of the moduli of the two-contacting materials, and the total equivalent flatness deviation. This method requires the measurement of flatness deviation and surface finish; the latter is readily obtained, but the former is more difficult to measure. This method was not applied since subsequent studies showed that the apparent contact area (the region adjacent to the bolts) represents only a small percent of the total joint area. However, the concept of constrictive heat flow is employed in the present study, except that it is applied in a much larger, gross scale. The method is discussed below.

The two methods discussed above considered a physical system without a disruptive element such as a bolt. Intuitively, the influence of fasteners should be great. An attempt at correlating joint conductance data is reported in Reference 16, and the resultant expression is semi-empirical. The method employed in the present study is semi-analytical and the close correlation with experimental results strongly suggests that the governing resistance is centered in the plate itself; at least for the type of joints considered here. The analytical method is discussed below.

7.2 ANALYTICAL DEVELOPMENT

The correlation of joint conductance data was limited to the component joint configurations. An anlytical model was postulated based on the work done by previous workers, experimental data and engineering judgement. The basic concept of the proposed method is that the controlling thermal resistance is the plate. It is postulated that the points of contact which contribute to the conductance are in the small region under and around the bolts. The problem is then to describe the heat flow in the plate to the bolt area. Two mathematical models were employed for this purpose.

7.2.1 ANALYTICAL MODEL I

The first model is shown in Figure 23(a). It is a disc with uniform heat flux over its surface and conduction to a central area at a constant temperature. The outside surface ($r = R$) is assumed to be insulated. This model is used to describe heat flow in a joint with only a few bolts in relation to the total area.

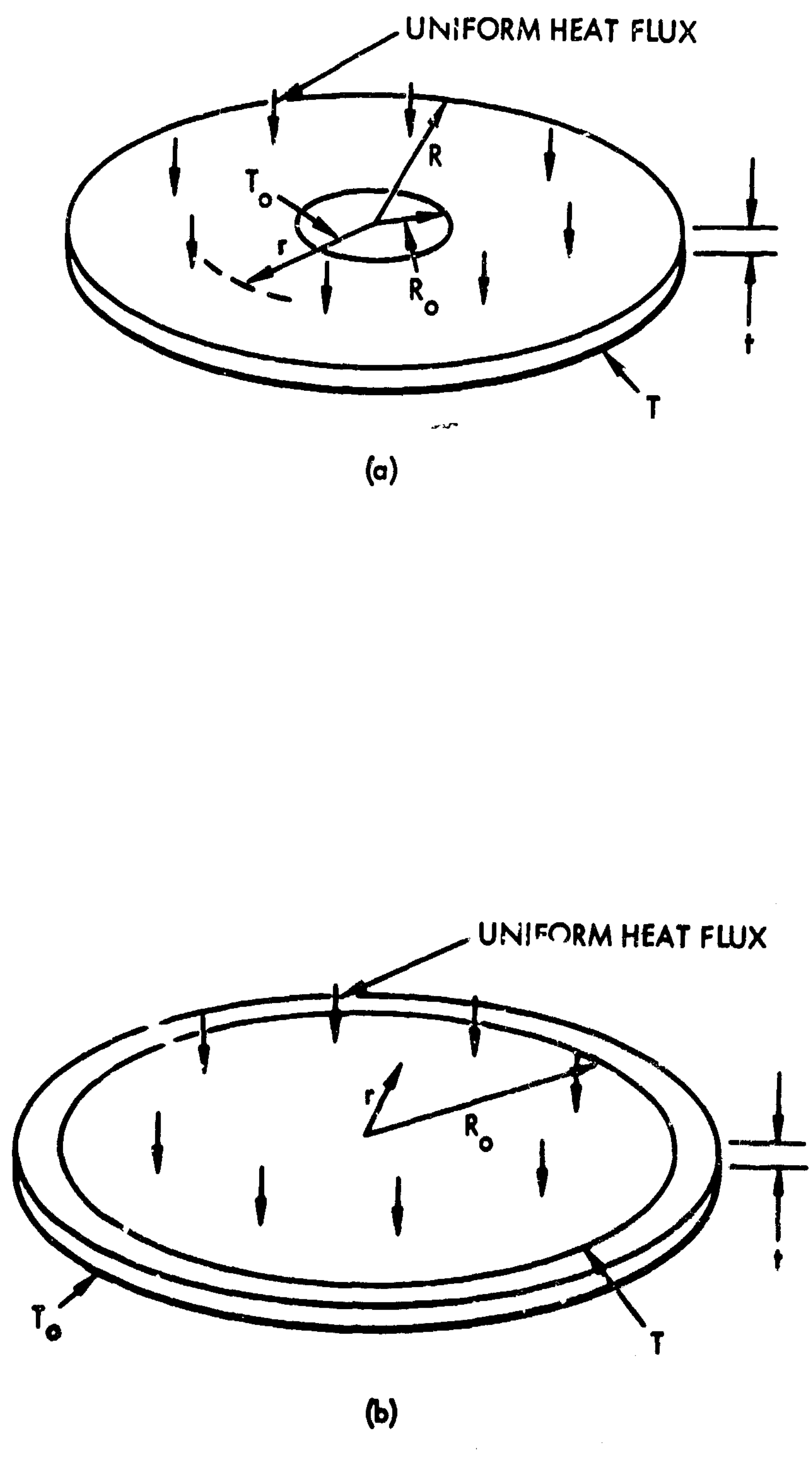

Figure 23. Analytical Models for Bolted Component Joint Correlation

For an incremental volume at radius r, a heat balance yields,

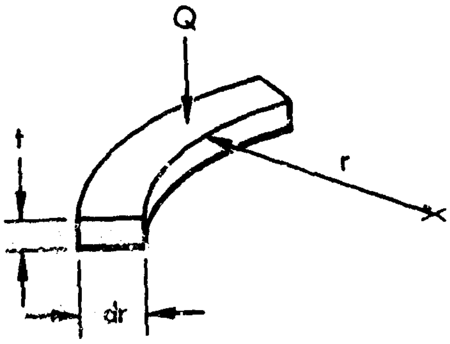

$$Q\,2\pi r\,dr = -2\pi ktr\left.\frac{dT}{dr}\right|_{r+dr} + 2\pi ktr\left.\frac{dT}{dr}\right|_{r} \qquad 7\text{-}1$$

or

$$Q = -\frac{kt}{r}\frac{d}{dr}\left(r\frac{dT}{dr}\right) \qquad 7\text{-}2$$

with boundary conditions:

at $r = R$, $\frac{dT}{dr} = 0$ (insulated) and

at $r = R_o$, $T = T_o$

Hence, $$T_o - T = \frac{Q}{Rt}\left[\frac{1}{4}(r^2-R_o^2) + \frac{1}{2}R^2\ln\frac{R_o}{r}\right] \qquad 7\text{-}3$$

Now let $\frac{r}{R} = \eta$, $\frac{R_o}{R} = \eta_o$

$$\therefore\; T_o - T = \frac{QR^2}{kt}\left[\frac{1}{4}(\eta^2-\eta_o^2) + \frac{1}{2}\ln\frac{\eta_o}{\eta}\right] = \Delta T \qquad 7\text{-}4$$

The conductance of one plate is:

$$h = \frac{Q\pi R^2}{\int_{R_o}^{R}(T-T_o)2\pi r\,dr} \qquad 7\text{-}5$$

57 (3)

Substituting ΔT from Equation 7-4 and changing the limits of integration gives:

$$h = \frac{Q\pi R^2}{\int_{\eta_o}^{1} \frac{QR^2}{kt} \left[\frac{1}{4}(\eta_o^2-\eta^2) + \frac{1}{2}\ln\frac{\eta}{\eta_o}\right] 2\pi\eta\, d\eta} \qquad 7\text{-}6$$

Integrating and substituting the limits yields

$$h = \frac{2kt}{R^2} \left[\frac{1}{\eta_o^2-\eta_o^4/4 - \ln\eta_o - 3/4}\right] \qquad 7\text{-}7$$

The bracketed term of Equation 7-7 is plotted in Figure 24 and the conductance versus radius for several effective contact radius values is shown in Figure 25.

7.2.2 ANALYTICAL MODEL II

The model which can be applied to a system having contact around the periphery is shown in Figure 23(b). The equation for this system is:

$$Q = -\frac{kt}{r}\frac{d}{dr}\left(r\frac{dt}{dr}\right) \qquad 7\text{-}8$$

The boundary conditions are:

$r = 0$, T is finite

$r = R_o$, $T = T_o$

Solution of Equation 7-8 yields,

$$T - T_o = \frac{Q}{4kt}\left[R_o^2-r^2\right] \qquad 7\text{-}9$$

The conductance of one plate is:

$$h = \frac{Q\pi R_o^2}{\int_0^{R_o} (T-T_o)\, 2\pi r\, dr} \qquad 7\text{-}10$$

Substituting ΔT from Equation 7-9 and integrating gives:

$$h = \frac{8kt}{R_o^2} \qquad 7\text{-}11$$

This equation is plotted in Figure 26.

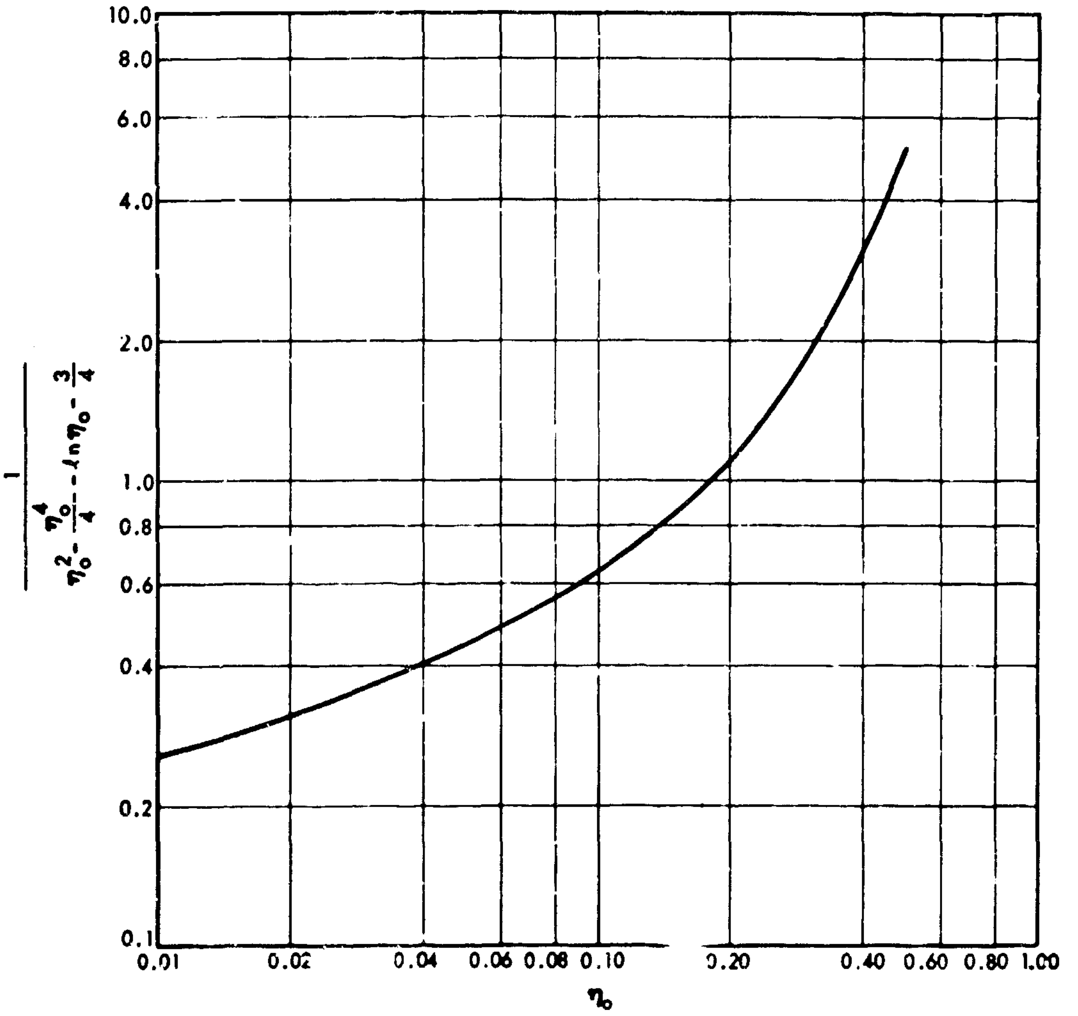

Figure 24. The Quantity $\left[\eta_o^2 - (\eta_o^4/4) - \ln \eta_o - 3/4\right]^{-1}$ as a Function of η_o

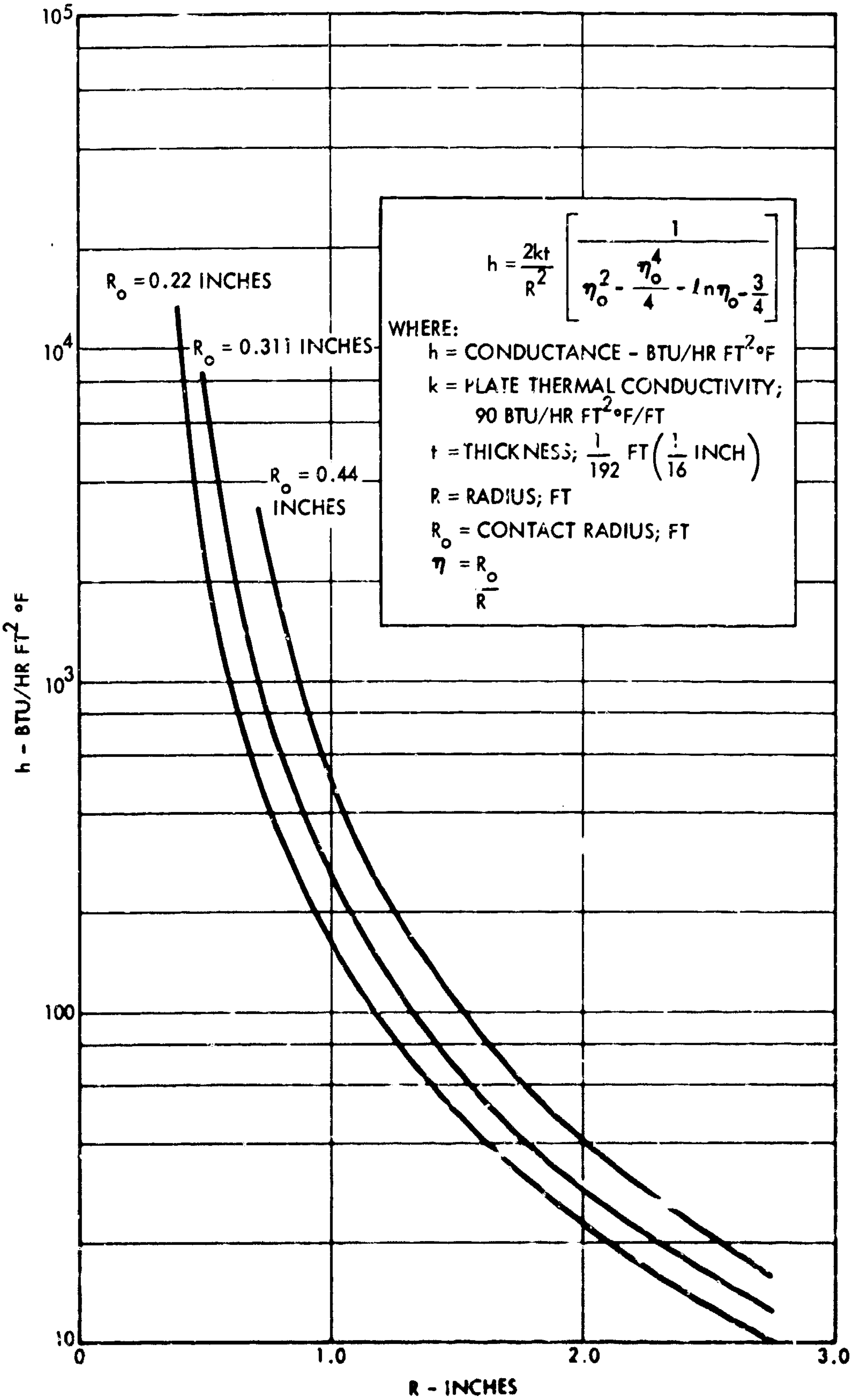

Figure 25. The Thermal Conductance of a Single Contact Junctio as a Function of Contact Radius (R_o) for an Aluminu Plate 1/16th Inch Thick

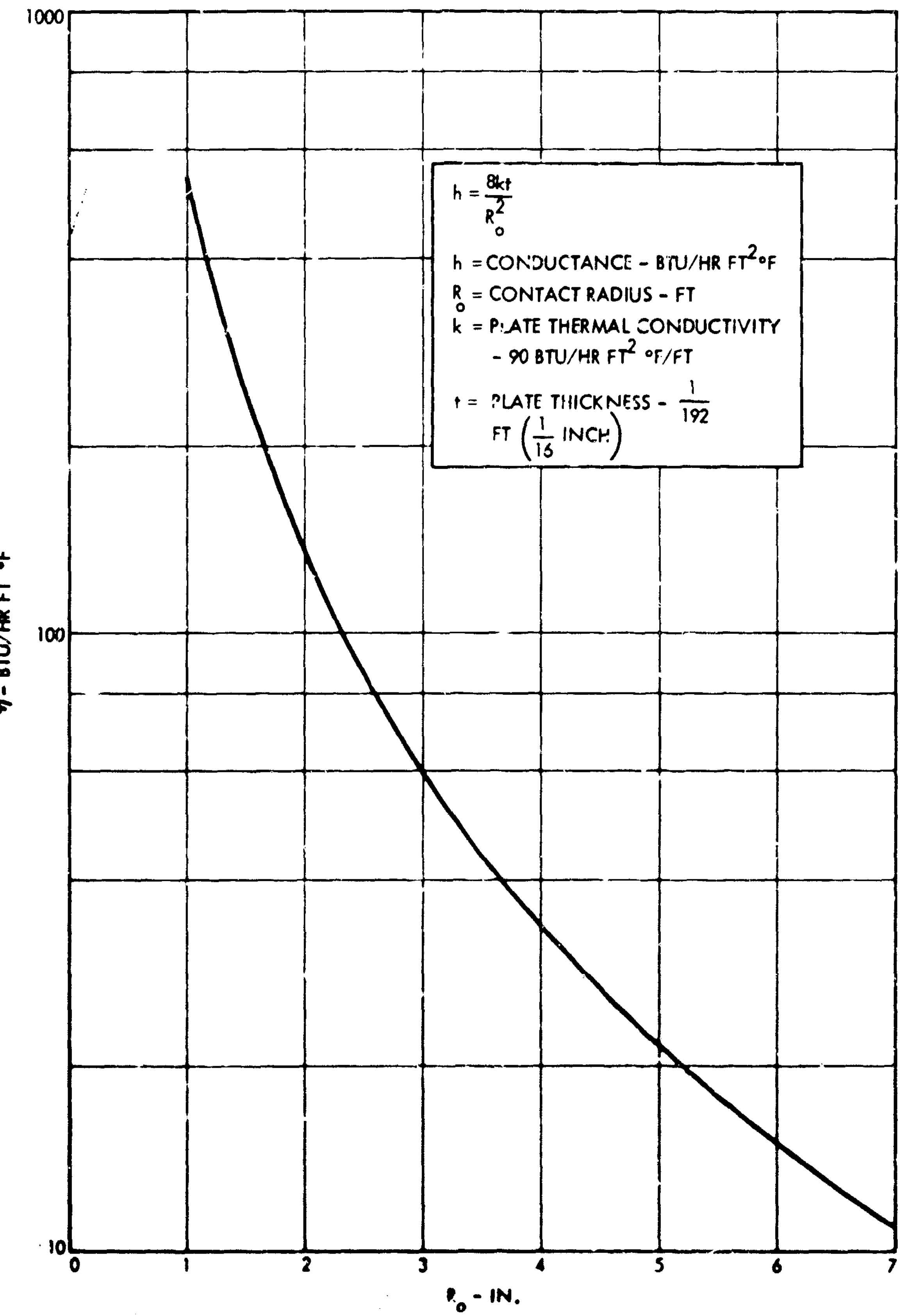

Figure 26. The Thermal Conductance of a Peripheral Contact Junction for an Aluminum Plate 1/16th Inch Thick

7.2.3 CONTACT REGION AROUND A BOLT

The contact area and conductance of a bolt is based on the deformation of the plates under bolt head. The method used to determine this quantity is that presented in reference (17). The analysis given by this reference assumes a uniform loading over the bolt area. The resultant stress distribution is shown in Figure 27 and can be expressed as (Equation 56, Reference 17):

$$\frac{\sigma_z}{\sigma_p} = 1 - \left(\frac{r}{c}\right)^{\left[\frac{2}{(c/a)^2 - 1}\right]} \qquad 7\text{-}12$$

The quantity c is dependent upon the bolt diameter, a, and the plate thickness, $\frac{b}{2}$. For a 1/16-inch plate in contact with a 1/8-inch plate, the effective contact radius, c, is given by Reference 17 as 1.35a.

The pressure under the bolt must be computed for use in the above expression. The tensile load in a bolt torqued to a preset value is determined from the approximate relation given in Reference 18.

$$T = 0.20\ Fd. \qquad 7\text{-}13$$

where

T = bolt torque, 24 in.-lb.

F = tensile load, lb.

d = major thread dia. = .190 in.

or

F = 630 lb.

This value is conservative for the present application; that is, it yields a lower conductance than values given by other references. Aron and Colombo (16), for example, use a value of 800 lb. for 22 in.-lb. torque in the same size bolt.

The bolt (NAS 563) has a measured bearing diameter of 0.344 inches and the nut (NAS 671) has a measured bearing diameter of 0.312 inches. The area under the nut was used to obtain the pressure, assuming uniform loading (σ_p = F)

$$P = \frac{F}{A} = \frac{630\ \text{lb.}}{.0468\ \text{in}^2} = 13,450\ \text{lb/in}^2 \qquad 7\text{-}14$$

This result was used with Equation 7-12 to obtain the pressure distribution and conductance at the bolt. The solution of Equation 7-12 for σ_z, using the results of Equation 7-14, are plotted in Figure 28. The pressure distribution was used by dividing the area into annular zones and evaluating each zone to estimate its conductance. The numerical values were obtained from the conductance versus pressure plot given in

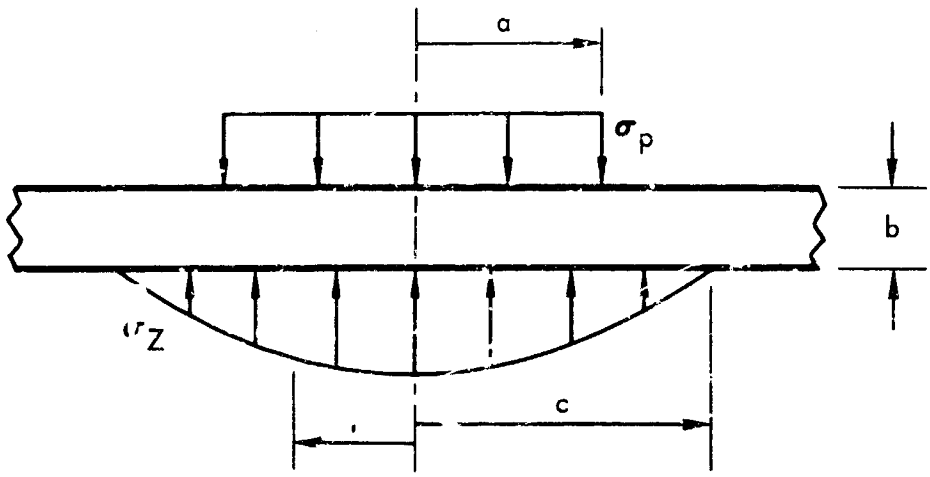

Figure 27. Stress Distribution in a Bolted Plate for Uniform Bolt Pressure

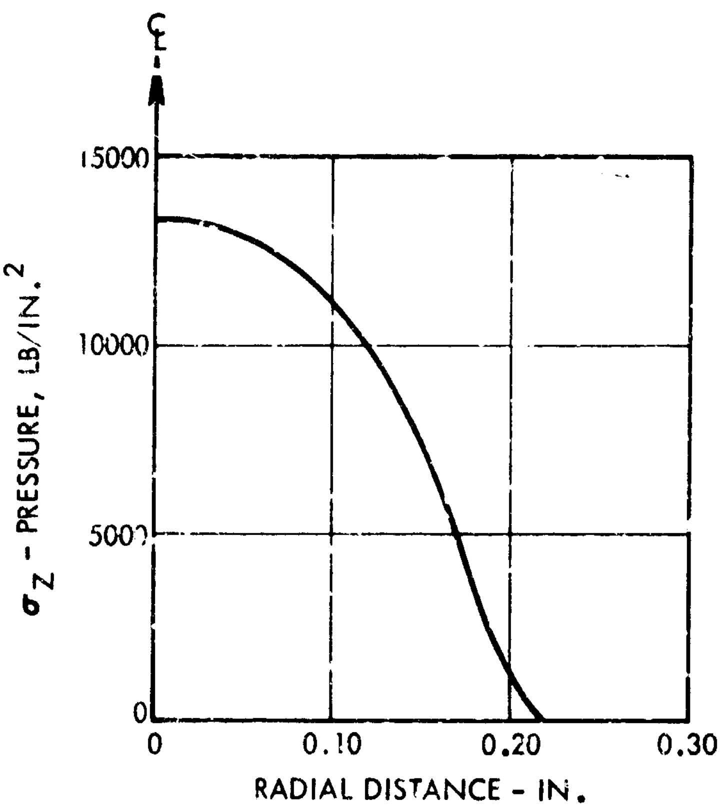

Figure 28. The Pressure Distribution Under the Nut of a Bolted Plate According to Equation 7-12

Figure 6-3 of Reference 19, labeled "Best line through most of the Aluminum (II) Data-Vacuum." The results of this calculation yield a conductance through the bolt of 21,000 Btu/hr ft^2 °F. This can be compared to the value of 10,000 Btu/hr ft^2 °F calculated in Reference 19 for a No. 10 bolt tightened to 22 in.-lb. torque. The area under the bolt in Reference 19 is given as 0.33 inches^2 (a washer was used in Reference 19). The contact area under the bolt in the present study was 0.12 in.^{2}. Thus, the thermal resistance of the two bolts can be compared:

Present Study:

$$R = \frac{1}{hA} = .0575 \frac{^{\circ}F\ hr}{BTU}$$

Reference (3)

$$R = \frac{1}{hA} = .044 \frac{^{\circ}F\ hr}{BTU}$$

7.3 APPLICATION TO TEST CONFIGURATIONS

Three component test configurations were run with fewer than the normal 12 bolts to evaluate bolt spacing effectiveness. These tests were in addition to those reported in Section 3.1. These configurations are shown in Figure 29 (a, b, and c). The sample size was 6 inches by 6 inches, the upper plate thickness was 1/16 inch, and the mounting plate was 1/8 inch thick. The bolt torque was 24 in. lb. for all cases.

Configuration 29-a was divided into four equal areas for purposes of analytical correlation. Each triangular section was assumed to be deformed into a semicircular shape of the same area and having a contact region at the center. The radius of the segment is then 2.38 in., and the bolt contact area, now semicircular, has an effective radius of 0.311 in. These dimensions were substituted in the equations described in Section 7.2.1. The resulting conductance of the upper plate was found to be: h_1 = 18.3 Btu/hr ft^2 °F.

The conductance of the lower plate will be computed using the same analytical procedure. Since the heat removal from the lower plate is not as uniform as heat supplied to the upper plate, the analytical model is now a poorer approximation of the real system. The results were used as an approximation since an analytical solution of the real heat flow in this plate would be a lengthy task. Applying this method to the lower plate, which has a thickness twice that of the upper plate, results in h_2 = 36.6 Btu/hr ft^2 °F. These two plate thermal conductances must be combined with the bolt thermal conductance. The thermal circuit for this system is:

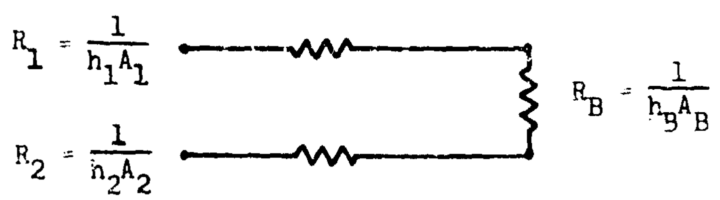

Figure 30. Thermal Circuit for Calculating Overall Thermal Conductance

The overall conductance is given by:

$$\frac{1}{hA} = \frac{1}{h_1 A_1} + \frac{1}{h_B A_B} + \frac{1}{h_2 A_2}$$

Substituting the values gives:

$$\frac{1}{hA} = \frac{1}{18.3\ (\frac{9}{144})} + \frac{1}{21{,}000\ (\frac{.12}{144})} + \frac{1}{36.6\ (\frac{9}{144})}$$

$$\frac{1}{hA} = .874 + .057 + .437$$

or

$$h = \frac{1}{1.368(\frac{9}{144})} = 11.7\ \text{Btu/hr ft}^2\ {}^{o}\text{F}$$

Applying this technique to Configuration 29-b, the corner bolts were close together and were lumped together to form a quarter circular area having an effective radius of 0.622 inches. The analytical method of Section 7.2.1 and thermal circuit substitutions yield an overall conductance of h = 8.0 Btu/hr ft^2 ^{o}F.

Configuration 29-c was divided by allotting to each corner bolt a hemicircular area of 4 in.^{2} and each center bolt a quarter circle of 5 in.^{2}. Using the same technique as above, the thermal circuit gave:

h = 22.0 Btu/hr ft^2 ^{o}F.

The twelve-bolt configuration was analyzed in the same manner by dividing this area into eight equal area segments as shown in Figure 29-d. The result was:

h = 26.7 Btu/hr ft^2 ^{o}F.

The 6 inch by 12 inch component configuration can be approached using the same technique by dividing the area into eight hemicircular sectors and four quarter circular sectors each with an effective area of 6 inch^2. Similarly the 12 by 12 configuration was divided into twelve hemicircles and four quarter circles of equal area, 9 inch^2. The results for these six configurations are shown in Table 8.

The 6 inch by 6 inch, 12 bolt and 12 inch by 12 inch, 24 bolt configurations can also be predicted using the method described in Section 7.2.2. An effective radius based on the plate area was used in Equation 7-11. The results are also given in Table 8. The results of these correlation attempts are compared to the measured values in Table 8. The agreement is adequate in all cases except 29-b where the predicted value is a little more than half of the measured conductance. In spite of this, the success of the technique is quite satisfactory. Further exploitation should be made of the approach described here. The results have been restricted to a bolted thin plate without a filler material.

EXPERIMENTAL SYSTEMS
AND
ANALYTICAL APPROXIMATIONS

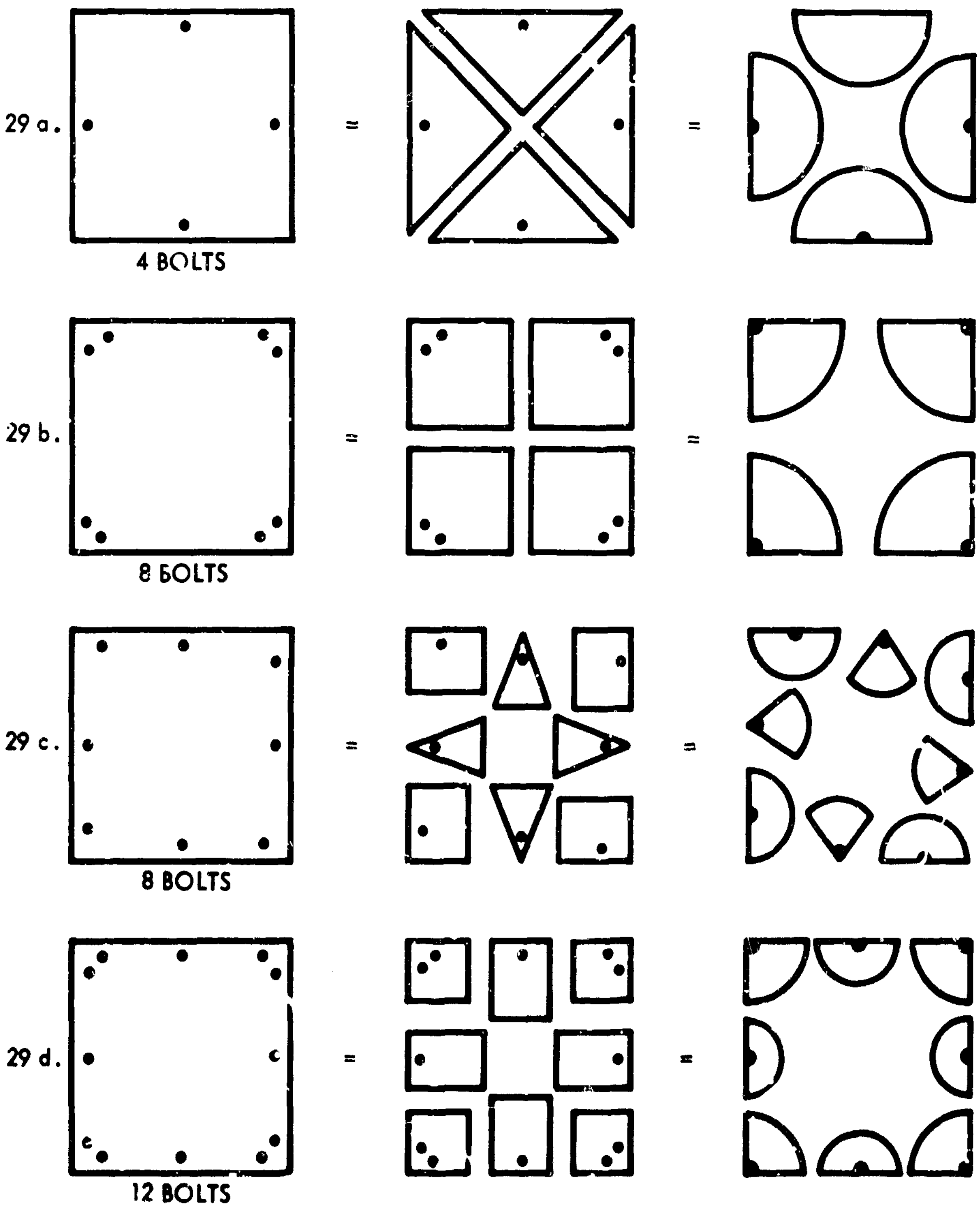

Figure 29. Method of Subdividing the Test Configurations to Predict Overall Thermal Conductance

TABLE 8

COMPARISON OF PREDICTED AND MEASURED COMPONENT JOINT CONDUCTANCES

Configuration	Experimental h, BTU/hr ft^2 ^oF	Method I (Sec. 7.2.1) h, BTU/hr ft^2 ^oF	Method II (Sec. 7.2.2) h, BTU/hr ft^2 ^oF
29-a	13.4	11.7	
29-b	13.7	8.0	
29-c	22.0	22.0	
29-d 6 x 6, 12 bolts	26.3	26.7	29
6 x 12, 18 bolts	18.5	18.1	
12 x 12, 24 bolts	8.3	10.5	7.8

An attempt should be made to extend this to thick plates with and without a filler and to thin plates with a filler.

8. CONCLUSIONS AND RECOMMENDATIONS

This report presents the results of the first phase of a program designed to improve the prediction of spacecraft thermal performance. The information necessary for the comparison of prediction and test of a spacecraft model has been gathered. The continuation of the program to this natural conclusion is the second phase of the study. There has been no decrease in the practical needs for this continuation and it is important to complete this program.

There have been several developments within this program which warrant further study. The first is the extension of the joint conductance testing to include a larger number of joint types. The techniques which have been developed in this program for experimentally measuring the conductance of practical joints have proven to be very simple and inexpensive. The accuracy which is obtained is adequate for such joints and is a satisfactory compromise with the cost of such experimentation. The joints for this additional work should not be chosen on the basis of a thermal test model but selected for the frequency with which they are used in actual practice, e.g., riveted joints, low conductance joints, etc.

The practical correlation of joint conductances should also be continued. The correlation for the thin plate unfilled component joints was obtained by assuming the primary resistance to heat flow was in the thin plates. This primary resistance was found to be adequately described by radial in the region surrounding each bolt fastener. The success with which the component joints were correlated by this procedure was very encouraging. The limitations of time and resources did not allow a similar attempt to be made to correlate filled joints or structural joints. However, such a correlation is believed to be feasible. This work could be included in the second phase of the program; correlation of other test joints would be performed as part of the experimental work described above or as a separate study. Regardless of the mechanism chosen for performing this correlation, this work should be continued and extended.

The application of the directional specular-diffuse method of analysis has indicated a major gap in our knowledge of thermal radiation properties. A critical part of this method is the separation of the thermal radiation properties into the diffuse and specular components. Additional experimental and analytical work is required to develop a basis for this separation from measurements of the directional and specular reflectances. Such a study should include an examination of the geometrical reflectances (and emittances) relative to the distribution of reflected (and emitted) radiation.

Although the comparisons of predicted and experimental radiation exchange in the simple geometries were close, further refinement of the predictions are desired. This problem is related in part to the separation of the diffuse and specular components discussed above. The effect of non-gray radiation properties is probably of equal or greater importance. Further study is needed for the improvement of the predicted temperatures and heat fluxes, e.g., a prediction using the band energy method.

In conclusion, the objectives of the first phase of the program have been satisfied; i.e., the data and methods required to compare the predicted and test thermal performance of a model spacecraft have been developed. Other areas for further study have also been found:

(1) practical joint conductance measurements
(2) correlation of measured joint conductances
(3) the separation of radiation properties into diffuse and specular components for the directional specular-diffuse analysis
(4) the importance of the non-gray property assumption

The development of additional problems is to be expected in a study of this nature. The second phase of the program should be expected to raise its own share of new problems.

REFERENCES

1. H. C. Hottel, "Radiant Heat Transmission," Chapter 4 of Heat Transmission, 3rd Ed., W. H. McAdams, McGraw-Hill Book Co., New York, 1954.
2. B. Gebhart, "Unified Treatment for Thermal Radiation Transfer Processes," Paper No. 57-A-34, Winter Meeting ASME, Dec. 1959.
3. A. K. Oppenheim, Trans. ASME 78:725-735 (1956).
4. J. T. Bevans and D. K. Edwards, "Radiation Exchange in an Enclosure with Directional Wall Properties," presented at the ASME Winter Meeting, Dec. 1965, Paper No. 64WA/HT-52, published in the August issue of the Journal of Heat Transfer 87:388-396 (1965).
5. C. D. Coulbert and Chien Liu, WADC TN 53-50 June 1953.
6. T. Ishimoto and J. T. Bevans, AIAA Journal 1:1428-9 (1963).
7. E. M. Sparrow, "On the Calculation of Radiant Interchange Between Surfaces," pp 181-212, W. Ibele editor Academic Press, New York, 1963.
8. J. T. Bevans and R. V. Dunkle, Trans. ASME, Series C 82:1-19 (1960).
9. E. M. Sparrow, et al., Trans. ASME, Series C 84:294-299 (1962).
10. D. K. Edwards and J. T. Bevans, "Effect of Polarization on Spacecraft Radiation Heat Transfer," to be published in the July issue of the AIAA Journal, 1965.
11. R. V. Dunkle, et al., "Heated Cavity Reflectometer for Angular Reflectance Measurements," Prog. in Intl. Research on Thermodynamics and Transport Properties Am. Soc. Mech. Engrs., pp 541-562 (1962).
12. A. M. Clausing and B. T. Chao, "Thermal Contact Resistance in a Vacuum Environment," University of Illinois Experimental Station Report, ME-TN-242-1, August 1963.
13. H. Atkins, "Bibliography on Thermal Metallic Contact Conductance," NASA TM X-53227, April 15, 1965, Marshall Space Flight Center.
14. H. Fenech and W. M. Rohsenow, "Prediction of Thermal Conductance of Metallic Surfaces in Contact," (Paper No. 62-HT-32) J. Heat Transfer, Vol. 85, pp 15-24, Feb.
15. J. J. Henry and H. Fenech, "The Use of Analogue Computers for Determining Surface Parameters Required for Prediction of Thermal Contact Conductance," ASME Paper 63-WA-104, 1963; also J. of Heat Transfer Transaction of ASME, Vol. 86, Series C, No. 4, Nov. 1964.
16. W. K. Aron and G. Colombo, "Controlling Factors of Thermal Conductance Across Bolted Joints in a Vacuum," ASME Paper 63-W-196.
17. K. G. Lindh, et al., "Studies in Heat Transfer in Aircraft Structure Joints," UCLA Report 57-50, May 1957.
18. J. E. Shigley, Machine Design, McGraw-Hill Book Co., Inc. New York, 1956.
19. M. F. Bloom, "Thermal Contact Conductance in a Vacuum Environment," Douglas Aircraft Report SM-47700, Dec. 1964.

APPENDICES

APPENDIX I

EXPERIMENTAL DATA—COMPONENT JOINTS

The experimental data for the 6 x 6 component joint is listed in Table 9 of this appendix. The thermocouple locations are shown on the full size drawing of Figure 31. In addition to these thermocouples, thermocouples were placed in the cooling water inlet and outlet lines. These are absolute thermocouples No. 3 and 4 respectively. The approximate cooling water flow rate was also recorded, but varied as the water pressure fluctuated. The heater voltage and current are also recorded.

Figure 31 also illustrates the zones which were used in computing the area weighted temperature difference. A sample calculation for run No. 1 is as follows:

$$\overline{\Delta T}_{①} = \frac{1.02 + 1.04 + 0.80 + 0.77}{4} = 0.91\ ^{\circ}F$$

$$\overline{\Delta T}_{②} = 1.98\ ^{\circ}F$$

$$\overline{\Delta T}_{③} = \frac{2.50 + 4.11 + 2.57}{3} = 3.06\ ^{\circ}F$$

$$\overline{\Delta T}_{④} = \frac{6.29 + 6.53}{2} = 6.41\ ^{\circ}F$$

These average ΔT's are for each zone, obtained by averaging the differential thermocouple readings in each zone. The overall ΔT is now computed by area weighting these values.

$$\Delta T_M = \Delta T_{①}\frac{A_{①}}{A_T} + \Delta T_{②}\frac{A_{②}}{A_T} + \Delta T_{③}\frac{A_{③}}{A_T} + \Delta T_{④}\frac{A_{④}}{A_T}$$

$$\Delta T_M = \frac{9.0}{36}(0.91) + \frac{7.50}{36}(1.98) + \frac{13.2}{36}(3.06) + \frac{6.25}{36}(6.41)$$

$$\Delta T_M = 0.229 + 0.412 + 1.121 + 1.11$$

$$\Delta T_M = 2.872^{\circ}F$$

$$Q_{IN} = 3.702\ (0.1314) = 4.864 \text{ watts}$$

$$= 16.6 \text{ Btu/hr}$$

$$h = \frac{Q}{A \Delta T_{M}}$$

$$= \frac{16.6 \text{ Btu/hr}}{1/4 \text{ ft}^2 \; 2.872^{\circ}F}$$

$$h = 23.1 \text{ Btu/hr ft}^2 \; {}^{\circ}F$$

The experimental data for the 6 inch x 12 inch and 12 inch x 12 inch component joints are given in Tables 10 and 11, respectively, of this appendix. The thermocouple locations and temperature weighting zones are shown in Figures 32 and 33 for these two experimental configurations.

Differential thermocouples are located at the same (x, y) coordinates on the back of the mounting plate and the component plate at the locations shown on Figures 31, 32 and 33.

The conductance is calculated using the following equation:

$$h = \frac{Q}{A \Delta T}$$

The area used in this calculation is the contact area of the mating parts. For the structural joints, this was the overlap area between the angle bracket and the panel. The ΔT is an area weighted average which is determined by the method explained in above.

6" x 6" COMPONENT THERMOCOUPLE LOCATION

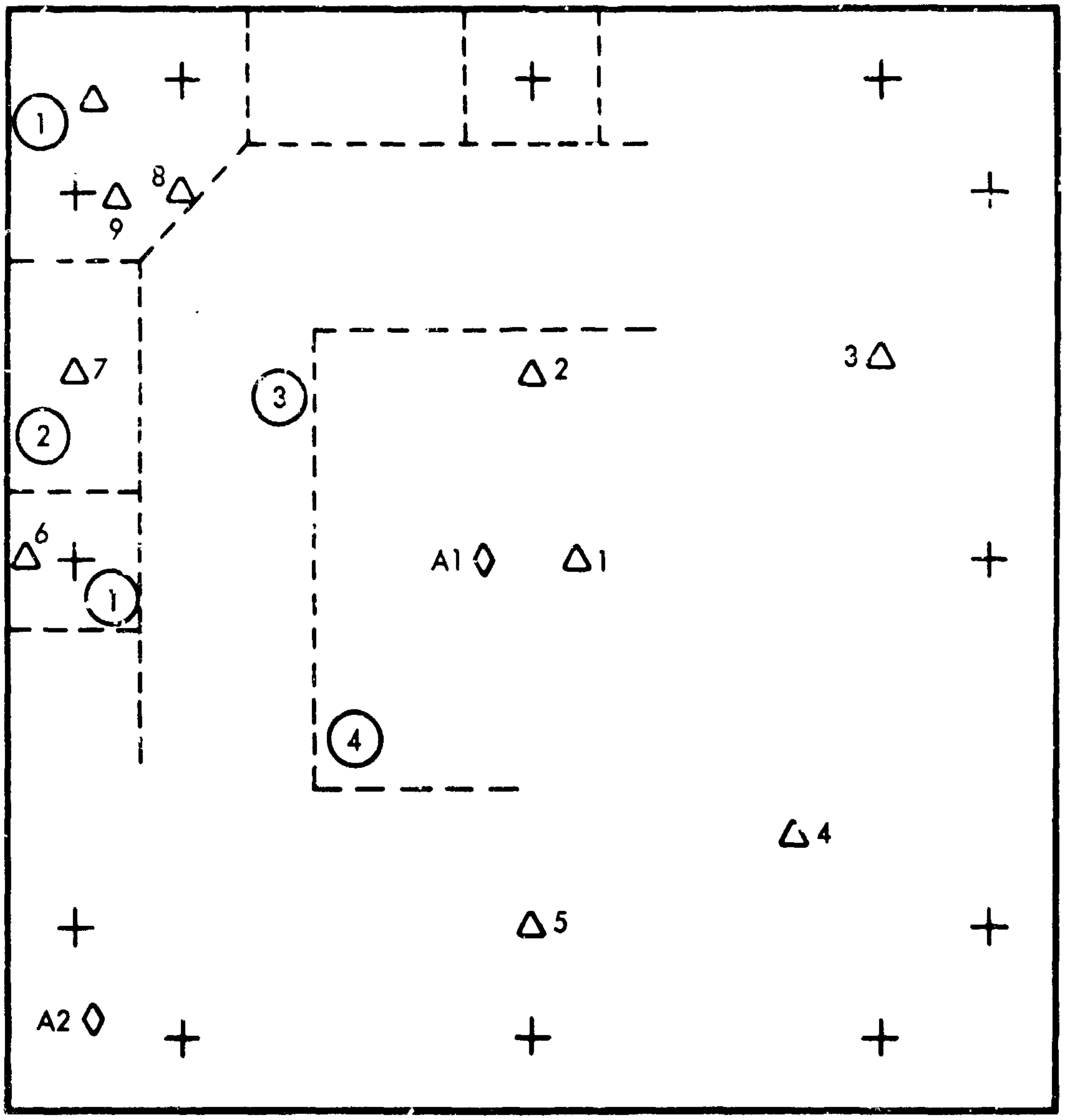

1 ZONE 1, AREA = 9.05 IN.^{2}

2 ZONE 2, AREA = 7.50 IN.^{2}

3 ZONE 3, AREA = 13.20 IN.^{2}

4 ZONE 4, AREA = 6.25 IN.^{2}

△ DIFFERENTIAL THERMOCOUPLES

◊ ABSOLUTE THERMOCOUPLES

+ BOLT LOCATION

○ ZONE AREAS USED TO CALCULATE AVERAGE ΔT

Figure 31. 6" x 6" Component Joint Thermocouple Location

6" x 12" COMPONENT THERMOCOUPLE LOCATION

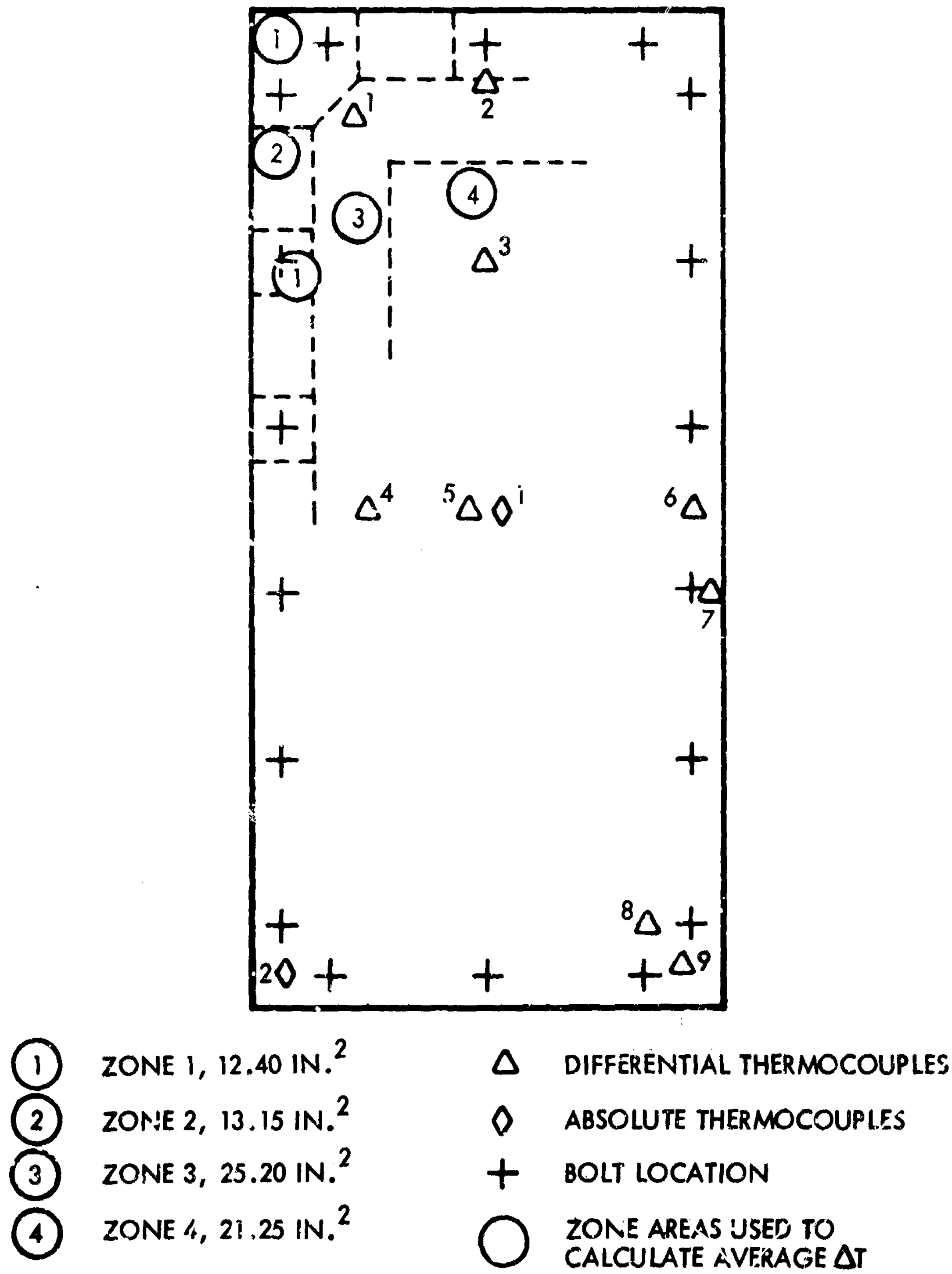

Figure 32. 6" x 12" Component Joint Thermocouple Location

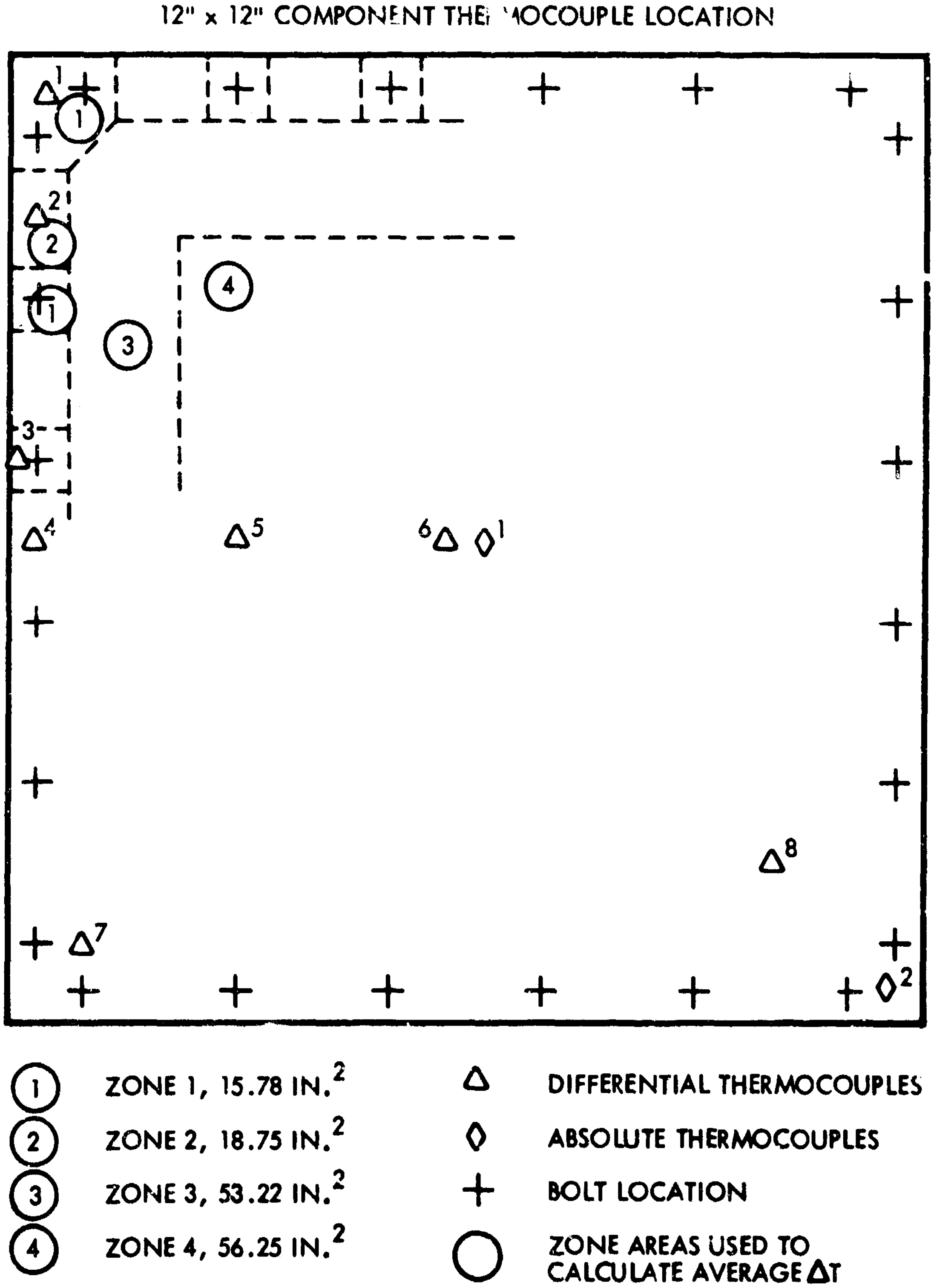

Figure 33. 12" x 12" Component Joint Thermocouple Location

Table 9. Experimental Data—6 by 6 Inch Component Joints

Run No.	1	2	3	4	5
Date	10/26/64	10/26/64	10/26/64	10/26/64	10/27/64
Pressure, Torr	6×10^{-7}	6×10^{-7}	6×10^{-7}	6×10^{-7}	5×10^{-7}
Absolute T. C.					
1 - °F	85.7	95.3	107.1	119.0	85.3
2 - °F	80.2	85.6	91.6	97.8	79.8
3 - °F	74.0	74.5	74.5	74.3	73.8
4 - °F	74.1	74.8	75.0	75.0	74.0
Differential T. C.					
1 - °F	6.53	11.78	18.28	24.72	6.72
2 - °F	6.29	11.38	17.60	23.78	6.48
3 - °F	2.50	4.56	7.25	9.85	2.52
4 - °F	4.11	7.06	10.95	14.90	4.05
5 - °F	2.57	4.64	7.25	9.81	2.63
6 - °F	1.02	1.81	2.81	3.81	1.02
7 - °F	1.98	3.52	5.46	7.40	2.00
8 - °F	1.04	1.88	2.92	3.96	1.07
9 - °F	0.80	1.41	2.19	2.97	0.81
10 - °F	0.77	1.31	2.04	2.77	0.74
Voltage, volts	37.02	49.31	61.54	72.04	36.99
Current, amps	0.1314	0.1750	0.2185	0.2560	0.1313
Water Flow, ml/min	725	650	650	650	575
Bolt Torque, in-lb	24	24	24	24	24
Filler	None	None	None	None	None
Sample Number	1	1	1	1	1
Number of Bolts	12	12	12	12	12
h, Btu/hr ft^2 °F	23.1	22.9	23.0	22.3	22.8

Table 9. Experimental Data—6 by 6 Inch Component Joints (Continued)

Run Number	6	7	8	9	10
Date	10/27/64	10/27/64	10/27/64	10/28/64	10/28/64
Pressure, Torr	5×10^{-7}	5×10^{-7}	5×10^{-7}	6×10^{-7}	7×10^{-7}
Absolute T. C.					
1 - °F	95.1	107.5	118.5	105.5	117.5
2 - °F	85.2	92.3	97.3	89.9	102.3
3 - °F	74.1	74.3	73.3	73.2	74.7
4 - °F	74.5	75.0	74.1	73.6	89.1
Differential T. C.					
1 - °F	11.78	18.30	24.72	18.27	18.68
2 - °F	11.31	17.65	23.89	17.68	17.82
3 - °F	4.48	7.25	9.85	7.22	7.95
4 - °F	7.03	10.95	14.88	10.90	11.32
5 - °F	4.60	7.50	9.79	7.19	7.44
6 - °F	1.78	2.77	3.77	2.78	2.53
7 - °F	3.50	5.45	7.37	5.50	5.04
8 - °F	1.86	2.92	3.96	2.94	2.87
9 - °F	1.40	2.16	2.94	2.19	2.00
10 - °F	1.30	2.00	2.71	2.02	1.82
Voltage, volts	49.[illegible]3	61.54	72.02	61.53	61.52
Current, amps	0.1751	0.2185	0.2559	0.2185	0.2185
Water Flow, ml/min	525	525	525	1175	21
Bolt Torque, in-lb	24	24	24	24	24
Filler	None	None	None	None	None
Sample Number	1	1	1	1	1
Number of Bolts	12	12	12	12	12
h, Btu/hr ft^2 °F	23.2	22.9	23.1	23.0	22.8

Table 9. Experimental Data—6 by 6 Inch Component Joints (Continued)

Run Number	11	12	13	14	15
Date	10/29/64	10/29/64	10/29/64	10/29/64	10/30/64
Pressure, Torr	7×10^{-7}	7×10^{-7}	7×10^{-7}	7×10^{-7}	5×10^{-7}
Absolute T.C.					
1 - °F	85.0	94.2	105.7	117.8	84.8
2 - °F	79.8	84.9	91.9	97.5	79.5
3 - °F	73.8	73.9	73.7	73.6	73.6
4 - °F	74.0	74.3	74.3	74.4	73.6
Differential T.C.					
1 - °F	6.22	10.90	17.20	23.37	6.27
2 - °F	5.88	10.29	16.30	22.10	5.93
3 - °F	2.23	4.02	6.62	9.10	2.90
4 - °F	3.88	6.74	10.52	14.31	3.90
5 - °F	2.45	4.30	6.80	9.30	2.55
6 - °F	0.62	1.10	1.73	2.32	0.68
7 - °F	1.83	3.21	5.04	6.81	1.84
8 - °F	0.91	1.61	2.57	3.50	0.95
9 - °F	0.66	1.19	1.87	2.53	0.70
10 - °F	0.74	1.31	2.04	2.73	0.79
Voltage, volts	37.00	49.32	61.54	72.02	37.0
Current, amps	0.1313	0.1751	0.2185	0.2559	0.1313
Water Flow, ml/min	525	550	550	550	500
Bolt Torque, in-lb	30	30	30	30	18
Filler	None	None	None	None	None
Sample Number	1	1	1	1	1
Number of Bolts	12	12	12	12	12
h, Btu/hr ft^2 °F	25.0	25.2	24.8	25.0	23.9

Table 9. Experimental Data- -6 by 6 Inch Component Joints (Continued)

Run Number	16	17	18	19	20
Date	10/30/64	11/2/64	11/2/64	11/2/64	11/2/64
Pressure, Torr	5×10^{-7}	6×10^{-7}	6×10^{-7}	6×10^{-7}	6×10^{-7}
Absolute T. C.					
1 - °F	94.1	81.5	88.4	96.1	104.5
2 - °F	84.8	78.9	84.0	88.9	94.7
3 - °F	73.7	73.2	73.6	73.4	0.891
4 - °F	74.1	73.4	73.9	73.9	
Differential T. C.					
1 - °F	10.99	2.20	3.76	5.76	7.83
2 - °F	10.34	2.25	3.87	5.94	8.05
3 - °F	4.10	0.50	0.83	1.27	1.73
4 - °F	6.76	1.49	2.50	3.90	5.27
5 - °F	4.46	0.43	0.72	1.11	1.52
6 - °F	1.19	0.27	0.47	0.71	0.98
7 - °F	3.21	0.52	0.83	1.26	1.71
8 - °F	1.67	0.15	0.25	0.38	0.53
9 - °F	1.24	0.28	0.44	0.67	0.91
10 - °F	1.38	0.45	0.73	1.11	1.49
Voltage, volts	49.30	37.00	49.34	61.50	72.04
Current, amps	0.1750	0.1313	0.1751	0.2183	0.2558
Water Flow, ml/min	525	600	600	600	600
Bolt Torque, in-lb	18	24	24	24	24
Filler	None	RTV 11	RTV 11	RTV 11	RTV 11
Sample Number	1	1	1	1	1
Number of Bolts	12	12	12	12	12
h, Btu/hr ft^2 °F	24.6	76.9	81.5	82.5	83.2

Table 9. Experimental Data—6 by 6 Inch Component Joints (Continued)

Run Number	21	22	23	24	25
Date	11/6/64	11/6/64	11/9/64	11/9/64	11/9/64
Pressure, Torr.	8×10^{-7}	8×10^{-7}	9×10^{-7}	9×10^{-7}	9×10^{-7}
Absolute T. C.					
1 - °F	81.4	91.0	83.7	86.8	95.5
2 - °F	76.0	80.2	74.2	77.5	80.9
3 - °F	73.3	73.8	70.9	71.7	72.1
4 - °F	73.4	74.1	71.1	72.1	72.5
Differential T. C.					
1 - °F	5.76	11.60	5.69	9.82	15.25
2 - °F	5.11	10.29	5.06	8.71	13.56
3 - °F	2.88	5.85	2.87	4.92	7.65
4 - °F	2.29	4.62	2.23	3.82	5.96
5 - °F	0.65	1.32	0.45	0.76	1.18
6 - °F	1.36	2.76	1.26	2.17	3.38
7 - °F	0.95	1.97	0.91	1.55	2.44
8 - °F	0.48	1.02	0.44	0.74	1.17
9 - °F					
10 - °F					
Voltage, volts	37.03	53.01	37.01	49.33	61.53
Current, amps	0.1315	0.1883	0.1314	0.1752	0.2186
Water Flow, ml/min	1300	675	575	575	575
Bolt Torque, in-lb	12	12	24	24	24
Filler	None	None	None	None	None
Sample Number	2	2	2	2	2
Number of Bolts	12	12	12	12	12
h, Btu/hr ft² °F	24.7	28.5	29.1	30.1	30.1

Table 9. Experimental Data—6 by 6 Inch Component Joints (Continued)

Run Number	26	27	28	29	30
Date	11/9/64	11/10/64	11/13/64	11/17/64	11/17/64
Pressure, Torr.	9×10^{-7}	1×10^{-6}	1×10^{-6}	1×10^{-6}	1×10^{-6}
Absolute T.C.					
1 - °F	104.7	88.2	81.2	71.6	75.7
2 - °F	84.5	77.4	75.4	69.0	70.9
3 - °F	72.1	70.8	69.9	66.0	70.9
4 - °F	73.0	71.3	70.4	66.4	66.5
Differential T.C.					
1 - °F	20.93	11.30	3.78	1.80	3.08
2 - °F	18.57	10.09	3.38	1.61	2.76
3 - °F	10.51	5.74	1.38	0.63	1.11
4 - °F	8.19	4.50	0.72	0.31	0.58
5 - °F	1.63	0.84	0.29	0.21	0.36
6 - °F	4.62	2.54	0.20	0.091	0.20
7 - °F	3.34	1.78	0.26	0.095	0.20
8 - °F	1.63	0.89	0.26	0.091	0.27
9 - °F					
10 - °F					
Voltage, volts	72.03	53.01	53.03	37.02	49.31
Current, amps	0.2560	0.1883	0.1883	0.1314	0.1751
Water Flow, ml/min	575	575	575	625	600
Bolt Torque, in-lb	24	30	12	24	24
Filler	None	None	RTV 11	RTV 11	RTV 11
Sample Number	2	2	2	2	2
Number of Bolts	12	12	12	12	12
h, Btu/hr ft^2 °F	30.1	30.0	123.0	128.1	127.0

Table 9. Experimental Data—6 by 6 Inch Component Joints (Continued)

Run Number	31	32	33	34	35
Date	11/17/64	11/17/64	11/19/64	11/20/64	11/23/64
Pressure, Torr	1×10^{-6}	1×10^{-6}	7×10^{-7}	1×10^{-6}	1×10^{-6}
Absolute T.C.					
1 - °F	81.7	87.0	78.8	80.6	72.1
2 - °F	74.2	76.5	73.4	72.5	68.2
3 - °F	66.2	66.1	67.7	66.7	65.2
4 - °F	67.0	67.0	68.[illegible]	67.1	65.4
Differential T.C.					
1 - °F	4.72	6.39	3.39	7.25	3.62
2 - °F	4.25	5.77	3.04	6.20	1.29
3 - °F	1.73	2.35	1.12	3.12	1.57
4 - °F	0.89	1.24	0.54	2.22	1.07
5 - °F	0.51	0.67	0.31	0.37	0.19
6 - °F	0.30	0.41	0.17	0.93	0.45
7 - °F	0.29	0.37	0.17	0.53	0.23
8 - °F	0.44	0.65	0.30	0.42	0.15
9 - °F					
10 - °F					
Voltage, volts	61.51	72.05	53.01	52.99	37.00
Current Amps	0.2185	0.2560	0.1883	0.1879	0.1312
Water Flow, ml/min	600	600	600	600	460
Bolt Torque, in-lb	24	24	30	12	24
Filler	RTV 11	RTV 11	RTV 11	G 683	G 683
Sample Number	2	2	2	2	2
Number of Bolts	12	12	12	12	12
h, Btu/hr ft^2 °F	129.0	130.0	142.0	55.5	63.0

Table 9. Experimental Data—6 by 6 Inch Component Joints (Continued)

Run Number	36	37	38	39	40
Date	11/23/64	11/23/64	11/23/64	11/23/64	11/24/64
Pressure, Torr	1×10^{-6}	1×10^{-6}	1×10^{-6}	1×10^{-6}	5×10^{-7}
Absolute T.C.					
1 - °F	78.3	85.7	92.4	79.9	88.1
2 - °F	71.4	74.7	77.4	71.7	73.9
3 - °F	66.0	66.7	66.5	65.9	66.7
4 - °F	66.5	67.4	67.5	66.4	67.1
Differential T.C.					
1 - °F	6.20	9.46	12.83	7.15	13.58
2 - °F	2.07	3.11	4.15	6.15	13.37
3 - °F	2.72	4.17	5.63	2.99	6.59
4 - °F	1.86	2.88	3.89	2.37	4.72
5 - °F	0.33	0.52	0.67	0.33	1.07
6 - °F	0.77	1.17	1.56	0.72	3.35
7 - °F	0.42	0.66	0.87	0.44	2.22
8 - °F	0.34	0.56	0.77	0.34	1.18
9 - °F					
10 - °F					
Voltage, volts	49.31	61.53	72.04	52.96	52.96
Current, amps	0.1749	0.2183	0.2556	0.1878	0.1880
Water Flow, ml/min	460	460	460	475	560
Bolt Torque, in-lb	24	24	24	30	12
Filler	G 683	G 683	G 683	G 683	None
Sample Number	2	2	2	2	3
Number of Bolts	12	12	12	12	12
h, Btu/hr ft^2 °F	65.0	66.1	67.1	57.0	24.8

Table 9. Experimental Data—6 by 6 Inch Component Joints (Continued)

Run Number	41	42	43	44	45
Date	11/24/64	11/25/64	11/25/64	11/25/64	11/25/64
Pressure, Torr	5×10^{-7}	5×10^{-6}	5×10^{-6}	5×10^{-7}	5×10^{-7}
Absolute T.C.					
1 - °F	92.6	88.4	92.7	77.5	85.0
2 - °F	81.8	74.9	75.0	70.7	72.9
3 - °F	66.6	65.9	66.4	66.8	66.2
4 - °F	67.0	66.4	66.9	67.0	66.7
Differential T.C.					
1 - °F	17.64	14.32	18.42	6.70	11.50
2 - °F	17.70	13.93	18.45	6.65	11.44
3 - °F	11.94	7.36	10.19	3.17	5.45
4 - °F	7.46	4.97	10.59	2.26	3.92
5 - °F	1.80	1.11	9.44	4.78	0.80
6 - °F	7.80	4.26	7.95	1.57	2.67
7 - °F	10.18	3.26	3.64	0.93	1.65
8 - °F	10.40	2.53	1.61	0.49	0.92
9 - °F					
10 - °F					
Voltage, volts	52.96	52.95	52.95	37.01	49.32
Current, amps	0.1880	0.1880	0.1880	0.1313	0.1751
Water Flow, ml/min	700	575	550	625	625
Bolt Torque, in-lb	24	24	24	24	24
Filler	None	None	None	None	None
Sample Number	3	3	3	3	3
Number of Bolts	4*	8*	8*	12	12
h, Btu/hr ft^2 °F	13.4	22.0	13.7	22.1	25.9

*See Appendix VI.

Table 9. Experimental Data—6 by 6 Inch Component Joints (Continued)

Run Number	46	47	48	49	50
Date	11/27/64	11/27/64	11/30/64	12/3/64	12/3/64
Pressure, Torr	5×10^{-7}	5×10^{-7}	6×10^{-7}	4×10^{-7}	4×10^{-7}
Absolute T. C.					
1 - °F	94.6	105.5	81.8	73.0	79.1
2 - °F	75.7	79.6	72.7	68.8	71.5
3 - °F	65.4	65.5	66.0	65.3	65.8
4 - °F	66.0	66.4	66.5	65.6	66.3
Differential T. C.					
1 - °F	17.67	23.95	5.63	2.63	4.54
2 - °F	17.59	23.80	6.21	3.00	5.14
3 - °F	8.36	11.31	1.81	0.76	1.32
4 - °F	6.02	8.20	0.75	0.27	0.45
5 - °F	1.26	1.69	0.24	0.14	0.21
6 - °F	4.14	5.60	0.24	0.13	0.20
7 - °F	2.59	3.54	0.24	0.12	0.23
8 - °F	1.49	2.02	0.37	0.05	0.23
9 - °F					
10 - °F					
Voltage, volts	61.52	72.06	53.01	37.00	49.34
Current, amps	0.2184	0.2560	0.1881	0.1313	0.1751
Water Flow, ml/min	600	600	600	550	550
Bolt Torque, in-lb	24	24	12	24	24
Filler	None	None	RTV 11	RTV 11	RTV 11
Sample Number	3	3	3	3	3
Number of Bolts	12	12	12	12	12
h, Btu/hr ft^2 °F	26.2	26.6	84.1	91.0	93.5

Table 9. Experimental Data — 6 by 6 Inch Component Joints (Continued)

Run Number	51	52	53	54
Date	12/3/64	12/3/64	12/4/64	12/4/64
Pressure, Torr	4×10^{-7}	4×10^{-7}	5×10^{-7}	2×10^{-6}
Absolute T. C.				
1 - ^{o}F	86.8	94.9	83.5	75.6
2 - ^{o}F	74.8	78.5	72.2	70.0
3 - ^{o}F	66.2	66.2	65.6	66.7
4 - ^{o}F	66.9	67.1	66.0	67.0
Differential T. C.				
1 - ^{o}F	6.95	9.44	8.95	4.52
2 - ^{o}F	7.86	10.62	9.19	4.48
3 - ^{o}F	2.03	2.77	3.22	1.59
4 - ^{o}F	0.70	0.96	2.25	1.09
5 - ^{o}F	0.30	0.40	0.26	0.12
6 - ^{o}F	0.29	0.40	0.92	0.42
7 - ^{o}F	0.37	0.52	0.70	0.28
8 - ^{o}F	0.44	0.67	0.42	0.11
9 - ^{o}F				
10 - ^{o}F				
Voltage, volts	61.54	72.05	53.01	37.05
Current, amps	0.2184	0.2558	0.1878	0.1312
Water Flow, ml/min	550	550	650	600
Bolt Torque, in-lb	24	24	12	24
Filler	RTV 11	RTV 11	G 683	G 683
Sample Number	3	3	3	3
Number of Bolts	12	12	12	12
h, Btu/hr ft^2 ^{o}F	94.8	95.4	47.0	47.3

Table 9. Experimental Data—6 by 6 Inch Component Joints (Continued)

Run Number	55	56	57	58
Date	12/4/64	12/7/64	12/7/64	12/8/64
Pressure, Torr	5×10^{-8}	1×10^{-6}	1×10^{-6}	5×10^{-7}
Absolute T. C.				
1 - °F	81.9	88.0	97.1	71.0
2 - °F	72.9	72.9	76.4	66.3
3 - °F	63.5	63.5	63.8	63.1
4 - °F	64.3	63.4	64.7	63.5
Differential T. C.				
1 - °F	7.70	11.80	15.93	3.12
2 - °F	7.74	11.88	16.05	3.25
3 - °F	2.76	4.25	5.74	0.85
4 - °F	1.91	2.98	4.02	0.48
5 - °F	0.22	0.36	0.48	0.15
6 - °F	0.74	1.09	1.48	0.18
7 - °F	0.54	0.81	1.10	0.73
8 - °F	0.33	0.51	0.76	0.
9 - °F				
10 - °F				
Voltage, volts	49.36	61.52	72.04	37.02
Current, amps	0.1748	0.2180	0.2554	0.1311
Water Flow, ml/min	600	500	500	525
Bolt Torque, in-lb	24	24	24	24
Filler	G 683	G 683	G 683	G 641
Sample Number	3	3	3	3
Number of Bolts	12	12	12	12
h, Btu/hr ft^2 °F	48.2	48.8	49.5	77.5

Table 9. Experimental Data—6 by 6 Inch Component Joints (Continued)

Run Number	59	60	61
Date	12/8/64	12/8/64	12/8/64
Pressure, Torr	5×10^{-7}	5×10^{-7}	5×10^{-7}
Absolute T.C.			
1 - °F	77.8	85.8	93.8
2 - °F	69.7	73.2	76.8
3 - °F	63.9	64.5	64.8
4 - °F	64.4	65.2	65.8
Differential T.C.			
1 - °F	5.36	8.20	11.10
2 - °F	5.58	8.56	11.56
3 - °F	1.47	2.27	3.07
4 - °F	0.85	1.34	1.81
5 - °F	0.22	0.32	0.40
6 - °F	0.33	0.51	0.70
7 - °F	0.20	0.37	0.54
8 - °F	0.19	0.45	0.69
9 - °F			
10 - °F			
Voltage, volts	49.35	61.52	72.02
Current, amps	0.1748	0.2180	0.2553
Water Flow, ml/min	525	525	525
Bolt Torque, in-lb	24	24	24
Fi er	G 641	G 641	G641
Sample Number	3	3	3
Number of Bolts	12	12	12
h, Btu/hr ft^2 °F	79.0	79.0	79.5

Table 10. Experimental Data—6 by 12 Inch Component Joints

Run Number	62	63	64	65	66
Date	12/9/64	12/9/64	12/9/64	12/10/64	12/10/64
Pressure, Torr	3×10^{-7}	3×10^{-7}	3×10^{-7}	5×10^{-7}	5×10^{-7}
Absolute T. C.					
1 - °F	74.4	84.9	106.0	74.9	70.0
2 - °F	67.7	71.6	79.0	68.1	66.7
3 - °F	63.3	63.9	63.5	64.0	64.5
4 - °F	64.3	64.8	65.2	64.6	64.9
Differential T. C.					
1 - °F	2.43	5.93	8.94	3.07	1.35
2 - °F	1.94	3.87	7.90	1.9	0.98
3 - °F	5.83	11.57	23.50	5.87	2.94
4 - °F	5.22	10.40	22.02	5.17	2.59
5 - °F	3.15	11.71	29.30	7.22	3.64
6 - °F	2.49	4.95	10.20	2.47	1.24
7 - °F	0.73	1.43	2.85	0.75	0.39
8 - °F	1.33	2.61	5.37	1.31	0.66
9 - °F	0.50	1.00	2.09	0.51	0.25
Voltage, volts	35.48	50.00	70.70	35.47	25.00
Currents, amps	0.2837	0.4000	0.5667	0.2840	0.2001
Water Flow, ml/min	575	600	600	550	550
Bolt Torque, in-lb	24	24	24	24	24
Filler	None	None	None	None	None
Sample Number	1	1	1	1	1
Number of Bolts	18	18	18	18	18
h, Btu/hr ft^2 °F	22.7	19.5	18.5	18.5	18.5

Table 10. Experimental Data — 6 by 12 Inch Component Joints

Run Number	67	68	69	70	71
Date	12/10/64	12/14/64	12/14/64	12/14/64	12/17/64
Pressure, Torr.	5×10^{-7}	4×10^{-7}	4×10^{-7}	4×10^{-7}	6×10^{-7}
Absolute T.C.					
1 - °F	86.5	70.4	76.0	88.3	68.6
2 - °F	73.3	67.9	70.8	77.6	65.2
3 - °F	65.2	64.6	65.0	66.5	62.0
4 - °F	66.2	65.1	65.9	67.7	62.6
Differential T.C.					
1 - °F	4.72	0.32	0.66	1.68	0.64
2 - °F	3.86	0.22	0.44	0.95	0.28
3 - °F	11.60	1.25	2.52	5.26	1.27
4 - °F	10.37	1.06	2.09	4.24	1.05
5 - °F	14.36	1.55	3.06	6.15	1.42
6 - °F	4.95	0.22	0.48	1.02	0.15
7 - °F	1.46	0.19	0.37	0.80	0.08
8 - °F	2.60	0.18	0.41	0.91	0.04
9 - °F	1.02	0.12	0.29	0.61	
Voltage, volts	50.00	35.47	50.00	70.73	35.49
Current, amps	0.4005	0.2839	0.4004	0.5669	0.2822
Water Flow, ml/min	550	625	625	625	575
Bolt Torque, in-lb	24	24	24	24	24
Filler	None	RTV 11	RTV 11	RTV 11	RTV 11
Sample Number	1	1	1	1	2
Number of Bolts	18	18	18	18	18
h, Btu/hr ft^2 °F	18.9	103.0	101.5	98.0	103.0

Table 10. Experimental Data—6 by 12 Inch Component Joints (Continued)

Run Number	72	73	74	75	76
Date	12/17/64	12/17/64	12/21/64	12/21/64	12/21/64
Pressure, Torr.	6×10^{-7}	6×10^{-7}	6×10^{-7}	6×10^{-7}	6×10^{-7}
Absolute T. C.					
1 - °F	75.5	88.5	67.5	73.5	86.2
2 - °F	68.8	75.0	64.2	67.0	73.4
3 - °F	62.6	62.8	61.1	61.1	61.6
4 - °F	63.6	64.8	61.6	61.9	63.3
Differential T. C.					
1 - °F	1.37	2.85	0.71	1.41	2.88
2 - °F	0.59	1.21	0.27	0.52	1.05
3 - °F	2.52	5.50	1.26	2.48	5.02
4 - °F	2.13	4.30	1.21	2.37	4.74
5 - °F	2.86	5.76	1.79	3.51	7.05
6 - °F	0.33	0.71	0.17	0.30	0.57
7 - °F	0.12	0.23	0.11	0.20	0.36
8 - °F	0.11	0.26	0.16	0.30	0.61
9 - °F		0	0.08	0.17	0.38
Voltage, volts	50.02	70.64	35.48	50.01	70.71
Current, amps	0.3980	0.5628	0.2834	0.3995	0.5651
Water Flow, ml/min	575	575	650	650	650
Bolt Torque, in-lb	24	24	24	24	24
Filler	RTV 11	RTV 11	RTV 11	RTV 11	RTV 11
Sample Number	2	2	3	3	3
Number of Bolts	18	18	18	18	18
h, Btu/hr ft^2 °F	101.0	97.0	90.0	92.0	92.0

Table 11. Experimental Data—12 by 12 Inch Component Joint

Run	77	78	79	80
Date	12/22/64	12/22/64	12/22/64	12/28/64
Pressure, Torr	4×10^{-7}	4×10^{-7}	4×10^{-7}	6×10^{-7}
Absolute T. C.				
1 - °F	80.5	100.2	138.6	69.9
2 - °F	66.3	71.6	82.3	65.6
3 - °F	61.1	60.9	61.4	61.8
4 - °F	62.0	62.8	65.2	62.8
Differential T. C.				
1 - °F	0.58	0.92	1.64	0.51
2 - °F	1.89	3.85	7.73	0.28
3 - °F	1.35	2.75	5.19	0.18
4 - °F	3.29	6.75	13.40	0.10
5 - °F	12.10	24.50	48.60	1.49
6 - °F	16.42	33.20	65.80	3.14
7 - °F	1.30	2.69	5.36	0.12
8 - °F	5.78	11.59	22.90	0.70
Voltage, volts	29.60	41.90	59.20	29.61
Current, amps	0.6753	0.9543	1.3407	0.6748
Water Flow, ml/min	550	550	550	600
Bolt Torque, in-lb	24	24	24	24
Filler	None	None	None	RTV 11
Sample Number	1	1	1	1
Number of Bolts	24	24	24	24
h, Btu/hr ft^2 °F	8.36	8.32	8.34	56.6

Table 11. Experimental Data—12 by 12 Inch Component Joint (Continued)

Run	81	82	83	84
Date	12/28/64	12/28/64	1/5/65	1/5/65
Pressure, Torr	6×10^{-7}	6×10^{-7}	8×10^{-8}	8×10^{-7}
Absolute T.C.				
1 - °F	77.7	93.3	68.7	77.3
2 - °F	69.0	76.0	64.5	69.5
3 - °F	61.5	61.7	60.5	61.4
4 - °F	63.4	65.3	61.7	63.5
Differential T.C.				
1 - °F	0.72	0.98	0.31	0.53
2 - °F	0.53	1.04	0.20	0.37
3 - °F	0.37	0.68	0.20	0.35
4 - °F	0.22	0.48	0.12	0.20
5 - °F	2.95	5.91	1.74	3.39
6 - °F	6.25	12.41	2.76	5.42
7 - °F	0.27	0.55	0.14	0.25
8 - °F	1.48	2.94	1.06	2.10
Voltage, volts	41.83	59.22	29.59	41.84
Current, amps	0.9527	1.3460	0.6747	0.9521
Water Flow, ml/min	600	600	550	550
Bolt Torque, in-lb	24	24	24	24
Filler	RTV 11	RTV 11	RTV 11	RTV 11
Sample Number	1	1	2	2
Number of Bolts	24	24	24	24
h, Btu/hr ft^2 °F	55.8	56.1	51.7	52.8

Table 11. Experimental Data — 12 by 12 Inch Component Joint (Continued)

Run	85	86	87	88
Date	1/5/65	1/7/65	1/7/65	1/8/65
Pressure, Torr	8×10^{-7}	8×10^{-7}	8×10^{-7}	5×10^{-7}
Absolute T. C.				
1 - °F	95.6	69.0	76.9	92.7
2 - °F	79.2	64.8	68.3	75.7
3 - °F	63.4	60.6	60.4	59.1
4 - °F	67.1	61.6	62.3	63.3
Differential T. C.				
1 - °F	1.06	0.42	0.57	0.87
2 - °F	0.77	0.17	0.32	0.66
3 - °F	0.65	0.13	0.28	0.60
4 - °F	0.37	-	-	-
5 - °F	6.80	1.89	3.76	7.54
6 - °F	10.80	2.91	5.72	11.40
7 - °F	0.63	0.14	0.30	0.64
8 - °F	4.64	0.93	1.85	3.58
Voltage, volts	59.26	29.[illegible]	41.85	59.25
Current, amps	1.3435	0.6750	0.9518	1.3440
Water Flow, ml/min	550	550	550	500
Bolt Torque, in-lb	24	24	24	24
Filler	RTV 11	RTV 11	RTV 11	RTV 11
Sample Number	2	3	3	3
Number of Bolts	24	24	24	24
h, Btu/hr ft^2 °F	51.0	51.4	51.9	52.4

APPENDIX II

STRUCTURAL JOINT TESTS

The experimental data for structural joint configuration No. 1 (Figure 3 of main report) is given in Table 12 of this appendix. The location of thermocouples is shown in Figures 34 and 35. The average ΔT for each joint, called "a" and "b," was obtained by dividing the joint area into zones. Two zones were used, a one inch square zone at each bolt, with the bolt in the center, and the remaining area as the other zone. The water flow rate and temperatures were monitored as in the component joints, and absolute thermocouples 2 and 3 measure inlet and outlet temperatures respectively. For run number 1, the conductance calculation for joint "a" is as follows:

$$\overline{\Delta T}_{①} = 3.56^{\circ}F$$

$$\overline{\Delta T}_{②} = \frac{6.10 + 8.17}{2} = 7.13^{\circ}F$$

$$\overline{\Delta T}_M = \frac{A_1}{A_T}\overline{\Delta T}_1 + \frac{A_2}{A_T}\overline{\Delta T}_2$$

$$\overline{\Delta T}_M = \frac{2}{6}(3.56) + \frac{4}{6}(7.13)$$

$$\overline{\Delta T}_M = 5.95^{\circ}F$$

$$Q_{IN} = 22.05(0.2310) = 5.099 \text{ watts}$$

$$= 17.4 \text{ Btu/hr}$$

$$h_a = \frac{Q}{A\overline{\Delta T}_M}$$

$$h_a = \frac{17.4}{\frac{6}{144} \times 5.95} = 70.3 \text{ Btu/hr ft}^2\ {}^{\circ}F$$

Thermocouples 1, 2, and 3 are used to calculate the conductance of joint "a," h_a, and thermocouples 6, 7, and 8 to calculate the conductance of joint "b," h_b.

Table 13 lists the experimental data for structural joint configuration 2. The thermocouple locations are shown in Figures 34 and 35. This configuration utilizes nut plates on one joint, called joint "b" in Table 13.

The results for configuration 3 are shown in Table 14, and the thermocouple locations in Figures 36 and 37. Differential thermocouples are located at the same (x, y) coordinates on the back of the angle brackets and panels at the locations shown on Figures 34, 35, 36, and 37.

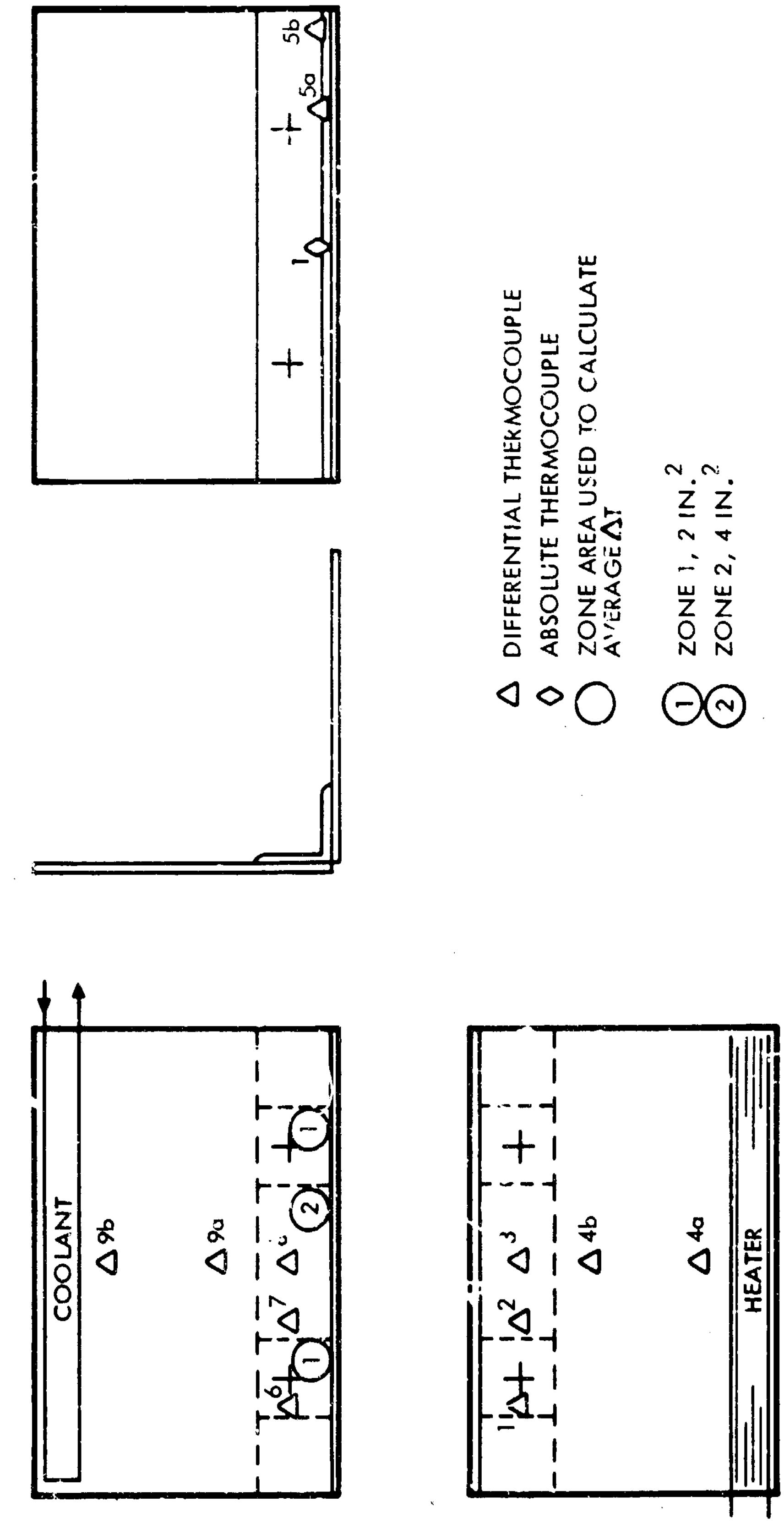

Figure 34. 6 Inch Structural Joint, Configurations 1 and 2, Thermocouple Locations

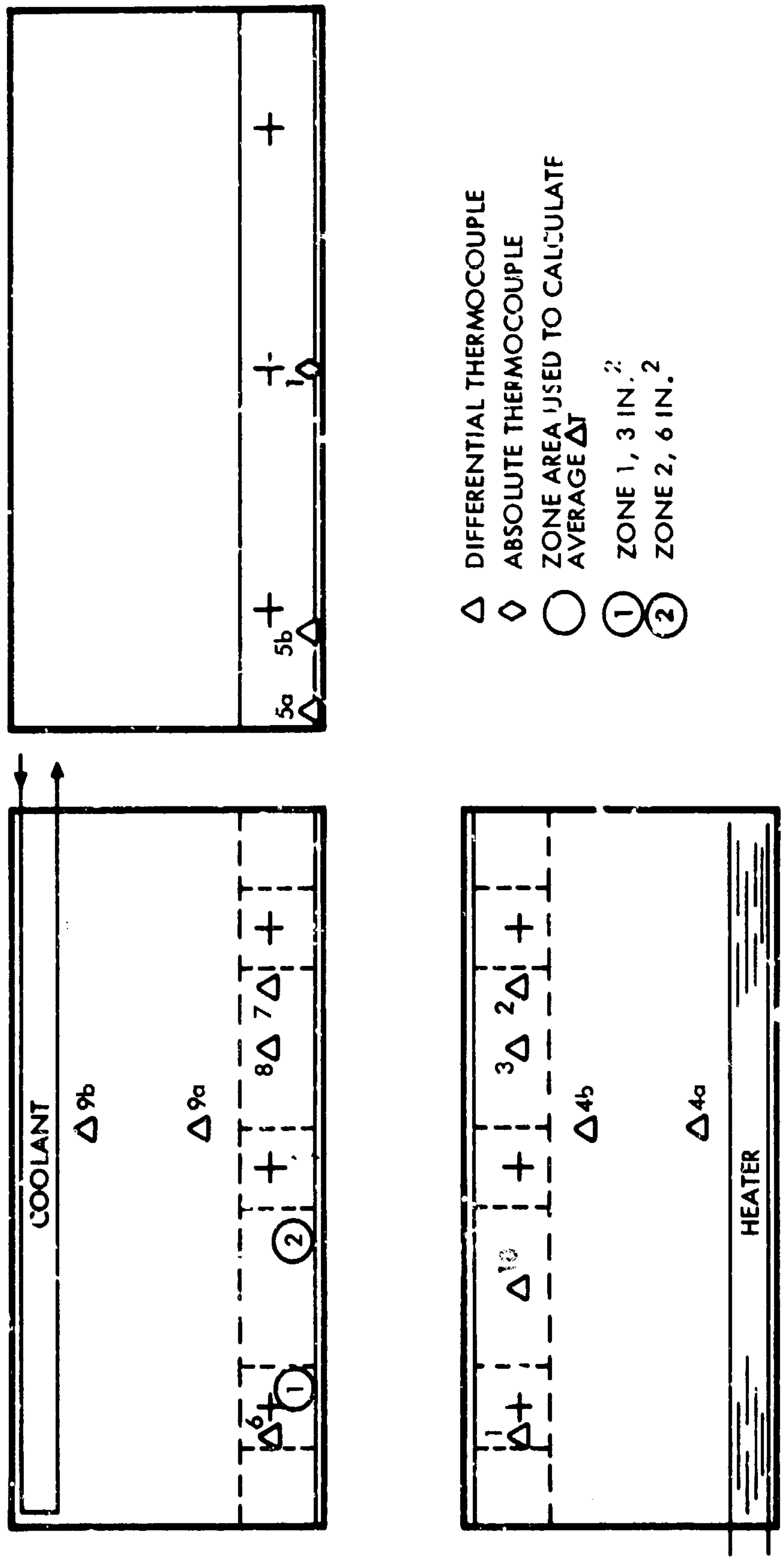

Figure 35. 9 Inch Structural Joint, Configurations 1 and 2, Thermocouple Locations

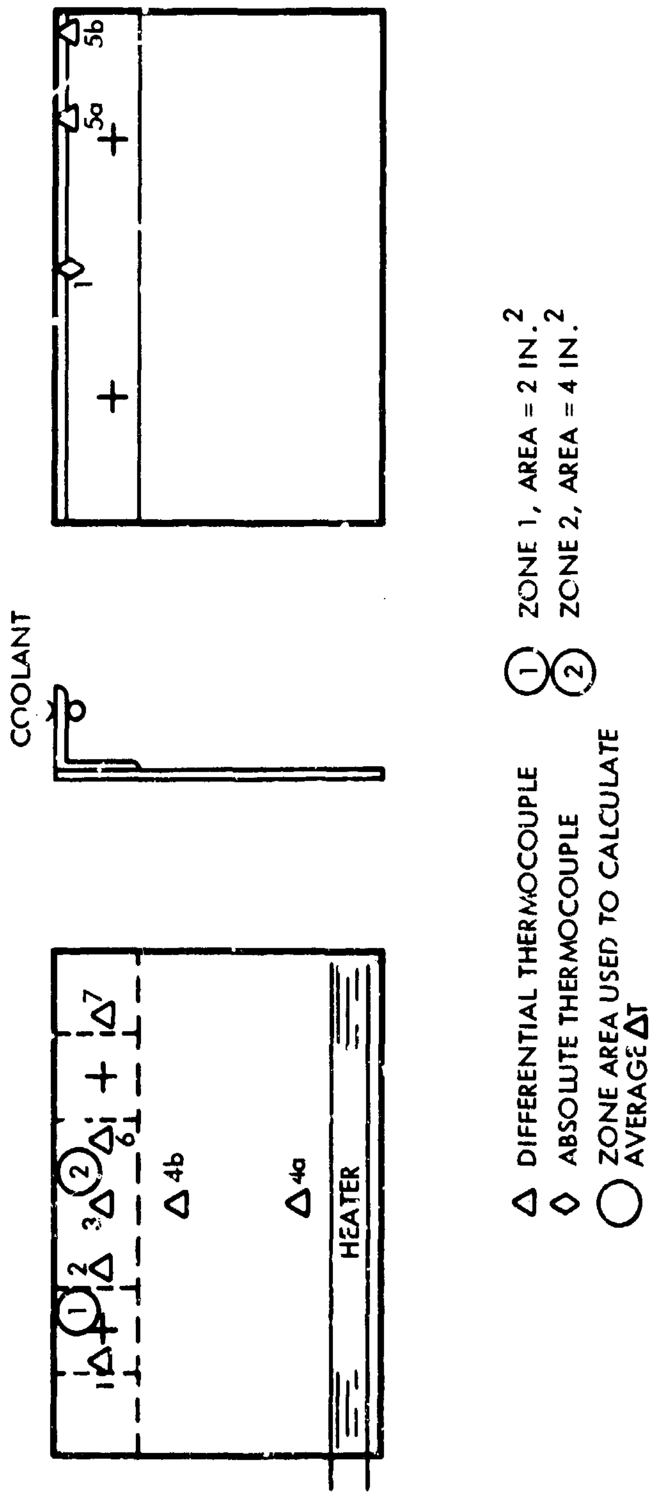

Figure 36. 6 Inch Structural Joint, Configuration 3. Thermocouple Locations

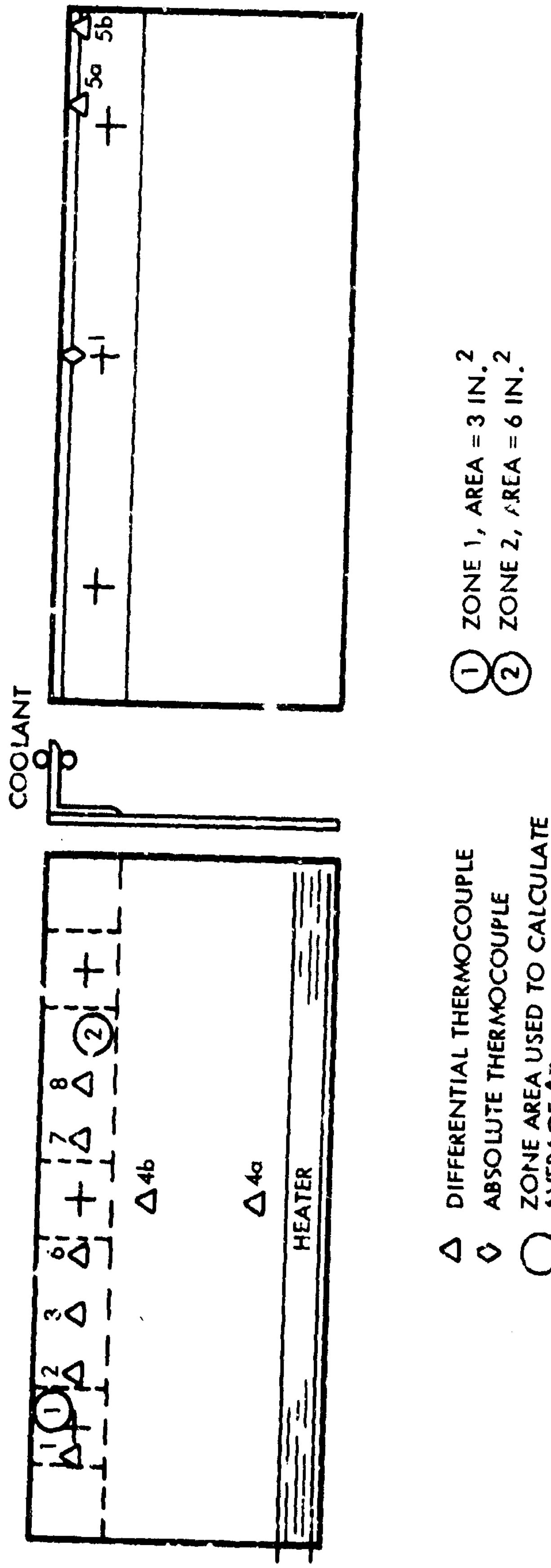

Figure 37. 9 Inch Structural Joint, Configuration 3, Thermocouple Locations

Table 12. Experimental Data — Structural Joint Configuration 1

Run Number	1	2	3	4	5
Date	2/16/65	2/16/65	2/16/65	2/17/65	3/1/65
Pressure, Torr	2×10^{-6}	2×10^{-6}	2×10^{-6}	1×10^{-6}	1×10^{-6}
Absolute T. C.					
1 - °F	93.0	126.2	158.4	196.7	88.0
2 - °F	63.5	63.8	63.0	60.2	63.1
3 - °F	63.9	64.4	63.9	61.4	63.5
Differential T. C.					
1 - °F	3.56	7.46	11.32	16.00	0.22
2 - °F	6.10	12.48	18.32	25.55	0.54
3 - °F	8.17	17.05	26.55	37.70	0.45
4 - °F	7.89	16.82	26.30	36.95	7.95
5 - °F	0.50	0.97	1.51	2.13	0.06
6 - °F	3.30	7.00	10.72	14.90	0.20
7 - °F	5.11	11.47	17.60	23.93	0.33
8 - °F	7.24	14.72	23.28	31.60	0.65
9 - °F	6.72	13.88	21.44	30.10	7.30
10 - °F					
Voltage, volts	22.05	32.21	40.17	48.17	22.00
Current, amps	0.2310	0.3376	0.4216	0.5061	0.2306
Water Flow, ml/min	750	750	750	550	700
Bolt Torque, in-lb	24	24	24	24	24
Filler	None	None	None	None	RTV 11
Sample Number	1	1	1	1	1
Joint Length, in.	6	6	6	6	6
Number of Bolts	2	2	2	2	2
h_a, Btu/hr ft^2 °F	70.3	72.0	74.2	75.7	1042
h_b, Btu/hr ft^2 °F	80.5	80.6	80.6	85.3	1042

Table 12. Experimental Data—Structural Joint Configuration 1 (Continued)

Run Number	6	7	8	9	10
Date	3/1/65	3/1/65	2/19/65	2/19/65	2/19/65
Pressure, Torr	1×10^{-6}	1×10^{-6}	1×10^{-6}	1×10^{-6}	1×10^{-6}
Absolute T. C.					
1 - °F	141.0	176.6	88.4	149.8	184.9
2 - °F	62.8	62.6	61.1	62.3	61.3
3 - °F	63.6	63.7	61.6	63.1	62.5
Differential T. C.					
1 - °F	0.88	2.30	2.58	8.25	11.31
2 - °F	1.95	3.36	4.08	14.20	20.52
3 - °F	1.64	2.77	5.44	18.88	27.42
4 - °F	25.10	38.60	8.06	26.22	37.95
5 - °F	0.33	2.75	0	0.04	0.13
6 - °F	0.68	0.82	3.50	11.24	15.88
7 - °F	1.08	2.05	4.50	14.80	19.80
8 - °F	2.28	3.89	6.17	19.93	26.08
9 - °F	22.58	33.75	7.82	24.17	34.85
10 - °F					
Voltage, volts	39.52	48.40	22.01	39.99	47.92
Current, amps	0.4149	0.5085	0.2319	0.4223	0.5067
Water Flow, ml/min	700	700	650	650	650
Bolt Torque, in-lb	24	24	24	24	24
Filler	RTV 11	RTV 11	None	None	None
Sample Number	1	1	2	2	2
Joint Length, in.	6	6	6	6	6
Number of Bolts	2	2	2	2	2
h_a, Btu/hr ft^2 °F	906	715	103.5	100.1	100.9
h_b, Btu/hr ft^2 °F	995	895	88.5	90	96.5

Table 12. Experimental Data —Structural Joint Configuration 1 (Continued)

Run Number	11	12	13	14	15
Date	3/5/65	3/5/65	3/8/65	3/9/65	3/9/65
Pressure, Torr	2×10^{-6}	2×10^{-6}	1×10^{-6}	8×10^{-7}	8×10^{-7}
Absolute T. C.					
1 - °F	90.5	142.5	192.1	87.7	134.7
2 - °F	63.5	63.4	62.9	62.8	62.5
3 - °F	63.9	64.1	64.0	63.1	63.1
Differential T. C.					
1 - °F	7.12	21.30	35.8	0.50	1.50
2 - °F	5.98	18.07	30.82	0.75	2.44
3 - °F	2.61	7.99	13.70	0.77	2.27
4 - °F	7.21	21.42	36.0	7.92	23.70
5 - °F	1.74	4.96	7.85	0.35	1.02
6 - °F	7.21	21.05	32.65	0	0.07
7 - °F	5.87	17.37	28.5	0.65	2.08
8 - °F	2.84	8.36	14.4	1.16	3.53
9 - °F	6.98	20.05	33.15	6.98	20.47
10 - °F	1.37	3.84	5.49		
Voltage, volts	21.58	37.50	48.22	21.83	37.83
Current, amps	0.2327	0.4050	0.5217	0.2289	0.3972
Water Flow, ml/min	675	675	700	750	750
Bolt Torque, in-lb	24	24	24	24	24
Filler	None	None	None	G 683	G 683
Sample Number	3	3	3	1	1
Joint Length, in.	6	6	6	6	6
Number of Bolts	2	2	2	2	2
h_a, Btu/hr ft^2 °F	78.5	79.4	77.0	602	595
h_b, Btu/hr ft^2 °F	77.5	79.8	81.9	681	652

Table 12. Experimental Data — Structural Joint Configuration 1 (Continued)

Run Number	16	17	18	19
Date	3/9/65	3/15/65	3/16/65	3/16/65
Pressure, Torr	8×10^{-7}	8×10^{-7}	6×10^{-7}	6×10^{-7}
Absolute T. C.				
1 - °F	176.5	88.5	138.9	189.1
2 - °F	62.7	62.5	62.2	62.6
3 - °F	63.8	63.0	63.3	64.2
Differential T. C.				
1 - °F	2.48	1.96	7.85	12.53
2 - °F	4.59	4.05	13.85	22.80
3 - °F	3.82	4.59	15.75	25.65
4 - °F	37.45	8.62	26.40	43.30
5 - °F	1.66	1.21	4.55	7.48
6 - °F	0.21	3.64	11.28	18.70
7 - °F	3.26	6.02	18.05	28.85
8 - °F	5.71	6.57	19.58	31.45
9 - °F	31.90	7.70	23.25	37.20
10 - °F		3.86	13.80	21.77
Voltage, volts	47.80	19.44	33.73	43.55
Current, amps	0.5024	0.3841	0.6672	0.8623
Water Flow, ml/min	750	700	625	625
Bolt Torque, in-lb	24	24	24	24
Filler	G 683	None	None	None
Sample Number	1	1	1	1
Joint Length, in.	6	9	9	9
Number of Bolts	2	3	3	3
h_a, Btu/hr ft^2 °F	542	116	98.5	100.8
h_b, Btu/hr ft^2 °F	645	74	75.3	77.9

Table 13. Experimental Data — Structural Joint Configuration 2

Run Number	20	21	22	23	24
Date	3/23/65	3/23/65	3/23/65	3/25/65	3/25/65
Pressure, Torr	5×10^{-7}	5×10^{-7}	5×10^{-7}	7×10^{-7}	7×10^{-7}
Absolute T. C.					
1 - °F	87.8	134.[illegible]	178.8	89.3	140.4
2 - °F	63.7	64.4	64.0	63.5	64.2
3 - °F	64.0	65.0	65.0	63.9	64.9
Differential T. C.					
1 - °F	2.61	8.02	12.75	2.14	6.53
2 - °F	5.20	16.10	25.80	3.93	12.42
3 - °F	6.79	20.95	33.75	5.55	17.25
4 - °F	8.03	24.35	38.65	7.37	21.60
5 - °F	-0.11	-0.23	0.05	0.35	0.94
6 - °F	3.32	9.70	15.35	3.53	10.44
7 - °F	3.75	10.81	16.33	5.25	15.20
8 - °F	5.35	15.91	24.62	6.72	19.88
9 - °F	7.24	21.40	34.10	7.07	20.22
10 - °F					
Voltage, volts	21.89	37.85	48.97	21.88	37.99
Current, amps	0.2284	0.3956	0.5126	0.2279	0.3964
Water Flow, ml/min	775	775	775	625	625
Bolt Torque, in-lb	24	24	24	24	24
Filler	None	None	None	None	None
Sample Number	1	1	1	2	2
Joint Length, in.	6	6	6	6	6
Number of Bolts	2	2	2	2	2
h_a, Btu/hr ft^2 °F	94.2	81.5	85.0	105.5	102.0
h_b, Btu/hr ft^2 °F	99.0	100.8	1[illegible].3	82.4	91.4

Table 13. Experimental Data — Structural Joint Configuration (Continued)

Run Number	25	26	27	28
Date	3/25/65	3/26/65	3/26/65	3/29/65
Pressure, Torr	7×10^{-7}	3×10^{-6}	3×10^{-6}	2×10^{-6}
Absolute T. C.				
1 - °F	188.6	94.0	149.7	206.2
2 - °F	63.8	64.7	64.5	64.8
3 - °F	65.1	65.0	65.2	65.8
Differential T. C.				
1 - °F	1[illegible].05	2.54	8.00	12.35
2 - °F	20.80	4.89	14.73	23.78
3 - °F	29.35	6.41	19.12	31.00
4 - °F	34.70	7.35	21.92	37.80
5 - °F	1.53	1.02	2.50	3.65
6 - °F	17.48	3.69	10.81	17.25
7 - °F	24.20	4.31	1[illegible].94	18.55
8 - °F	32.45	5.24	14.55	23.10
9 - °F	32.80	6.91	19.87	32.10
10 - °F				
Voltage, volts	49.00	21.86	37.75	48.88
Current, amps	0.5121	0.2308	0.3993	0.5179
Water Flow, ml/min	550	750	700	650
Bolt Torque, in-lb	24	24	24	24
Filler	None	None	None	None
Sample Number	2	3	3	3
Joint Length, in.	6	6	6	6
Number of Bolts	2	2	2	2
h_a, Btu/hr ft^2 °F	100.8	89.5	88.5	92.6
h_b, Btu/hr ft^2 °F	83.2	93.5	[illegible]9.3	105.2

Table 13. Experimental Data — Structural Joint Configuration 2 (Continued)

Run Number	29	30	31	32
Date	3/31/65	3/31/65	3/31/65	4/1/65
Pressure, Torr	7×10^{-7}	7×10^{-7}	7×10^{-7}	1×10^{-6}
Absolute T. C.				
1 - °F	84.2	124.7	165.0	84.0
2 - °F	63.3	63.5	63.5	62.7
3 - °F	63.6	64.1	64.7	63.0
Differential T. C.				
1 - °F	0.70	2.51	4.46	0.95
2 - °F	0.07	0.08	0.34	0.67
3 - °F	0.09	0.40	1.05	1.17
4 - °F	7.73	22.85	37.85	7.53
5 - °F	0.33	0.91	1.37	0.20
6 - °F	0.48	1.50	2.19	0.54
7 - °F	0.64	1.90	3.70	0.80
8 - °F	1.24	3.72	6.65	2.24
9 - °F	7.42	21.50	34.75	7.49
10 - °F				
Voltage, volts	21.93	37.87	48.93	21.83
Current, amps	0.2289	0.3958	0.5120	0.2279
Water Flow, ml/min	650	650	650	575
Bolt Torque, in-lb	24	24	24	24
Filler	RTV 11	RTV 11	RTV 11	G 683
Sample Number	1	1	1	1
Joint Length, in.	6	6	6	6
Number of Bolts	2	2	2	2
h_a, Btu/hr ft^2 °F	1427	1227	1050	438
h_b, Btu/hr ft^2 °F	520	514	490	341

Table 13. Experimental Data—Structural Joint Configuration 2 (Continued)

Run Number	33	34	35	36
Date	4/1/65	4/2/65	4/5/65	4/5/65
Pressure, Torr	1×10^{-6}	7×10^{-7}	1×10^{-6}	1×10^{-6}
Absolute T. C.				
1 - °F	126.0	167.2	88.8	137.0
2 - °F	62.9	63.1	64.2	65.1
3 - °F	63.8	64.5	64.6	66.0
Differential T. C.				
1 - °F	3.54	6.13	2.78	8.04
2 - °F	1.89	3.10	4.03	11.92
3 - °F	3.33	5.44	6.31	18.92
4 - °F	22.40	36.95	8.51	26.80
5 - °F	0.50	0.91	0.25	0.74
6 - °F	1.73	2.66	2.76	8.35
7 - °F	2.44	3.74	5.23	15.50
8 - °F	6.53	10.03	6.21	18.28
9 - °F	21.75	35.15	7.97	23.00
10 - °F			5.13	14.95
Voltage, volts	37.96	48.96	19.43	33.66
Current, amps	0.3967	0.5124	0.3865	0.6710
Water Flow, ml/min	575	550	600	600
Bolt Torque, in-lb	24	24	24	24
Filler	G 683	G 683	None	None
Sample Number	1	1	1	1
Joint Length, in.	6	6	9	9
Number of Bolts	2	2	3	3
h_a, Btu/hr ft^2 °F	425	420	93.5	95.2
h_b, Btu/hr ft^2 °F	345	375	84.1	87.8

Table 13. Experimental Data — Structural Joint Configuration 2 (Continued)

Run	37	38	39	40
Date	4/5/65	4/6/65	4/6/65	4/6/65
Pressure, Torr	1×10^{-6}	8×10^{-7}	8×10^{-7}	8×10^{-7}
Absolute T. C.				
1 - °F	182.2	85.1	126.0	162.2
2 - °F	64.6	64.0	64.4	64.0
3 - °F	66.2	64.4	65.1	65.0
Differential T. C.				
1 - °F	12.58	0.16	0.60	1.26
2 - °F	20.59	0.39	1.44	2.99
3 - °F	32.44	0.83	2.61	4.95
4 - °F	45.32	7.33	22.00	36.10
5 - °F	1.28	0.35	1.05	1.87
6 - °F	12.05	0.17	0.65	3.43
7 - °F	23.56	0.13	0.51	1.44
8 - °F	27.59	0.35	1.36	2.86
9 - °F	36.90	7.41	21.60	35.02
10 - °F	25.22			
Voltage, volts	43.44	21.89	37.99	48.99
Current, amps	0.8674	0.2281	0.3960	0.5119
Water Flow, ml/min	600	625	625	625
Bolt Torque, in-lb	24	24	24	24
Filler	None	RTV 11	RTV 11	RTV 11
Sample Number	1	2	2	2
Joint Length, in.	9	6	6	6
Number of Bolts	3	2	2	2
h_a, Btu/hr ft^2 °F	94.1	889	795	669
h_b, Btu/hr ft^2 °F	97.6	1892	1466	800

Table 14. Experimental Data—Structural Joint Configuration 3

Run Number	41	42	43	44	45
Date	5/8/65	5/8/65	5/8/65	5/9/65	5/9/65
Pressure, Torr	1×10^{-6}	1×10^{-6}	1×10^{-6}	1×10^{-6}	1×10^{-6}
Absolute T. C.					
1 - °F	70.3	84.5	98.1	69.6	80.0
2 - °F	62.7	62.6	62.2	63.5	63.1
3 - °F	63.0	63.3	63.4	63.9	64.0
Differential T. C.					
1 - °F	1.42	4.55	7.80	1.11	4.06
2 - °F	3.12	9.34	15.78	2.35	7.48
3 - °F	3.83	11.61	19.67	2.84	8.90
4 - °F	3.62	10.91	18.90	3.64	11.20
5 - °F	-0.22	0.36	1.15	0.43	1.55
6 - °F	2.66	8.30	14.35	1.92	6.15
7 - °F	3.11	9.55	16.40	1.98	6.41
8 - °F					
Voltage, volts	21.93	37.94	49.01	21.89	38.01
Current, amps	0.2281	0.3949	0.5106	0.2268	0.3943
Water Flow, ml/min	600	600	600	575	575
Bolt Torque, in-lb	24	24	24	24	24
Filler	None	None	None	None	None
Sample Number	1	1	1	2	2
Joint Length, in.	6	6	6	6	6
Number of Bolts	2	2	2	2	2
h, Btu/hr ft^2 °F	147	144.2	142	194	180

Table 14. Experimental Data—Structural Joint Configuration 3 (Continued)

Run Number	46	47	48	49	50
Date	5/9/65	5/13/65	5/13/65	5/13/65	5/15/65
Pressure, Torr	1×10^{-6}	6×10^{-7}	6×10^{-7}	6×10^{-7}	5×10^{-7}
Absolute T. C.					
1 - °F	89.7	72.2	86.8	98.3	70.7
2 - °F	62.5	65.0	66.0	64.1	62.4
3 - °F	63.7	65.3	66.9	65.4	62.8
Differential T. C.					
1 - °F	7.11	2.69	7.94	13.30	0.107
2 - °F	12.79	3.82	11.62	19.90	0.583
3 - °F	15.31	4.91	14.60	24.80	0.414
4 - °F	19.00	4.01	11.79	20.30	3.84
5 - °F	1.94	0.07	0.43	0.76	-0.458
6 - °F	10.50	3.71	11.08	18.82	0.307
7 - °F	10.81	3.66	10.52	17.78	0.222
8 - °F					
Voltage, volts	49.01	21.88	37.20	48.00	21.91
Current, amps	0.5084	0.2385	0.4059	0.5244	0.2279
Water Flow, ml/min	575	575	575	575	425
Bolt Torque, in-lb	24	24	24	24	24
Filler	None	None	None	None	RTV 11
Sample Number	2	3	3	3	1
Joint Length, in.	6	6	6	6	6
Number of Bolts	2	2	2	2	2
h, Btu/hr ft^2 °F	174.0	112.2	108.5	106.5	1110

Table 14. Experimental Data — Structural Joint Configuration 3 (Continued)

Run Number	51	52	53	54
Date	5/15/65	5/15/65	5/16/65	5/16/65
Pressure, Torr	5×10^{-7}	5×10^{-7}	4×10^{-7}	4×10^{-7}
Absolute T. C.				
1 - °F	87.7	102.5	74.3	91.3
2 - °F	63.7	63.4	66.0	68.0
3 - °F	64.8	65.0	66.3	68.9
Differential T. C.				
1 - °F	0.461	0.827	0.222	0.723
2 - °F	1.560	2.441	0.284	0.991
3 - °F	0.979	1.672	0.418	1.208
4 - °F	11.52	19.50	3.89	11.71
5 - °F	-0.282	-0.218	-0.515	0.491
6 - °F	0.735	1.260	0.391	1.104
7 - °F	0.630	1.088	0.311	0.835
8 - °F				
Voltage, volts	38.00	48.99	21.90	38.00
Current, amps	0.3956	0.5104	0.2278	0.3955
Water Flow, ml/min	375	450	450	575
Bolt Torque, in-lb	24	24	24	24
Filler	RTV 11	RTV 11	G 683	G 683
Sample Number	1	1	1	1
Joint Length, in.	6	6	6	6
Number of Bolts	2	2	2	2
h, Btu/hr ft^2 °F	1273	1242	1328	1262

Table 14. Experimental Data—Structural Joint Configuration 3 (Continued)

Run Number	55	56	57	58
Date	5/16/65	5/19/65	5/19/65	5/20/65
Pressure, Torr	4×10^{-7}	7×10^{-7}	7×10^{-7}	4×10^{-7}
Absolute T.C.				
1 - °F	103.2	75.0	87.0	96.8
2 - °F	63.9	68.6	69.2	67.2
3 - °F	65.1	69.2	70.2	68.9
Differential T.C.				
1 - °F	1.273	1.44	4.41	7.60
2 - °F	1.678	3.10	9.46	16.21
3 - °F	2.043	4.10	12.64	21.63
4 - °F	19.85	4.10	12.39	21.08
5 - °F	0.80	0.40	1.50	2.78
6 - °F	1.905	4.64	14.00	23.78
7 - °F	1.440	3.84	11.61	19.60
8 - °F		3.00	9.18	15.47
Voltage, volts	49.01	18.98	32.84	42.45
Current, amps	0.5105	0.3958	0.6852	0.8860
Water Flow, ml/min	625	575	575	575
Bolt Torque, in-lb	24	24	24	24
Filler	G 683	None	None	None
Sample Number	1	1	1	1
Joint Length, in.	6	9	9	9
Number of Bolts	2	3	3	3
h, Btu/hr ft^2 °F	1231	142.2	139	135.5

APPENDIX III

SCRIPT F COMPUTER PROGRAM PRINT OUT

```
$IBFTC MAIN     LIST,REF,DECK
C      DRIVER FOR SPECULAR-DIRECTIONAL SCRIPT F PROGRAM (AH052A) 10/28/64
       DIMENSION ID(22)
       DIMENSION RHO(20,20),F(20,20),AREA(20)
     1  ,SF(20,20),SFA(20,20)
     2  ,D(800),D1(400)
       DIMENSION R(20,20,20),R1(20,20),R2(20,20),R3(20,20),R4(20,20)
     1  ,R5(20,20),R6(20,20),R7(20,20),R8(20,20),R9(20,20),R10(20,20)
     2  ,R11(20,20),R12(20,20),R13(20,20),R14(20,20),R15(20,20)
     3  ,R16(20,20),R17(20,20),R18(20,20),R19(20,20),R20(20,20)
C
       EQUIVALENCE (R1(1,1),R(1,1,1)),(R2(1,1),R(1,1,2)),(R3(1,1),R(1,1,3
     1  )),(R4(1,1),R(1,1,4)),(R5(1,1),R(1,1,5)),(R6(1,1),R(1,1,6))
     2  ,(R7(1,1),R(1,1,7)),(R8(1,1),R(1,1,8)),(R9(1,1),R(1,1,9))
     3  ,(R10(1,1),R(1,1,10)),(R11(1,1),R(1,1,11)),(R12(1,1),R(1,1,12))
     4  ,(R13(1,1),R(1,1,13)),(R14(1,1),R(1,1,14)),(R15(1,1),R(1,1,15))
     5  ,(R16(1,1),R(1,1,16)),(R17(1,1),R(1,1,17)),(R18(1,1),R(1,1,18))
     6  ,(R19(1,1),R(1,1,19)),(R20(1,1),R(1,1,20))
C
C      CLEAR STORAGE REGIONS
  300  DO 310 I=1,20
       AREA(I)= 0.
  310  CONTINUE
       DO 320 I=1,400
       RHO(I,1)= 0.
       F(I,1)= 0.
  320  CONTINUE
       DO 330 I= 1,8000
       R(I,1,1)= 0.
  330  CONTINUE
C
  100  WRITE (3,1000)
 1000  FORMAT ( 1H1,5X,13HINPUT FOLLOWS)
C
       CALL FSMP(-26,2,CLR,RHO,F,AREA,R1,R2,R3,R4,R5,R6,R7,R8,R9,R10,R11
     1  ,R12,R13,R14,R15,R16,R17,R18,R19,R20,ID
     2  , 156HN        CLR     RHO     F       AREA    R1      R2      R3      R4      R5
     3   R6      R7      R8      R9      R10     R11     R12     R13     R14     R15     R16
     4   R17     R18     R19     R20     ID      )
C
       N= 2+.25
```

```
      NN= N+N
 2000 DO 2100 I=1,N
      IF(RHO(I,1))2020,2070,2070
 2020 RHO(I,1)=-RHO(I,1)
      DO 2060 J=1,N
      RHO(I,J)=RHO(I,1)
      DO 2060 K=1,J
 2060 R(K,I,J)=RHO(I,1)
 2070 DO 2100 J=1,N
      IF(J.LT.I)F(J,I)=AREA(I)*F(I,J)/AREA(J)
      DO 2100 K=1,J
 2100 R(J,I,K)=R(K,I,J)
      WRITE (1,1001)
 1001 FORMAT ( 1H0,5X,12HEND OF INPUT)
      WRITE (3,1010) ID
 1010 FORMAT (1H1,26X,56HSPECULAR-DIRECTIONAL SCRIPT F PROGRAM (AH052A),
     1 10/28/64 /(1H0,21X,11A6) )
C
      WRITE (3,1002)
 1002 FORMAT (1H1,5X,15HRHO(I,J) MATRIX)
      CALL MPRT (RHO,N)
      WRITE (3,1003)
 1003 FORMAT (1H1,5X,13HF(I,J) MATRIX)
      CALL MPRT (F,N)
      WRITE (3,1004) (AREA(I),I=1,N)
 1004 FORMAT (1H1,5X,11HAREA VECTOR//(5E20.8))
      WRITE (3,1005)
 1005 FORMAT (1H1,5X,14HR(I,J,K) ARRAY)
      DO 150 K=1,N
      WRITE (3,1009) K
 1009 FORMAT (1H0/1H0,5X,9HBLOCK NO. I4)
      CALL MPRT (R(1,1,K),N)
 150  CONTINUE
      CALL SCRF (N,NN,RHO,F,AREA,R,D,DI,SF,SFA,IERR)
      WRITE (3,1007)
 1007 FORMAT (1H1,5X,15HSCRIPT F MATRIX)
      CALL MPRT (SF,N)
      WRITE (3,1008)
 1008 FORMAT (1H1,5X,16HSCRIPT FA MATRIX)
      CALL MPRT (SFA,N)
      IF (CLR) 300,100,300
```

END

```
$IBMAP ERRS     LIST,REF,DECK                                   ERRS0000
       ENTRY    ERRS                                            ERRS0001
ERRS   SAVE     4,2,1                                           ERRS0002
       SXA      EA,4                                            ERRS0003
       LAC      EA,2                                            ERRS0004
       SXA      EA,2                                            ERRS0005
       TXI      *+1,4,-2                                        ERRS0006
       CLA      1,4                                             ERRS0007
       STA      IDENT2                                          ERRS0008
       CLA*     1,4                                             ERRS0009
       PAX      ,1                                              ERRS0010
       SXA      CODEO,1                                         ERRS0011
       CAL      2,4                                             ERRS0012
       ANA      (PDT)                                           ERRS0013
       TNZ      ER23                                            ERRS0014
       CAL*     2,4                                             ERRS0015
       TRA      ER24                                            ERRS0016
ER23   CAL      2,4                                             ERRS0017
ER24   SLW      NAME                                            ERRS0018
       STZ      ER7                                             ERRS0019
       CAL      3,4                                             ERRS0020
       ANA      (PDT)                                           ERRS0021
       TNZ      ER31                                            ERRS0022
       CAL      3,4                                             ERRS0023
       STA      LEAV1                                           ERRS0024
       AXT      1,2                                             ERRS0025
       SXA      ER7,2                                           ERRS0026
       SXD      *+2,4                                           ERRS0027
       AXC      14,2                                            ERRS0028
       TXI      *+1,2,**                                        ERRS0029
       SXA      BEG1,2                                          ERRS0030
       LAC      BEG1,2                                          ERRS0031
       SXA      BEG1,2                                          ERRS0032
       SXA      BEG1+3,2                                        ERRS0033
       AXT      10,4                                            ERRS0034
BEG1   CAL      **,4                                            ERRS0035
       ANA      (PDT)                                           ERRS0036
       TNZ      ER31                                            ERRS0037
       CLA      **,4                                            ERRS0038
       STA      ARG+10,4                                        ERRS0039
       TIX      BEG1,4,1                                        ERRS0040
```

```
ER31     CALL     .FWRD.(.UN03.,A)                                        ERRS0041
         CLA      EA                                                      ERRS0042
         TSX      .FCNV.,4                                                ERRS0043
         CLA      NAME                                                    ERRS0044
         TSX      .FCNV.,4                                                ERRS0045
         CLA      CODEO                                                   ERRS0046
         TSX      .FCNV.,4                                                ERRS0047
IDENT2   CLA      **                                                      ERRS0048
         TSX      .FCNV.,4                                                ERRS0049
         TSX      .FFIL.,4                                                ERRS0050
EA8      ZET      ER7                                                     ERRS0051
         TRA      LEAV1                                                   ERRS0052
RTN      RETURN   ERRS                                                    ERRS0053
         REM                                                              ERRS0054
         REM      SIMULATE CALL TO SUBPROGRAM (CNTRL) FROM MAIN PROGRAM   ERRS0055
         REM      ...UP TO 10 ARGUMENTS PERMITTED                         ERRS0056
         REM                                                              ERRS0057
LEAV1    TSX      **,4                                                    ERRS0058
         TRA      RTN                                                     ERRS0059
         NOP                                                              ERRS0060
ARG      PZE                                                              ERRS0061
         PZE                                                              ERRS0062
         PZE                                                              ERRS0063
         PZE                                                              ERRS0064
         PZE                                                              ERRS0065
         PZE                                                              ERRS0066
         PZE                                                              ERRS0067
         PZE                                                              ERRS0068
         PZE                                                              ERRS0069
         PZE                                                              ERRS0070
NAME     BCI      1,                                                      ERRS0071
EA       PZE                                                              ERRS0072
ALIST    PZE                                                              ERRS0073
CODEO    BSS      1                                                       ERRS0074
(PDT)    OCT      777777700000                                            ERRS0075
ER7      BSS      1                                                       ERRS0076
A        BCI      1,(1H0 3                                                ERRS0077
         BCI      1,5H ***                                                ERRS0078
         BCI      1,*ERRS-                                                ERRS0079
         BCI      1,-ERROR                                                ERRS0080
         BCI      1, EXIT                                                 ERRS0081
```

```
      BCI     1,FROM L                                        ERRS0082
      BCI     1,OCATIO                                        ERRS0083
      BCI     1,N 03.                                         ERRS0084
      BCI     1,10H, P                                        ERRS0085
      BCI     1,ROGRAM                                        ERRS0086
      BCI     1, A6, 8                                        ERRS0087
      BCI     1,H, I.D                                        ERRS0088
      BCI     1,. = 06                                        ERRS0089
      BCI     1,, 5H(8                                        ERRS0090
      BCI     1,) = I6                                        ERRS0091
      BCI     1,, 9H(1                                        ERRS0092
      BCI     1,0).***                                        ERRS0093
      BCI     1,*)                                            ERRS0094
      END                                                     ERRS0095
```

```
SIBMAP FINP     LIST,REF,DECK                                                   FINP0000
*      FINP-FORTRAN IV DECEMBER 1964                                            FINP0001
TBL    ENTRY    TBLOO                                                           FINP0002
FINP   SAVE     (4,1,2)I                                                        FINP0003
       TXI      *+1,4,-2                                                        FINP0004
       CLA*     1,4                                                             FINP0005
       STO      COMMON+28           FLAG TO USE PREVIOUS CALL                   FINP0006
       TZE      INPT2                                                           FINP0007
       SXD      FINPT,4                                                         FINP0008
INPT2  LXD      FINPT,4                                                         FINP0009
       PXA      0,4                                                             FINP0010
       SBM*     1,4                                                             FINP0011
       SUB      1B35                                                            FINP0012
       COM                                                                      FINP0013
       STA      TBLO2               ALPHA+N                                     FINP0014
       CLA      1,4                                                             FINP0015
       STA      TBLOC                                                           FINP0016
       CLA*     1,4                                                             FINP0017
       STO      COMMON+29           N OR O                                      FINP0018
       ALS      18                                                              FINP0019
       COM                                                                      FINP0020
       STD      *+1                                                             FINP0021
       TXI      *+1,4,0                                                         FINP0022
       CLA      0,4                                                             FINP0023
       STO      GINOO               FOR HEADER COMPATABILITY                    FINP0024
       STO      RLOC                RELATIVE ORIGIN                             FINP0025
       CLA      1,4                                                             FINP0026
       ADM      COMMON+29           N                                           FINP0027
       STA      TBLO1                                                           FINP0028
       STO      ERROR                                                           FINP0029
*      READ ONE BCD CARD IMAGE FROM INPUT TAPE                                  FINP0030
GINA   CALL     .FRDD.(.UNO2.,=H(14A6))                                         FINP0031
       AXT      14,1                                                            FINP0032
A      TSX      .FCNV.,4                                                        FINP0033
       STO      COMMON+14,1                                                     FINP0034
       TIX      A,1,1                                                           FINP0035
       TSX      .FRTN.,4                                                        FINP0036
       CLA      COMMON+29           N                                           FINP0037
       TPL      GINA1               NO INPUT LIST                               FINP0038
*      WRITE CARD IMAGE ON OUTPUT TAPE.                                         FINP0039
       CALL     .FWRD.(.UNO3.,=H(15A6))                                         FINP0040
```

```
       CLA    =H                                                  FINP0041
       TSX    .FCNV.,4                                            FINP0042
       AXT    14,1                                                FINP0043
       CLA    COMMON+14,1                                         FINP0044
       TSX    .FCNV.,4                                            FINP0045
       TIX    *-2,1,1                                             FINP0046
       CALL   .FFIL.                                              FINP0047
GINA1  AXC    COMMON,1                                            FINP0048
       TXI    *+1,1,-12                                           FINP0049
       SXD    GINC,1                                              FINP0050
       SXD    GIN11+1,1                                           FINP0051
       AXC    COMMON,1                                            FINP0052
       CLA    BLANK                                               FINP0053
GINB   CAS    0,1                                                 FINP0054
       TXL    GINC+2                                              FINP0055
       TXI    *+2,1,-1                                            FINP0056
       TXL    GINC+2                                              FINP0057
GINC   TXH    GINB,',**                                           FINP0058
       TXL    GINA              INGORE BLANK CZRD                 FINP0059
       AXC    COMMON,1                                            FINP0060
       LDQ 0,1                                                    FINP0061
GIND1  PXD **                 SAVE PREFIX CODE                    FINP0062
       LGL 6                                                      FINP0063
       STO PREFIX                                                 FINP0064
       STQ 0,1                                                    FINP0065
       SUB    ME                  E                               FINP0066
       TZE    GIN13               END                             FINP0067
       LGL 30                 SAVE LAST DIGIT OF ADDRESS          FINP0068
       ANA MASK1                                                  FINP0069
       STO ADDIND                                                 FINP0070
       STZ SUM                TEST FOR BLANK ADDRESS              FINP0071
       STZ SIGN                                                   FINP0072
       CLA    0,1                                                 FINP0073
       CAS    MASK2                                               FINP0074
       TXL    *+2                                                 FINP0075
       TX.    GIN06               BLANK                           FINP0076
       LDQ    0,1                 DETERMINE COMMA POSITION        FINP0077
       LGL    5                                                   FINP0078
       AXT    2,4                                                 FINP0079
       PXD    0,0                                                 FINP0080
       LGL    6                                                   FINP0081
```

```
        SUB   MASK4               COMMA                               FINP0082
        TZE   *+3                                                     FINP0083
        TXH   GIN17-2,4,3         NOT MATRIX                          FINP0084
        TXI   *-5,4,1                                                 FINP0085
        PXA   ,4                  POSITION OF COMMA                   FINP0086
GIN6    TSX   MTX00,4             MATRIX                              FINP0087
        TRA   GINER               OUTSIDE MATRIX                      FINP0088
        TRA   GIN20                                                   FINP0089
MASK4   OCT   73                                                      FINP0090
        AXT   5,4                                                     FINP0091
        LDQ   0,1                                                     FINP0092
GIN17   PXD                                                           FINP0093
        LGL   6                                                       FINP0094
        PAX   0,2                                                     FINP0095
        TXL   GIN18,2,9                                               FINP0096
        TXH   GIN19,2,48                                              FINP0097
        TXL   GIN19,2,47                                              FINP0098
GIN18   TIX   GIN17,4,1                                               FINP0099
        TXL   GIN16                                                   FINP0100
GIN19   CLA   0,1                SYMBOLIC                             FINP0101
        ORA   MASK3                                                   FINP0102
        TSX   TBL00,4                                                 FINP0103
        LLS   35                                                      FINP0104
        STA   GIN00                                                   FINP0105
        STA   SGIN03                                                  FINP0106
GIN20   CLA   MASK3                                                   FINP0107
        STO   ADDIND                                                  FINP0108
        TXL   GIN07                                                   FINP0109
GIN16   CLA   ADDIND              TEST FOR OCTAL                      FINP0110
        SUB MASK3                                                     FINP0111
        TZE GIN04                                                     FINP0112
        LXA 5B35,2               SET-UP OCTAL ADDRESS                 FINP0113
        TSX OCTAL,4                                                   FINP0114
GIN02   TXH 5,,**                                                     FINP0115
GIN03   TXL GIN07,,**                                                 FINP0116
GIN04   LXA 100B35,2             SET UP DECIMAL ADDRESS               FINP0117
        CLA 4B35                                                      FINP0118
        TSX DECIM,4                                                   FINP0119
        TRA     GINER             ERROR                               FINP0120
GIN05   TXH 6,,**                                                     FINP0121
        TXL GINER,2,100                                               FINP0122
```

```
         TXL       GIN07                                            FINP0123
GIN06    LDQ MASK2                                                  FINP0124
GIN07    STQ       CRDADD                                           FINP0125
         LXA PREFIX,4            SET-UP TRA TO                      FINP0126
         TXH GINER,4,48               SUB-PROGRAM                   FINP0127
         TXL GIN08,4,47                                             FINP0128
         LXD 100B35,4                                               FINP0129
         TXL GIN09                                                  FINP0130
GIN08    TXH       GINER,4,41                                       FINP0131
         TXL       *+2,4,32                                         FINP0132
         TXI       GIN09,4,-23                                      FINP0133
         TXH       GINER,4,25                                       FINP0134
         TNX GINER,4,16                                             FINP0135
GIN09    TXI GIN09+1,1,-1                                           FINP0136
         TRA GIN10,4                                                FINP0137
         TXL       RGIN00           R RELATIVE ORIGIN               FINP0138
         TXL       GINER            Q                               FINP0139
         TXL       GINER            P                               FINP0140
         TXL       GINER            O                               FINP0141
         TXL       NGIN00           N RELATIVE INDEX VALUE          FINP0142
         TXL       MCD00            M MATRIX IJ:ZERO                FINP0143
         TXL       MCD00            L MATRIX IJ-NO ZERO             FINP0144
         TXL       KGIN00           K SKIP CELLS                    FINP0145
         HTR*      CRDADD           J                               FINP0146
         TXL       IGIN00           I       INTEGER                 FINP0147
         TXL       HGIN00           H       HEADER                  FINP0148
         TXL       GGIN00           G       TABLE ORIGIN            FINP0149
         TXL       FGIN00           F       FIXED FOINT             FINP0150
         TXL GINER               E                                  FINP0151
         TXL       DGIN00           D       BCD                     FINP0152
         TXL       CGIN00           C SAVE NEXT LOCATION            FINP0153
         TXL       BGIN00           B       OCTAL                   FINP0154
         TXL       ACD0             A       SYMBOLIC                FINP0155
GIN10    TXL       LGIN00,,12       BLANK  FLOATING                 FINP0156
GIN11    TXI GIN11+1,1,-1             TEST END CARD                 FINP0157
         TXH       GIN01-1,1,**                                     FINP0158
GIN12    TXL       GINA             TO NEXT CARD                    FINP0159
GIN13    NZT       ERROR                                            FINP0160
         TRA       GIN15                                            FINP0161
         RETURN    FINP                                             FINP0162
GIN15    CALL      .FXEM.(CODE40)   ERROR EXIT                      FINP0163
```

```
         CALL    EXIT                                             FINP0164
GINER    STZ     ERROR                                            FINP0165
         CLA     COMMON+29                                        FINP0166
         TPL     GIN12                                            FINP0167
         CALL    .FWRD.(.UN03.,=H(14A6))                          FINP0168
         AXT     10,1                                             FINP0169
         CLA     =H                                               FINP0170
         TSX     .FCNV.,4                                         FINP0171
         TIX     *-2,1,1                                          FINP0172
         AXT     4,1                                              FINP0173
         CLA     GINRRC+4,1                                       FINP0174
         TSX     .FCNV.,4                                         FINP0175
         TIX     *-2,1,1                                          FINP0176
         CALL    .FFIL.                                           FINP0177
         TXL     GIN12                                            FINP0178
GINRRC   BCI     4,     ABOVE CARD IN ERROR                       FINP0179
NE       BCI     1,00000E                                         FINP0180
BLANK    BCI     1,                                               FINP0181
MGINOO   CLA     CRDADD                                           FINP0182
         CAS     MASK2                                            FINP0183
         TXL     *+2                                              FINP0184
         TXL     GIN12                    BLANK                   FINP0185
         LDQ     CRDADD                                           FINP0186
         MPY     11B35                                            FINP0187
         LLS     35                                               FINP0188
         TZE     *+2                      SYMBOLIC                FINP0189
         SUB     10B35                                            FINP0190
         STO     CRDADD                                           FINP0191
         AXT     11,1                                             FINP0192
         LDQ     COMMON+12,1                                      FINP0193
         TSX     SGINOO,4                                         FINP0194
         CLA     MASK2                    SET TO BLANK            FINP0195
         STO     CRDADD                                           FINP0196
         TIX     *-4,1,1                                          FINP0197
         TXL GIN12                                                FINP0198
GGINOO   CLA ADDIND                                               FINP0199
         SUB MASK3                                                FINP0200
         TZE GGIN01                                               FINP0201
         PXD                                                      FINP0202
         TRA GGIN02                                               FINP0203
GGIN01   CAL GINOO                                                FINP0204
```

```
GGINO2 SUB       1B35                                            FINP0205
       ADD CRDADO                                                FINP0206
       STA SGINO3                                                FINP0207
       TXL GIN12                                                 FINP0208
BGINOO STZ SUM                                                   FINP0209
       STZ SIGN                                                  FINP0210
       LXA M6B35,2                      6                        FINP0211
       TSX OCTAL,4                                               FINP0212
       TXI       BGINO4,1,-1                                     FINP0213
       TXI BGINO1,1,-1                                           FINP0214
BGINO1 LXA M6B35,2                      6                        FINP0215
       TSX OCTAL,4                                               FINP0216
       TXH 4                                                     FINP0217
BGINO2 TSX SGINOO,4                                              FINP0218
BGINO3 TXL GIM11,,**                    EXIT FOR NEW PREFIX      FINP0219
BGINO4 TXH       BGINO3,2,5                BLANK                 FINP0220
       TXL       BGINO2                                          FINP0221
IGINOO TSX DECNO,4                     INTERGER FORMAT           FINP0222
       TXH       GINER,2,1                 DECIMAL PLACES        FINP0223
       TXL       BGINO2,2,0                STORE INTEGER         FINP0224
       CLM                                                       FINP0225
       DVP       10B35                                           FINP0226
       TNZ       GINER                     NOT .0                FINP0227
       TRA       BGINO2                    STORE INTEGER         FINP0228
DGINOO LDQ 0,1                                                   FINP0229
       TSX SGINOO,4                                              FINP0230
       CLA MASK2                                                 FINP0231
       STO CRDADO                                                FINP0232
       LDQ 1,1                                                   FINP0233
       TXI BGINO2,1,-1                                           FINP0234
DECNO  SXD BGINO3,4                                              FINP0235
       CLA       0,1                                             FINP0236
       STO       COMMON+33                                       FINP0237
       CLA       1,1                                             FINP0238
       STO       COMMON+34                                       FINP0239
       ALS 24                                                    FINP0240
       SLW COMMON+20                                             FINP0241
       STZ SUM                                                   FINP0242
       STZ SIGN                                                  FINP0243
       LXA 100B35,2                                              FINP0244
       CLS M6B35                        6                        FINP0245
```

```
          TSX DECIM,4                                      FINP0246
          TRA      DECER               ERROR               FINP0247
          TXI DECN2+1,1,-1          END ON BLANK           FINP0248
          TXI DECN1,1,-1                                   FINP0249
DECN1     CLA 4B99                  4                      FINP0250
          TSX DECIM,4                                      FINP0251
          TXI      DECER,1,1           ERROR               FINP0252
DECN2     TXH 2,,**                                        FINP0253
          TXL DECN4,2,99                                   FINP0254
          TXL GIN11,2,100                                  FINP0255
DECN3     LXD 1B99,2                                       FINP0256
DECN4     LXD BGINO3,4                                     FINP0257
          LXD BGINO3,4                                     FINP0258
          TRA 1,4                                          FINP0259
DECEN     SXD GINO3,4                                      FINP0260
          TSX DECNO,4                                      FINP0261
          STO COMMON+13                                    FINP0262
          SXD DECN2,2                                      FINP0263
          CLA DECN2                                        FINP0264
          STZ SUM                                          FINP0265
          STZ SIGN                                         FINP0266
          LDQ COMMON+20                                    FINP0267
          STO 0,1                                          FINP0268
          TSX DECIM,4                                      FINP0269
          TXI      DECER,1,1           ERROR               FINP0270
          TXH                                              FINP0271
          LXD GINO3,4                                      FINP0272
          TRA 1,4                                          FINP0273
DECER     CLA      COMMON+33                               FINP0274
          STO      0,1                                     FINP0275
          CLA      COMMON+34                               FINP0276
          STO      1,1                                     FINP0277
          TRA      ACDO                                    FINP0278
FGINOO    TSX DECEN,4               FIXED PT. CONVERSION   FINP0279
          STO COMMON                                       FINP0280
          CAL DECN2                                        FINP0281
          COM                                              FINP0282
          ADD 1B17                                         FINP0283
          PDX 0,2                                          FINP0284
          CLA COMMON                                       FINP0285
          SUB BREF,2                                       FINP0286
```

```
        TMI GINER                                            FINP0287
        STA FGINO1                                           FINP0288
        LDQ COMMON+13                                        FINP0289
        MPY FREF,2                                           FINP0290
FGINO1  LRS **                                               FINP0291
        TMZ GINER                                            FINP0292
        TXL BGINO2,,**                                       FINP0293
LGINOO  TSX DECEN,4              FLTG. PT. CONVERSION        FINP0294
        STQ COMMON                                           FINP0295
        LXD DECN2,2                                          FINP0296
        PXD ,2                                               FINP0297
        ARS 18                                               FINP0298
        SSM                                                  FINP0299
        ADD COMMON                                           FINP0300
        LRS 35                                               FINP0301
        DVP 10B35                                            FINP0302
        SUB M9B35                                            FINP0303
        PAX ,2                                               FINP0304
        CLM                                                  FINP0305
        LLS 35                                               FINP0306
        ADD 5B35                 HIGH DIGIT                  FINP0307
        TMI GINER                                            FINP0308
        PAX ,4                                               FINP0309
        SXD FGINO1+2,1           SAVE ADD REFERENCE          FINP0310
        CLA XREF1,2                                          FINP0311
        ADD XREF2,4                                          FINP0312
        ADD 126B35                                           FINP0313
        TPL LGINOA                                           FINP0314
        STZ COMMON+13                                        FINP0315
LGINOA  PAX 0,1                                              FINP0316
        LDQ FREF1,2                                          FINP0317
        MPR FREF2,4                                          FINP0318
        LRS 35                                               FINP0319
        MPY COMMON+13                                        FINP0320
        LLS 2                                                FINP0321
        TZE LGINO3                                           FINP0322
LGINO1  TZE LGINO2                                           FINP0323
        LRS 1                                                FINP0324
        TXI LGINO1,1,1                                       FINP0325
LGINO2  LLS     27                                           FINP0326
        RND                                                  FINP0327
```

```
        LRS      27                                    FINP0328
        TZE      *+3                                   FINP0329
        LRS      1                                     FINP0330
        TXI      *+1,1,1                               FINP0331
        PXA      ,1                                    FINP0332
        LLS 0                                          FINP0333
        LRS 8                                          FINP0334
LGINO3  LXD FGINO1+2,1                                 FINP0335
        TNZ GINER                                      FINP0336
        TXL BGINO2             EXIT TO STORE           FINP0337
SGINOO  CLA CRCADD             STORE ROUTINE           FINP0338
        SUB MASK2                                      FINP0339
        TZE      SGINO1                                FINP0340
        CLA ADDIND                                     FINP0341
        SUB MASK3                                      FINP0342
        TZE      SAA1                                  FINP0343
        CLA CRDADD                                     FINP0344
        TXL SGINO2                                     FINP0345
SAA1    CLA      CRDADD           ONLY IF CRDADD HAS   FINP0346
        TZE      SGINOA                                FINP0347
        CAL      CRDADD                                FINP0348
        SUB      1B35             RELATIVE LOCATION IN FINP0349
        STA      CRDADD                                FINP0350
SGINOA  CAL      GINOO                                 FINP0351
        ACL      CRDADD                                FINP0352
        TXL      SGINO2                                FINP0353
SGINO1  CAL SGINO3             ADD 1 TO OLD ADDRESS    FINP0354
        ACL 1B35                                       FINP0355
SGINO2  STA SGINO3                                     FINP0356
SGINO3  STQ **                                         FINP0357
        TRA 1,4                                        FINP0358
*                                                      FINP0359
KGINOO  TSX      DECNO,4          SKIP CELLS           FINP0360
        TXH      GINER,2,0        NON INTEGER          FINP0361
        XCA                                            FINP0362
        TMI      GINER                                 FINP0363
        ADM      SGINO3                                FINP0364
        STA      SGINO3                                FINP0365
        TRA      GIN11                                 FINP0366
*                                                      FINP0367
CGINOO  CLA      0,1                                   FINP0368
```

```
        TSX     TBLOO,4                                        FINP0369
        CAL     SGINO3                                         FINP0370
        ADD     1B35                                           FINP0371
CGINO1  AXT     **,2                                           FINP0372
        STA*    TBLO2                                          FINP0373
        TXI     GIN11,1,-1                                     FINP0374
*       SAVE RELATIVE LOCATION AND ABSOLUTE LOCATION           FINP0375
NGINOO  CLA     0,1                                            FINP0376
        TSX     TBLOO,4                                        FINP0377
        LXA     CGINO1,2                                       FINP0378
        TXI     *+1,2,1                                        FINP0379
        CLA*    TBLO1               SYMLOC LOCATION            FINP0380
        SUB     BLANK                                          FINP0381
        TNZ     GINER               NOT BLANK-RELATIVE INDEX   FINP0382
        TXI     *+1,2,-2                                       FINP0383
        XEC     TBLO2                                          FINP0384
        XCA                                                    FINP0385
        STA     NGINO1                                         FINP0386
        TXI     *+1,2,1                                        FINP0387
        CAL     SGINO3                                         FINP0388
        ADD     1B35                                           FINP0389
        STA*    TBLO2                                          FINP0390
        ADD     1B35                                           FINP0391
        SUB     RLOC                                           FINP0392
        STZ*    *+1                                            FINP0393
NGINO1  STA     **                                             FINP0394
        TXI     GIN11,1,-1                                     FINP0395
RGINOO  CLA     0,1                                            FINP0396
        TSX     TBLOO,4                                        FINP0397
        STZ     RLOC                                           FINP0398
        XCA                                                    FINP0399
        STA     RLOC                                           FINP0400
        TXI     GIN11,1,-1                                     FINP0401
*                                                              FINP0402
OCTAL   LDQ 0,1                     SET-UP OCTAL INTEGER       FINP0403
OCTAL1  PXD                                                    FINP0404
        LGL 3                                                  FINP0405
        TNZ OCTAL2                                             FINP0406
        CAL SUM                                                FINP0407
        LGL 3                                                  FINP0408
        SLW SUM                                                FINP0409
```

```
         TIX OCTAL1,2,1                                      FINP0410
         TXI OCTAL3,4,-1                                     FINP0411
OCTAL2   LGL 3                                               FINP0412
         SUM MASK3                                           FINP0413
         TNZ GINER                                           FINP0414
OCTAL3   LDQ SUM                                             FINP0415
         TRA 1,4                                             FINP0416
DECIM    SXD DECIM2,4            GENERATE DECIMAL  INTEGER   FINP0417
         PAX ,4                                              FINP0418
DECIM1   CLM                                                 FINP0419
         LDQ 0,1                                             FINP0420
         LGL 6                                               FINP0421
         STQ 0,1                                             FINP0422
         SUB 10B35                                           FINP0423
         TMI DECIM6                                          FINP0424
         SBM     M6B35                                       FINP0425
         TZE     DECIM7          =+                          FINP0426
         SUB     11B35                                       FINP0427
         TNZ DECIM3                                          FINP0428
         LXD 10B35,2                                         FINP0429
DECIM2   TXL DECIM7,,**                                      FINP0430
DECIM3   SUB 5B35                                            FINP0431
         TMI     DECIM9                                      FINP0432
         SUB 10B35                                           FINP0433
         TNZ DECIM4                                          FINP0434
         SUB 10B35                                           FINP0435
DECIM4   TPL DECIM5                                          FINP0436
         STO SIGN                                            FINP0437
         TXL DECIM6                                          FINP0438
DECIM5   ADD M6B35                                           FINP0439
         TZE     DECIM8             BLANK                    FINP0440
         SUB     11B35                                       FINP0441
         TNZ     DECIM9                                      FINP0442
         TRA     DECIM7             IGNORE COMMA             FINP0443
DECIM8   LXD DECIM2,4            END ON BLANK                FINP0444
         LDQ SUM                                             FINP0445
         CLA SIGN                                            FINP0446
         LRS 0                                               FINP0447
         TRA     2,4                                         FINP0448
DECIM6   ADD 10B35                                           FINP0449
         STO COMMON+14                                       FINP0450
```

```
        LDQ SUM                                                    FINP0451
        MPY 10B35                                                  FINP0452
        LLS 35                                                     FINP0453
        ADD COMMON+14                                              FINP0454
        STO SUM                                                    FINP0455
        TXI DECIM7,2,1                                             FINP0456
DECIM7  TIX DECIM1,4,1                                             FINP0457
        LXD DECIM2,4                                               FINP0458
        TXI DECIM8+1,4,-1        END ON DIGIT COUNT                FINP0459
DECIM9  LXD      DECIM2,4                                          FINP0460
        TRA      1,4                 ERROR EXIT                    FINP0461
        DEC 133                                                    FINP0462
100B35  DEC 100                                                    FINP0463
        DEC 67                                                     FINP0464
        DEC 34                                                     FINP0465
1B35    DEC 1                                                      FINP0466
        DEC -33                                                    FINP0467
        DEC -66                                                    FINP0468
        DEC -99                                                    FINP0469
        DEC -132                                                   FINP0470
XREF2   DEC .9183549616B0                                          FINP0471
        DEC .7888609053B0                                          FINP0472
        DEC .6776263579B0                                          FINP0473
        DEC .5820766092B0                                          FINP0474
        DEC .5B0                                                   FINP0475
        DEC .8589934592B0                                          FINP0476
        DEC .7378697630B0                                          FINP0477
        DEC .6338253002B0                                          FINP0478
        DEC .5444517871B0                                          FINP0479
FREF2   DEC 30                                                     FINP0480
        DEC 27                                                     FINP0481
        DEC 24                                                     FINP0482
        DEC 20                                                     FINP0483
17B35   DEC 17                                                     FINP0484
        DEC 14                                                     FINP0485
10B35   DEC 10                                                     FINP0486
        DEC 7                                                      FINP0487
4B35    DEC 4                                                      FINP0488
BREF    DEC 1                                                      FINP0489
        DEC -3                                                     FINP0490
M6B35   DEC -6                                                     FINP0491
```

```
M9B35   DEC -9                                                  FINP0492
        DEC -13                                                 FINP0493
        DEC -16                                                 FINP0494
        DEC -19                                                 FINP0495
        DEC -23                                                 FINP0496
        DEC -26                                                 FINP0497
XREF1   DEC -29                                                 FINP0498
        DEC .9313225747B0                                       FINP0499
        DEC .7450580597B0                                       FINP0500
        DEC .5960464477B0                                       FINP0501
        DEC .9536743164B0                                       FINP0502
        DEC .7629394531B0                                       FINP0503
        DEC .6103515625B0                                       FINP0504
        DEC .9765625B0                                          FINP0505
        DEC .78125B0                                            FINP0506
        DEC .625B0                                              FINP0507
FREF    DEC .5B0                                                FINP0508
        DEC .8B0                                                FINP0509
        DEC .64B0                                               FINP0510
        DEC .512B0                                              FINP0511
        DEC .8192B0                                             FINP0512
        DEC .65536B0                                            FINP0513
        DEC .524288B0                                           FINP0514
        DEC .8388608B0                                          FINP0515
        DEC .67108864B0                                         FINP0516
FREF1   DEC .536870912B0                                        FINP0517
5B35    DEC 5                                                   FINP0518
126B35  PZE 126                                                 FINP0519
MASK1   OCT 000000000077                                        FINP0520
MASK2   OCT 606060606000                                        FINP0521
MASK3   OCT 000000000060                                        FINP0522
1B17    OCT 1000000                                             FINP0523
 2B35   DEC 2B35                                                FINP0524
 3B35   PZE 3                                                   FINP0525
 8B35   DEC 8B35                                                FINP0526
11B35   PZE     11                                              FINP0527
12B35   PZE 12                                                  FINP0528
*                                 CLA LOC COMMA                 FINP0529
MTX00   SXA     MTX10,4           TSX MTX00,4                   FINP0530
        STO     COMMON+35         NO CHAR I                     FINP0531
        SSM                                                     FINP0532
```

143

```
        ADD     5B35                                          FINP0533
        STO     COMMON+36       NO CHAR J                     FINP0534
        AXT     2,4             IJ RETURN                     FINP0535
MTX01   SXA     MTX02,4         NORMAL RETURN                 FINP0536
        STZ     SIGN                                          FINP0537
        STZ     SUM                                           FINP0538
        LXA     100B35,2                                      FINP0539
        CLA     COMMON+37,4                                   FINP0540
        TSX     DECIM,4                                       FINP0541
        TRA     GINER                                         FINP0542
        TRA     MTX11           LES THAN N CHADS              FINP0543
        TXL     GINER,2,100                                   FINP0544
MTX02   AXT     **,4                                          FINP0545
        STQ     I+2,4           I,J                           FINP0546
        TIX     MTX01,4,1                                     FINP0547
MTX10   AXT     **,4                                          FINP0548
        CLA     J                                             FINP0549
        SUB     1B35                                          FINP0550
        XCA                                                   FINP0551
        MPY     IMAX                                          FINP0552
        XCA                                                   FINP0553
        ADD     I                                             FINP0554
        LDQ     IJ                                            FINP0555
        TLQ     1,4             LOC GTR MAX                   FINP0556
        XCA                                                   FINP0557
        TRA     2,4                                           FINP0558
MTX11   LXA     MTX02,4                                       FINP0559
        TXH     GINER,4,1       I ERROR                       FINP0560
        TRA     MTX02-1         J                             FINP0561
*       SET UP IJ WORD                                        FINP0562
MCD00   SXA     MCD02,4                                       FINP0563
        CAL     GIN00                                         FINP0564
        SUB     1B35                                          FINP0565
        STA     SGIN03                                        FINP0566
        LDQ     0,1             DETERMINE COMMA POSITION      FINP0567
        LGL     6                                             FINP0568
        AXT     2,4                                           FINP0569
        PXD     0,0                                           FINP0570
        LGL     6                                             FINP0571
        SUB     MASK4           COMMA                         FINP0572
        TZE     *+3                                           FINP0573
```

```
          TXH     GINER,4,3           NOT MATRIX                          FIMP0574
          TXI     *-5,4,1                                                 FIMP0575
          PXA     ,4                  POSITION OF COMMA                   FIMP0576
          TSX     MTX00,4                                                 FIMP0577
MCD02     NOP     **                                                      FIMP0578
          LDQ     I                                                       FIMP0579
          STQ     IMAX                                                    FIMP0580
          MPY     J                                                       FIMP0581
          STQ     IJ                                                      FIMP0582
          LXA     MCD02,4                                                 FIMP0583
          TXL     MCD04,4,12                                              FIMP0584
          LXA     IJ,4                                                    FIMP0585
          CAL     GIN00                                                   FIMP0586
          ADM     IJ                                                      FIMP0587
          STA     *+1                 ZERO MATRIX                         FIMP0588
          STZ     **,4                                                    FIMP0589
          TIX     *-1,4,1                                                 FIMP0590
MCD04     TXI     GIK11,1,-1                                              FIMP0591
*                                                                         FIMP0592
ACD0      STZ     CTR                                                     FIMP0593
          STZ     PASS                                                    FIMP0594
ACD1      STZ     PF                                                      FIMP0595
          AXT     5,2                                                     FIMP0596
          TSX     SYM00,4                                                 FIMP0597
          AXT     0,4                 BLANK                               FIMP0598
          TXH     ACD6,2,1                                                FIMP0599
          TXL     ACD12,4,0           NULL AND BLANK                      FIMP0600
          TXL     ACD6+1              NULL                                FIMP0601
ACD6      STQ     PF                                                      FIMP0602
          TXL     ACD10,4,0           BLANK                               FIMP0603
          AXT     1,2                                                     FIMP0604
          TSX     SYM00,4                                                 FIMP0605
          AXT     0,4                 BLANK                               FIMP0606
          TXL     ACD10,2,1           NULL                                FIMP0607
          XCL                                                             FIMP0608
          ALS     15                                                      FIMP0609
          STT     PF                                                      FIMP0610
ACD10     LDQ     PF                                                      FIMP0611
          CLS     PASS                                                    FIMP0612
          STO     PASS                                                    FIMP0613
          TPL     ACD15                                                   FIMP0614
```

```
         STQ    WORD                                                   FINP0615
         TXH    ACD1,4,0              NOT BLANK                        FINP0616
ACD12    LXA    CTR,4                                                  FINP0617
         TXH    ACD14,4,6                                              FINP0618
         TXI    *+1,1,-1                                               FINP0619
         TXL    *+3,4,1               BLANK                            FINP0620
ACD14    LDQ    WORD                                                   FINP0621
         TSX    SGIN00,4                                               FINP0622
         TXL    GIN11                                                  FINP0623
ACD15    ROL    18                                                     FINP0624
         SLQ    WORD                                                   FINP0625
         TXL    ACD12                                                  FINP0626
*                                                                      FINP0627
SYM00    SXD    SYM02,2                                                FINP0628
         SXA    SYM14,4               LXA L(NO CHARACTERS),2           FINP0629
         STZ    PSYM                  TSX SYM00,4                      FINP0630
         AXT    1,2                   BALNK                            FINP0631
SYM01    CLA    CTR                   NORMAL IR2=1 IF NULL             FINP0632
         ADD    1B35                                                   FINP0633
         STO    CTR                                                    FINP0634
         SUB    10B35+1               7                                FINP0635
         TNZ    *+2                                                    FINP0636
         TXI    *+1,1,-1                                               FINP0637
         LDQ    0,1                                                    FINP0638
         CAL    PSYM                                                   FINP0639
         LGL    6                                                      FINP0640
         SLW    PSYM                                                   FINP0641
         STQ    0,1                                                    FINP0642
         ANA    MASK1                                                  FINP0643
         SUB    MASK3                                                  FINP0644
         TZE    SYM20                 BLANK                            FINP0645
         SUB    11B35                                                  FINP0646
         TZE    SYM21                 COMMA                            FINP0647
         TXI    *+1,2,1                                                FINP0648
SYM02    TXL    SYM01,2,**                                             FINP0649
         CAL    PSYM                                                   FINP0650
SYM03    TXI    *+1,2,-1                                               FINP0651
         SXA    SYM06,2               NO CHARACTERS                    FINP0652
         LDQ    MASK2                                                  FINP0653
SYM04    LGL    6                     LEFT JUSTIFY                     FINP0654
         TXI    *+1,2,1                                                FINP0655
```

```
         TXL    SYM04,2,5                       FINP0656
         SLW    SYMBL                           FINP0657
         CAL    PSYM                            FINP0658
         ANA    BLANK                           FINP0659
         TNZ    SYM10        SYMBOLIC           FINP0660
SYM06    AXT    **,2         NO CHARACTERS      FINP0661
         LDQ    SYMBL                           FINP0662
         STZ    SUM                             FINP0663
         STZ    SIGN                            FINP0664
         TXL    SYM08,2,4    DECIMAL            FINP0665
         TSX    OCTAL1,4     OCTAL              FINP0666
         TXL    GINER                           FINP0667
         TSX    SYM14,2                         FINP0668
SYM08    CLA    0,1                             FINP0669
         STQ    0,1                             FINP0670
         STO    SYMBL                           FINP0671
         PXA    ,2                              FINP0672
         TSX    DECIN,4                         FINP0673
         TRA    GINER        ERROR              FINP0674
         TXL    GINER                           FINP0675
         CLA    SYMBL                           FINP0676
         STO    0,1                             FINP0677
         TSX    SYM14,2                         FINP0678
SYM10    CLA    SYMBL                           FINP0679
         TSX    TBL00,4                         FINP0680
SYM14    AXT    **,4                            FINP0681
         TRA    2,4          EXIT               FINP0682
SYM20    TXI    *+1,4,1      BLANK              FINP0683
         SXA    SYM14,4                         FINP0684
SYM21    TXL    SYM14+1,2,1  NULL FIELD         FINP0685
SYM25    CAL    PSYM                            FINP0686
         ARS    6                               FINP0687
         SLW    PSYM                            FINP0688
         TXL    SYM03                           FINP0689
TBL00    LXA    **,2         N                  FINP0690
TBL01    CAS    **,2         BCD+N-N            FINP0691
         TXL    *+2                             FINP0692
         TXI    TBL02,2,-2                      FINP0693
         TIX    TBL01,2,1                       FINP0694
TBL03    TXL    GINER,0,-1                      FINP0695
TBL02    LDQ    **,2         ALPHA+N-(N-2)      FINP0696
```

```
         SXA    CGIN01,2                                        FINP0697
         LXD    TBL03,2                                         FINP0698
         TRA    1,4                                             FINP0699
IMAX     PZE                                                    FINP0700
IJ       PZE                                                    FINP0701
PF       SYN    COMMON+15                                       FINP0702
PASS     SYN    COMMON+16                                       FINP0703
CTR      EQU    COMMON+17                                       FINP0704
SYMBL    EQU    COMMON+18                                       FINP0705
PSYM     EQU    COMMON+19                                       FINP0706
CRDADD   EQU    COMMON+21                                       FINP0707
SIGN     EQU    COMMON+22                                       FINP0708
SUM      EQU    COMMON+23                                       FINP0709
ADDIND   EQU    COMMON+24                                       FINP0710
PREFIX   EQU    COMMON+25                                       FINP0711
WORD     SYN    COMMON+26                                       FINP0712
ERROR    SYN    COMMON+27                                       FINP0713
I        SYN    PASS                                            FINP0714
GIN00    SYN    COMMON+30                                       FINP0715
RLOC     SYN    COMMON+32                                       FINP0716
J        SYN    CTR                                             FINP0717
FINPT    PZE                                                    FINP0718
CODE40   PZE    40                                              FINP0719
ER40MS   PZE    E40MES,,6                                       FINP0720
E40MES   BCI    6,0FINP INPUT DATA ERROR...JOB DELETED          FINP0721
COMMON   BSS    37                                              FINP0722
         END                                                    FINP0723
```

```
$IBFTC MAT9    LIST,REF,DECK
      SUBROUTINE MAT9(A,X,KR,KC,LC,LA)                                  MAT90000
      DIMENSION A(KR,KC),X(KR,LC)                                       MAT90001
      N=KR                                                              MAT90002
      M=LC                                                              MAT90003
      MM=KC                                                             MAT90004
      DO 15 I=2,N                                                       MAT90005
      II=I-1                                                            MAT90006
      DO 15 J=1,II                                                      MAT90007
      IF(A(I,J))9,15,9                                                  MAT90008
    9 IF (ABS(A(J,J))-ABS(A(I,J))) 11,10,10                             MAT90009
   10 R=A(I,J)/A(J,J)                                                   MAT90010
      GO TO 13                                                          MAT90011
   11 R=A(J,J)/A(I,J)                                                   MAT90012
      DO 12 K=1,MM                                                      MAT90013
      B=A(J,K)                                                          MAT90014
      A(J,K)=A(I,K)                                                     MAT90015
   12 A(I,K)=B                                                          MAT90016
   13 JJ=J+1                                                            MAT90017
      DO 14 K=JJ,MM                                                     MAT90018
   14 A(I,K)=A(I,K)-R*A(J,K)                                            MAT90019
   15 CONTINUE                                                          MAT90020
      IF (ABS(A(N,N))-1.0E-10)16,16,17                                  MAT90021
   16 CALL ERRS(1,4HMAT9)                                               MAT90022
      LA=-1                                                             MAT90023
      RETURN                                                            MAT90024
   17 DO28J=1,M                                                         MAT90025
      KK=N+J                                                            MAT90026
      X(N,J)=A(N,KK)/A(N,N)                                             MAT90027
      DO28I=2,N                                                         MAT90028
      JJ=N-I+1                                                          MAT90029
      B=0.                                                              MAT90030
      II=N-I+2                                                          MAT90031
      DO 25 K=II,N                                                      MAT90032
   25 B=B+A(JJ,K)*X(K,J)                                                MAT90033
      IF (ABS(A(JJ,JJ))-1.0E-10)26,26,28                                MAT90034
   26 CALL ERRS(2,4HMAT9)                                               MAT90035
      LA=-1                                                             MAT90036
      RETURN                                                            MAT90037
   28 X(JJ,J)=(A(JJ,KK)-B)/A(JJ,JJ)                                     MAT90038
      LA=+1                                                             MAT90039
                                                                        MAT90040
```

```
      RETURN                                                  MAT90041
      END                                                     MAT9004+
```

```
$IBFTC MPRT    LIST,REF,DECK
C      MPRT PRINTS THE FIRST N ROWS AND COLUMNS OF A 20X20 ARRAY
       SUBROUTINE MPRT (A,N)
       DIMENSION A(20,20)
       DO 100 I=1,N
       WRITE (3,1001) I,(A(I,J),J=1,N)
 1001  FORMAT (4HOROW,I4,5E20.8/(8X,5E20.8))
 100   CONTINUE
       RETURN
       END
```

```
$IBFTC SCRF     LIST,REF,DECK
C      SCRF COMPUTES AN NXN SCRIPT F MATRIX (( SCRIPT F(I,J) ))
C
       SUBROUTINE SCRF (N,NN,RHO,F,AREA,R,D,DI,SF,SFA,IERR)
C
       DIMENSION RHO(20,20),F(20,20),AREA(20),R(20,20,20)
     1  ,ALPHA(20,20),A(20,20),B(20,20),C(20,20),DD(20,20)
     2  ,D(N,NN),DI(N,N)
     3  ,SF(20,20),SFA(20,20)
     4  ,WK(10)
C
  100  N2= N*N
       NN2= 2*N2
       IERR= 0
C      CLEAR STORAGE PEGIONS
       DO 120 I=1,400
       DD(I,1)= 0.
       SF(I,1)= 0.
       SFA(I,1)= 0.
  120  CONTINUE
       DO 150 I=1,NN2
       D(I,1)= 0.
  150  CONTINUE
C
C      COMPUTE ABSORBITIVITIES AND EMISSITIVITIES.
  200  DO 210 I=1,N
       DO 210 J=1,N
       ALPHA(I,J)= 1.-RHO(I,J)
  210  CONTINUE
C
C      COMPUTE MATRICES A,B,C,AND D.
  300  DO 390 I=1,N
       DO 390 J=1,N
       WK(3)= ALPHA( J,I)*F(I,J)
       WK(1)= ALPHA(I,J)*WK(3)
       WK(2)= 0.
       WK(4)= 0.
C
       DO 320 K=1,N
       WK(5)= R(J,K,I)*F(I,K)*F(K,J)
       WK(6)= WK(5)*RHO(J,K)
```

```
      WK(7)= WK(5)*ALPHA(J,K)
C
      WK(1)= WK(1) +      (I,K)*WK(7)
      WK(2)= WK(2) +  LPHA(I,K)*WK(6)
      WK(3)= WK(3) +      (7)
      WK(4)= WK(4) + WK(6)
  320 CONTINUE
C
      A(I,J)= -WK(1)
      B(I,J)= -WK(2)
      C(I,J)=  WK(3)
      D(I,J)= -WK(4)
      IF (I-J) 390,330,390
C     I=J, DIAGONAL ELEMENTS
  330 D(I,J)= 1.-WK(4)
      IN= I+N
      B(I,IN)= 1.
  390 CONTINUE
C
C
C     COMPUTE SMALL P MATRIX
  400 LA= 1
C     [illegible]
      CALL MAI9 (D,DI,N,NN,N,LA)
      IF (LA) 410,410,500
  410 WRITE (3,1000)
 1000 FORMAT (68H1 ERROR, MATRIX D CAN NOT BE INVERTED, CHECK DIAGONAL E
     1LEMENTS OF D,/1H0,5X, 8HMATRIX DI)
      IERR=1
      CALL VMPRT (D,N)
      GO TO 900
C
C     COMPUTE CAPITAL D MATRIX
  500 DO 590 I=1,N
      DO 590 J=1,N
      WK=0.
      DO 520 K=1,N
      WK= WK + DI(J,K)*C(K,I)
  520 CONTINUE
      DD(I,J)= WK
  590 CONTINUE
```

```
C
C     COMPUTE SCRIPT F MATRIX
  600 DO 690 I=1,N
      DO 690 J=1,N
      WK= A(I,J)
      DO 620 K=1,N
      WK= WK + B(I,K)*DD(J,K)
  620 CONTINUE
      SF(I,J)= -WK
      SFA(I,J)= -WK*AREA(I)
  690 CONTINUE
  900 RETURN
      END
```

```
$IBFTC VMPRT    LIST,REF,DECK
C       VMPRT PRINTS AN NXN ARRAY
        SUBROUTINE VMPRT (A,N)
        DIMENSION A(N,N)
        DO 100 I=1,N
        WRITE (3,1001) I,(A(I,J),J=1,N)
 1001   FORMAT (4HOROW,I4,5E20.8/(8X,5E20.8))
 100    CONTINUE
        RETURN
        END
```

```
INPUT FOLLOWS
H1     DIRECTIONAL SPECULAR, ALUM. PAINT
H2     BLACK, BLACK
 N      4
 01,030.7075         01,040.7283                MRHO  20,20        01,020.7075
 02,030.07           02,040.1275                                   02,010.1275
 03,020.07           03,040.1275                                   03,010.1275
MF       20,20       02,010.2               03,010.2               03,020.2
 04,010.2            04,020.2               04,030.2               04,040.4
                     AREA                   1      0.25            2     0.25
 3      0.25         4      0.75
MR1     20,20        01,020.07              01,030.07
MR2     20,20        01,030.07              02,030.07
MR3     20,20        C1,020.07              02,011.519             03,C20.07
                                                                  MR4    20,20
 01,020.16583        C1,030.16583           02,010.692613          02,030.07
                     03,010.692813          03,020.07
 04,010.752091       04,020.13388           04,030.13388
                                                                  END
END OF INPUT
```

SPECULAR-DIRECTIONAL SCRIPT F PROGRAM (AH052A), 10/28/64

DIRECTIONAL SPECULAR, ALUM. PAINT

BLACK, BLACK

RHO(I,J) MATRIX

ROW	1	0.	0.70750000E 00	0.70750000E 00	0.72830000E 00
ROW	2	0.12750000E-00	0.	0.70000000E-01	0.12750000E-00
ROW	3	0.12750000E-00	0.70000000E-01	0.	0.12750000E-00
ROW	4	0.	0.	0.	0.

F(I,J) MATRIX

ROW	1	0.	0.20000000E-00	0.20000000E-00	0.59999999E 00
ROW	2	0.20000000E-00	0.	0.20000000E-00	0.59999999E 00
ROW	3	0.20000000E-00	0.20000000E-00	0.	0.59999999E 00
ROW	4	0.20000000E-00	0.20000000E-00	0.20000000E-00	0.40000000E-00

AREA VECTOR

0.25000000E-00 0.25000000E-00 0.25000000E-00 0.75000000E 00

R(I,J,K) ARRAY

BLOCK NO. 1

ROW	1	0.	0.70000000E-01	0.70000000E-01	0.
ROW	2	0.	0.	0.70000000E-01	0.
ROW	3	0.	0.70000000E-01	0.	0.
ROW	4	0.	0.16582999E-00	0.16582999E-00	0.

BLOCK NO. 2

ROW	1	0.	0.	0.70000000E-01	0.
ROW	2	0.	0.	0.70000000E-01	0.
ROW	3	0.15189999E 01	0.	0.	0.
ROW	4	0.69261300E 00	0.	0.70000000E-01	0.

BLOCK NO. 3

ROW	1	0.	0.70000000E-01	0.	0.
ROW	2	0.15189999E 01	0.	0.	0.
ROW	3	0.	0.70000000E-01	0.	0.
ROW	4	0.69261300E 00	0.70000000E-01	0.	0.

BLOCK NO. 4

ROW	1	0.	0.16582999E-00	0.16582999E-00	0.

ROW	2	0.69261300E 00	0.	0.70000000E-01	0.
ROW	3	0.69261300E 00	0.70000000E-01	0.	0.
ROW	4	0.75209100E 00	0.13388000E-00	0.13388000E-00	0.

SCRIPT F MATRIX

ROW	1	0.48790440E-03	0.52023036E-01	0.52023036E-01	0.17548605E-00
ROW	2	0.52221070E-01	0.43687483E-02	0.21963776E-00	0.60985991E 00
ROW	3	0.52221070E-01	0.21963776E-00	0.43687482E-02	0.60985991E 00
ROW	4	0.58881963E-01	0.20385623E-00	0.20385623E-00	0.53362094E 00

SCRIPT FA MATRIX

ROW	1	0.12197610E-03	0.13005759E-01	0.13005759E-01	0.43871512E-01
ROW	2	0.13055267E-01	0.10921870E-02	0.54909441E-01	0.15246497E-00
ROW	3	0.13055267E-01	0.54909441E-01	0.10921870E-02	0.15246497E-00
ROW	4	0.44011472E-01	0.15289217E-00	0.15289217E-00	0.40021570E-00

APPENDIX IV

EXPERIMENTAL DATA—
RADIATION EXCHANGE EXPERIMENT

The experimental data used in the verification of the analytical techniques described in Section 6 are shown in Table 15. The predicted receiver temperature was calculated from a heat balance between the surfaces of the experimental enclosure. The heat balance equation for the receiver is

$$A_S \mathfrak{F}_{S-R}\left(\sigma T_S^{\,4} - \sigma T_R^{\,4}\right) + A_M \mathfrak{F}_{M-R}\left(\sigma T_M^{\,4} - \sigma T_R^{\,4}\right) = A_R \mathfrak{F}_{R-O}\left(\sigma T_R^{\,4} - \sigma T_O^{\,4}\right) + Q_{LOSS}$$

$$\sigma T_R^{\,4} = \frac{A_S \mathfrak{F}_{S-R} \sigma T_S^{\,4} + A_M \mathfrak{F}_{M-R} \sigma T_M^{\,4} + A_R \mathfrak{F}_{R-O} \sigma T_O^{\,4} - Q_{LOSS}}{A_S \mathfrak{F}_{S-R} + A_M \mathfrak{F}_{M-R} + A_R \mathfrak{F}_{R-O}}$$

For Configuration 3, run number 7, using the directional analysis to obtain the $\mathfrak{F}$'s

$$\sigma T_R^{\,4} = \frac{0.0593(201.84) + 0.0013(62.85) + 0.159(1.0) - 0.57}{0.2196}$$

$$\sigma T_R^{\,4} = 53.0$$

$$T_R = 419.4^{\circ}R$$

This temperature can be compared to the experimentally measured value of $428.2^{\circ}R$.

The net heat lost by the source, Q_S, is computed by summing the heat leaving the source and received by each surrounding surface

$$Q_S = Q_{S-M} + Q_{S-R} + Q_{S-O} + Q_{LOSS}$$

$$Q_{S-M} = A_S \mathfrak{F}_{S-M}\left(\sigma T_S^{\,4} - \sigma T_M^{\,4}\right)$$

$$Q_{S-R} = A_S \mathfrak{F}_{R-S}\left(\sigma T_S^{\,4} - \sigma T_R^{\,4}\right)$$

$$Q_{S-O} = A_S \mathfrak{F}_{R-O}\left(\sigma T_S^{\,4} - \sigma T_O^{\,4}\right)$$

Using the data from Run 7, directional analysis

$$Q_S = 0.0013(201.84 - 62.85) + 0.0593(201.84 - 57.62) + 0.159(201.84 - 1.0)$$

$$Q_S = 40.68 \text{ Btu/hr}$$

This value compares to the experimental quantity of 41.29 Btu/hr.

As described in Section 6, a guard heater method was used to minimize the extraneous heat losses from each test surface. Figure 38 shows the measured heat losses from a vacuum deposited aluminum coated surface and a 3M black paint coated surface. These results were used to correct the experimentally measured source radiation and in the prediction of the temperature of the receiver temperature.

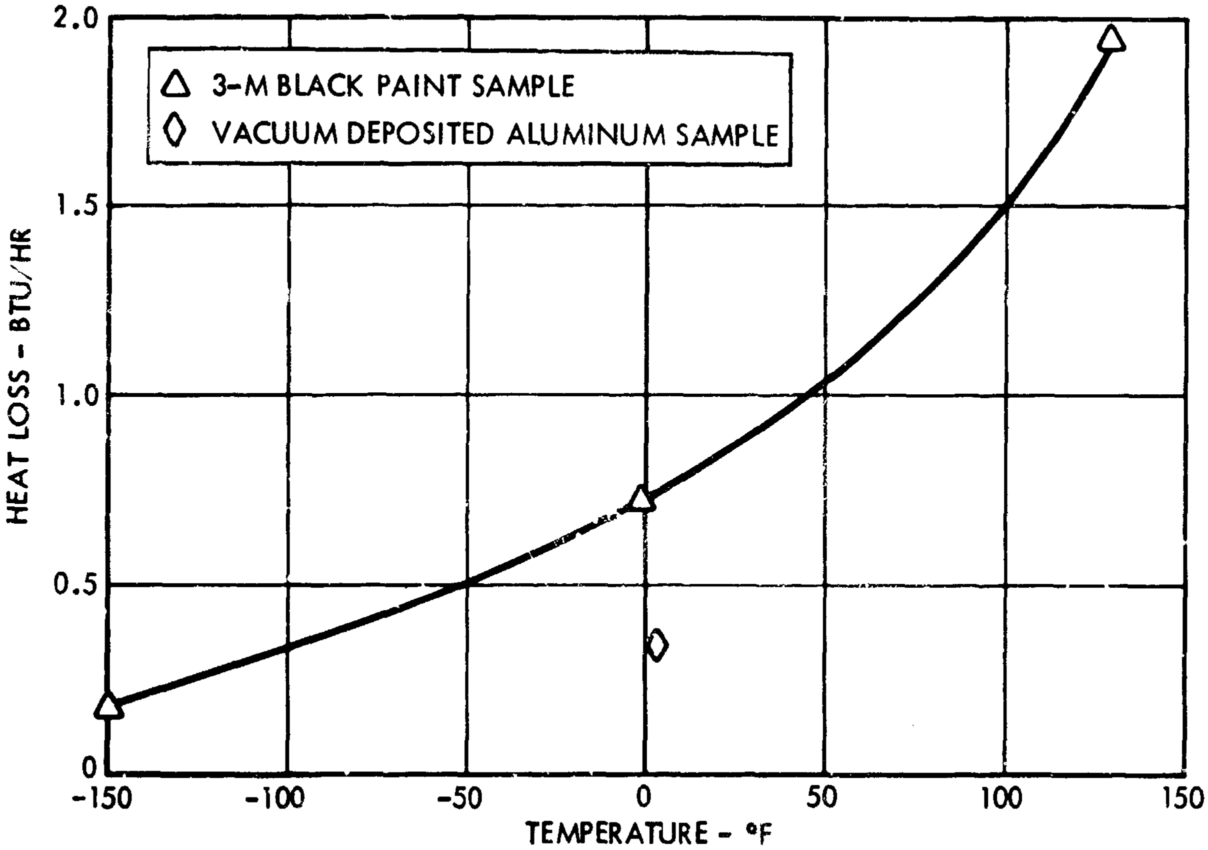

Figure 38. Measured Heat Loss from Test Surfaces of Radiation Experiment

Table 15. Summary of the Data Obtained in the Experimental Testing of the Analytical Prediction

Run Number	1	2	3	4	5
Date	3/18/65	3/19/65	3/19/65	3/23/65	3/4/65
Pressure	4×10^{-6}	4×10^{-6}	3×10^{-6}	4×10^{-6}	5×10^{-6}
Configuration	*	*	*	**	1
Source					
Center T.C. - °F	129.9	-1.0	-150.9	+4.4	73.8
Corner T.C. - °F	129.1	-1.5	-151.7	+4.1	72.2
Guard T.C. - °F	129.9	-0.3	-147.4	+1.0	73.1
Mirror					
Center T.C. - °F					
Corner T.C. - °F					
Guard T.C. - °F					
Receiver					
Center T.C. - °F					-114.5
Corner T.C. - °F					-115.0
Guard T.C. - °F					-114.8
Source Voltage, volts	50.5	30.4	13.5	6.86	41.11
Source Current, amps	0.276	0.167	0.0776	0.0373	0.2266

*Single black plate

**Single vacuum deposited aluminum plate

Table 15. Summary of the Data Obtained in the Experimental Testing of the Analytical Prediction (Continued)

Run Number	6	7	8	9	10
Date	3/28/65	4/1/65	4/5/65	4/6/65	4/8/65
Pressure	2×10^{-6}	3×10^{-6}	4×10^{-6}	5×10^{-6}	7×10^{-6}
Configuration	2	3	4	5	6
Source					
Center T. C. - ^{o}F	124.6	125.8	124.7	125.0	124.5
Corner T. C. - ^{o}F	124.5	125.8	124.3	124.6	124.1
Guard T. C. - ^{o}F	125.1	125.3	123.7	126.7	125.5
Mirror					
Center T. C. - ^{o}F		-22.4	-51.8	-74.7	-63.5
Corner T. C. - ^{o}F		-22.4	-51.7	-74.7	-62.6
Guard T. C. - ^{o}F		-23.7	-51.7	-73.5	-60.3
Receiver					
Center T. C. - ^{o}F	-66.1	-31.0	-36.5	-50.3	-61.3
Corner T. C. - ^{o}F	-66.4	-31.7	-37.0	-50.3	-61.3
Guard T. C. - ^{o}F	-65.4	-24.4	-35.2	-52.4	-61.7
Source Voltage, volts	48.7	48.0	47.7	47.3	47.4
Source Current, amps	0.267	0.2635	0.2615	0.259	0.2592

APPENDIX V

BIBLIOGRAPHY FOR

JOINT THERMAL CONDUCTANCE

APPENDIX V

BIBLIOGRAPHY FOR JOINT THERMAL CONDUCTANCE

1. Ambrosio, A. and Lindh, K. "Thermal Contact Resistance of Riveted Joints," UCLA Engineering Report No. C55-4, February 1955.

2. Ambrosio, A. and Lindh, K. "Thermal Contact Resistance of Spot Welded Titanium Joints," UCLA Engineering Report No. C55-12, March 1955.

3. Blum, H. A. and Moore, C. J. "Heat Transfer Across Surfaces in Contact Transient Effects of Ambient Temperatures and Pressures," NASA-CR-57137, 1964.

4. Bernard, J. "The Thermal Resistance of Joints: Translation 951," AD 202, 822, 1961.

5. Clausing, A. H. and Chao, B. T. "Thermal Contact Resistance in a Vacuum Environment," ASME Journal of Heat Transfer, 87:243-251, May 1965.

6. Gurr, G. V. and Cote, H. S. "A Study of the Thermal Conductance of Metallic Joints," Engineering Report No. LB-25705, Douglas Aircraft Company, 23 January 1958.

7. Lindh, K. "Measurement of Thermal Contact Resistance," UCLA Engineering Report No. C14-53, July 1953.

8. Lindh, K. "Thermal Contact Resistance Study," UCLA Engineering Report No. C15-53, August 1953.

9. Lindh, K. "Progress Report Contract," North American P. O. No. L522-138792, Thermal Resistance, UCLA Engineering Report No. 56-28, 1 June 1956.

10. Lindh, K., Lieb, B. A., Knuth, E. L., Ishimoto, T., and Kaysen, H. M. "Studies in Heat Transfer in Aircraft Structure Joints," UCLA Engineering Report No. 57-50, May 1957.

11. Little, R., Smith, S., et al. "Electrical Breakdown in Vacuum NRL 5671," AD 266603, 2 October 1961.

12. Lobbet, J. and Robb, E. "Thermo-Mechanical Analysis of Structural Joint Study," WADD TR 61-151, January 1962.

13. Miller, Y. S. "Thermal Resistances in Contact Areas of Heating Elements," (Prokontak TUI TERMICHNI OPORY U TEPLOVYDILYA YUCHYKH ELEMENTAKH) March 1964, Translation into English from Akad. Nauk Ukr RSR, Inst. Teploenerg, 2b Prats (Kiev) no 24, 1962, NASA-TT-F-8839.

APPENDIX VI

COMPONENT JOINT TEST DATA

USED FOR CORRELATION TASK

Three experimental tests were conducted to verify the results of the correlation task. The experimental measurements are given in Table 16. The thermocouple locations and data reduction technique are described in Appendix I. The bolt locations for these three tests are shown in Figure 39.

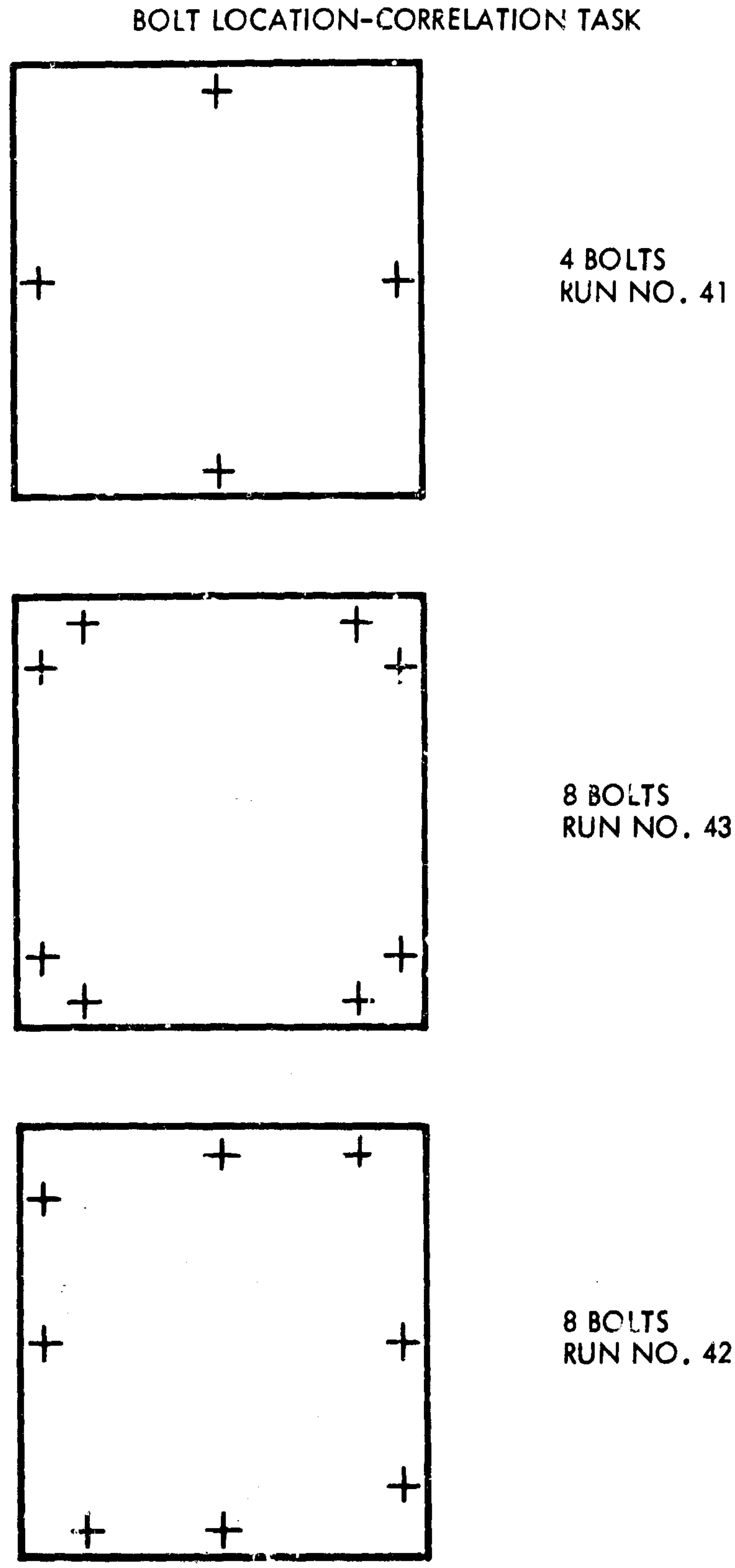

Figure 39. Bolt Locations for Correlation Task Experiments

Table 16. Additional Component Joint Correlation Data

Run Number	41	42	43
Date	11/24/64	11/25/64	11/25/64
Pressure	5×10^{-7}	5×10^{-6}	5×10^{-6}
Absolute T. C.			
1 - °F	92.6	88.4	92.7
2 - °F	81.8	74.9	75.0
3 - °F	66.6	65.9	66.4
4 - °F	67.0	66.4	66.9
Differential T. C.			
1 - °F	17.64	14.32	18.42
2 - °F	17.70	13.93	18.45
3 - °F	11.94	7.36	10.19
4 - °F	7.46	4.97	10.59
5 - °F	1.80	1.11	9.44
6 - °F	7.80	4.26	7.95
7 - °F	10.18	3.26	3.64
8 - °F	10.40	2.53	1.61
Voltage, volts	52.96	52.95	52.95
Current, amps	0.1880	0.1880	0.1880
Water Flow, ml/min	700	575	550
Bolt Torque, in-lb	24	24	24
Filler	None	None	None
Sample Number	3	3	3
Number of Bolts	4	8	8
h, Btu/hr ft^2 °F	13.4	22.0	13.7

Unclassified

Security Classification

DOCUMENT CONTROL DATA - R&D

(Security classification of title, body of abstract and indexing annotation must be entered when the overall report is classified)

1. ORIGINATING ACTIVITY (Corporate author) AFFDL (FDFE WPAFB, Ohio	2a. REPORT SECURITY CLASSIFICATION Unclassified 2b. GROUP

3. REPORT TITLE

Prediction of Space Vehicle Thermal Characteristics

4. DESCRIPTIVE NOTES (Type of report and inclusive dates)

TR

5. AUTHOR(S) (Last name, first name, initial)

J. T. Bevans, T. Ishimoto, B. R. Loya, E. E. Luedke

6. REPORT DATE	7a. TOTAL NO. OF PAGES	7b. NO. OF REFS
August 1965		

8a. CONTRACT OR GRANT NO.	9a. ORIGINATOR'S REPORT NUMBER(S)
b. PROJECT NO. 614617	
c.	9b. OTHER REPORT NO(S) (Any other numbers that may be assigned this report)
d.	

10. AVAILABILITY/LIMITATION NOTICES

Not to be released to the U.S. Department of Commerce, OTS, for a period of two years from date of publication.

11. SUPPLEMENTARY NOTES	12. SPONSORING MILITARY ACTIVITY
	AF Flight Dynamics Laboratory

13. ABSTRACT

The work reported herein is the first phase of a program to improve the prediction of spacecraft thermal performance. The study has consisted of measuring actual joint thermal conductances, correlation of the measured joint conductances, programing an improved method of thermal radiation analysis, and performing an experimental comparison of predicted radiation exchange for a simple geometrical system.

Three types of structural and three sizes of component mounting joints were tested and the conductances measured. A successful method of correlation was developed for the unfilled component mounting joints.

A method of radiation analysis has been programed which uses directional thermal radiation properties and accounts for the specularity and/or diffuseness of these properties. The results of this program can be readily incorporated into most existing thermal analysis programs. The user has the choice of the specular, the diffuse, or the specular-diffuse assumption. The prediction of radiation exchange using these assumptions for simple geometrical arrangements has been compared to experiment. Although the results were within the overall experimental tolerances, further improvement in the predicted values is believed possible.

DD FORM 1 JAN 64 1473

Security Classification

14. KEY WORDS	LINK A		LINK B		LINK C	
	ROLE	WT	ROLE	WT	ROLE	WT
1. Space vehicles.						
2. Passive temperature control systems.						
3. Radiant heat transfer.						
4. Thermal conductance of joints.						

INSTRUCTIONS

1. ORIGINATING ACTIVITY: Enter the name and address of the contractor, subcontractor, grantee, Department of Defense activity or other organization *(corporate author)* issuing the report.

2a. REPORT SECURITY CLASSIFICATION: Enter the overall security classification of the report. Indicate whether "Restricted Data" is included. Marking is to be in accordance with appropriate security regulations.

2b. GROUP: Automatic downgrading is specified in DoD Directive 5200.10 and Armed Forces Industrial Manual. Enter the group number. Also, when applicable, show that optional markings have been used for Group 3 and Group 4 as authorized.

3. REPORT TITLE: Enter the complete report title in all capital letters. Titles in all cases should be unclassified. If a meaningful title cannot be selected without classification, show title classification in all capitals in parenthesis immediately following the title.

4. DESCRIPTIVE NOTES: If appropriate, enter the type of report, e.g., interim, progress, summary, annual, or final. Give the inclusive dates when a specific reporting period is covered.

5. AUTHOR(S): Enter the name(s) of author(s) as shown on or in the report. Enter last name, first name, middle initial. If military, show rank and branch of service. The name of the principal author is an absolute minimum requirement.

6. REPORT DATE: Enter the date of the report as day, month, year; or month, year. If more than one date appears on the report, use date of publication.

7a. TOTAL NUMBER OF PAGES: The total page count should follow normal pagination procedures, i.e., enter the number of pages containing information.

7b. NUMBER OF REFERENCES: Enter the total number of references cited in the report.

8a. CONTRACT OR GRANT NUMBER: If appropriate, enter the applicable number of the contract or grant under which the report was written.

8b, 8c, & 8d. PROJECT NUMBER: Enter the appropriate military department identification, such as project number, subproject number, system numbers, task number, etc.

9a. ORIGINATOR'S REPORT NUMBER(S): Enter the official report number by which the document will be identified and controlled by the originating activity. This number must be unique to this report.

9b. OTHER REPORT NUMBER(S): If the report has been assigned any other report numbers *(either by the originator or by the sponsor)*, also enter this number(s).

10. AVAILABILITY/LIMITATION NOTICES: Enter any limitations on further dissemination of the report, other than those imposed by security classification, using standard statements such as:

(1) "Qualified requesters may obtain copies of this report from DDC."

(2) "Foreign announcement and dissemination of this report by DDC is not authorized."

(3) "U. S. Government agencies may obtain copies of this report directly from DDC. Other qualified DDC users shall request through
____________________________________."

(4) "U. S. military agencies may obtain copies of this report directly from DDC. Other qualified users shall request through
____________________________________."

(5) "All distribution of this report is controlled. Qualified DDC users shall request through
____________________________________."

If the report has been furnished to the Office of Technical Services, Department of Commerce, for sale to the public, indicate this fact and enter the price, if known.

11. SUPPLEMENTARY NOTES: Use for additional explanatory notes.

12. SPONSORING MILITARY ACTIVITY: Enter the name of the departmental project office or laboratory sponsoring *(paying for)* the research and development. Include address.

13. ABSTRACT: Enter an abstract giving a brief and factual summary of the document indicative of the report, even though it may also appear elsewhere in the body of the technical report. If additional space is required, a continuation sheet shall be attached.

It is highly desirable that the abstract of classified reports be unclassified. Each paragraph of the abstract shall end with an indication of the military security classification of the information in the paragraph, represented as *(TS), (S), (C), or (U)*.

There is no limitation on the length of the abstract. However, the suggested length is from 150 to 225 words.

14. KEY WORDS: Key words are technically meaningful terms or short phrases that characterize a report and may be used as index entries for cataloging the report. Key words must be selected so that no security classification is required. Identifiers, such as equipment model designation, trade name, military project code name, geographic location, may be used as key words but will be followed by an indication of technical context. The assignment of links, rules, and weights is optional.